FINITE ELEMENT ANALYSIS MODELING OF CHEMICAL VAPOR DEPOSITION OF SILICON CARBIDE

THESIS
JUNE 2014

Brandon M. Allen, Civilian

AFIT-ENP-T-14-J-38

DEPARTMENT OF THE AIR FORCE
AIR UNIVERSITY
AIR FORCE INSTITUTE OF TECHNOLOGY

Wright-Patterson Air Force Base, Ohio

This thesis was sponsored by Dr. Ming Chen at the Air Force Research Laboratory through a program administered by the Oak Ridge Institute for Science and Education.

AFIT-ENP-T-14-J-38

FINITE ELEMENT ANALYSIS MODELING OF CHEMICAL VAPOR DEPOSITION OF SILICON CARBIDE

THESIS

Presented to the Faculty

Department of Engineering Physics

Graduate School of Engineering and Management

Air Force Institute of Technology

Air University

Air Education and Training Command

In Partial Fulfillment of the Requirements for the

Degree of Master of Science in Applied Physics

Brandon M. Allen, BS

Civilian

June 2014

AFIT-ENP-T-14-J-38

FINITE ELEMENT ANALYSIS MODELING OF CHEMICAL VAPOR DEPOSITION OF SILICON CARBIDE

Brandon M. Allen, BS

Civilian

Approved:

Alex G. Li, PhD (Chairman)	Date
Larry W. Burggraf, PhD (Member)	Date
James L. Blackshire, PhD (Member)	Date

Abstract

Fiber-reinforced silicon carbide (SiC) composite materials are important for many applications due to their high temperature strength, excellent thermal shock and impact resistance, high hardness, and good chemical stability. The microstructure and phase composition of SiC composites can be tailored by fiber surface modification, the process parameters, and/or fiber preform architecture. One process by which SiC composites can be produced is chemical vapor deposition (CVD). This thesis primarily focuses on mass transport by gas-phase flow and diffusion, chemical reaction in gas phase and on solid surfaces, and thin film formation on curved surfaces, which are fundamental to the CVD process. We highlighted process parameters that can potentially affect the structures and properties of the CMCs using simple model material systems. We also analyzed the use of a finite element modeling tool, COMSOL Multiphysics, to build the series of models.

Acknowledgments

I would like to express my sincere appreciation to my faculty advisor, Dr. Alex Li, for his guidance and support throughout the course of this thesis effort. The insight and experience was certainly appreciated. I would also like to thank Dr. Larry Burggraf and Dr. James Blackshire whose probing questions were excellent at pointing out ways to strengthen my research. I give great thanks to Dr. Ming Chen at the Air Force Research Laboratory for sponsoring this work through the Oak Ridge Institute for Science and Education.

Brandon M. Allen

Table of Contents

Page

Page

List of Figures

Figure Page

List of Tables

Table Page

FINITE ELEMENT ANALYSIS MODELING OF CHEMICAL VAPOR DEPOSITION OF SILICON CARBIDE

I. Introduction

Overview

Ceramics and ceramic composites are versatile materials used in almost every industry. Silicon carbide (SiC) in particular is capable of high hardness, good chemical stability across a range of temperatures, low thermal expansion, and very good thermal shock resistance. These properties are made even better by the excellent impact resistance that can be achieved with the addition of ceramic fibers reinforcing the SiC matrix into a ceramic matrix composite (CMC). The abundance of methods for achieving SiC production also make it a versatile material. Silicon carbide is often produced from polymer precursors which can be utilized in any phase of matter. For example, slurried solid particulates can be layered with ceramic fibers or fabrics and then pyrolyzed; liquid polymers can be infused via capillary action or injection molding and also pyrolyzed; gaseous polymers can deposit directly upon a preform surface. These methods, though completely viable, are often expensive in material costs, energy expended, and time required [1-3].

Such factors are significantly affected by the particular manufacturing process that is used. In this thesis the focus is on the process of chemical vapor deposition (CVD). This is a process that uses the reactions of gaseous precursor chemicals to deposit the desired material (i.e. SiC) on a substrate or preform [4]. Optimizing

manufacturing processes by experiment requires a great deal of effort and cost to generate more data to fill the gaps in our collective database o f knowledge. Modeling and simulation plays a strong role in searching for effective solutions at lower cost. One powerful method of modeling a system is by means of finite element analysis where the large domain is divided into a mesh of small subdomains.

Purpose of Research

A goal of this thesis is to gain an understanding of ceramic matrix composite processing by way of computer modeling. There can be great difficulty during the manufacturing process of CMCs in determining all that is occurring at any given moment. *In situ* measurements of material properties are problematic if not impossible to obtain. It is nearly impossible, for example, to determine the deposition rate at an specific interior point using traditional methods during the deposition process. However, computer models contain all material properties at all times and locations; digital "probes" can thus be inserted into the model and material properties can be calculated.

The understanding developed from selected model material systems can also aid in guiding ceramic design. Model parameters can be parameterized over a range of values. The resulting output can lead to understanding of how, for example, temperature affects the properties of the final CMC. Input parameters can then be optimized for a desired result in final properties. All this is not only faster than performing physical experiments, but much cheaper in material and energy costs.

While computer modeling and simulation is a relatively low-cost and versatile approach towards better understanding of a CVD system, it can still be quite difficult to generate an effective model. CVD processes involve macro-scale material transport, complex chemical reactions, and sub-micro-scale kinetics on surfaces that result in changes in material geometry. Of the various literature that were reviewed, two main points of modeling research focus were presented. Some authors discussed the macroscopic chemical interactions and large-scale deposition growth rates of the SiC, many of which uses a finite element method model [5-16]. Other researchers discussed the microscopic changes in geometry resulting from the growth without discussing in detail the chemical interactions leading to the growth. They modeled the growth by using various methods, a random walk algorithm being popular [17-24]. Two research papers were found that incorporated both aspects of this ceramic production [25, 26]. Both used two separate modeling systems, one for each spatial scale, that were connected, but neither used a single unified model. In both cases, the models would be run iteratively and alternately. Geometry changes affect gas flow, which can affect chemical reactions, which in turn affect further changes in geometry, all at the same time. As they are so interconnected, a simulation strategy that can include, simultaneously, both detailed chemical reactions and geometry changes is tremendously helpful in evaluating any manufacturing process.

A secondary purpose of this research project is to provide an investigation into one viable option for a complete chemical and geometric simulation of SiC deposition.

In searching for an appropriate modeling and simulation tool, desirable qualities are that it utilizes first principles to simulate multi-physics problems and that it be user-friendly, having preprogrammed physics modules with automatic integration. Due to its module-based, customizable, multi-physics architecture, its utilization of finite element methods, and its general user-friendliness, COMSOL Multiphysics®, produced by COMSOL, Inc., was chosen as the software platform. This project seeks to explore the feasibility of using this software to model and simulate the chemical and geometric growth of SiC CMCs via CVD.

Research Objectives

This thesis is focused on producing a set of relatively simple models of the production of fiber reinforced silicon carbide (SiC/substrate). These models are meant to build understanding of the chemical vapor deposition (CVD) process with which the SiC/substrate is produced. These models are also meant to show that it is possible to build a single model that combines simultaneously running models of macroscopic flow and chemistry with microscopic geometry changes. The specific SiC CVD process to be modeled uses silane and propane as the infiltration chemicals carried by gaseous hydrogen. In this case, the hydrogen acts as both a carrier and a reactant.

The process of producing a model for any complex system can be made much easier by breaking down the system into separate, relatively simple parts. Once the smaller models are generated and their properties understood individually, they can be brought together in a unified whole. These sub-models include a model of laminar flow

of gaseous materials through and around the fabric preform; a model of the diffusion of chemical species, heat transport, and chemical reactions involved with the deposition process; and a growth process implemented by a deformation of the finite element mesh. Each of these models have its own complexity in coupling several physics phenomena coherently. These complexities are to be explored by investigating the relationship between initial variables and predicted results. How does the input pressure effect fluid flow characteristics? How does temperature effect deposition rates? Once these and other questions are answered, the three sub-models will be combined into a overarching model for the entire process. In the event that a working combined model is achieved, higher levels of complexity and realism will be added.

Assumptions/Limitations

Ceramic production methods are so complex that it is difficult to achieve a single modeling module that will contend with them all. Therefore, for the purpose of this thesis, only a single process is investigated, specifically a chemical vapor deposition process. The models to be used are also fairly simplistic. The substrate fibers that make up a fabric preform are, for example, modeled as perfectly shaped and completely solid. True fibers have imperfections and porous behavior. The geometry of the initial experimental setups only include the areas around the substrates and ignore the inflow and outflow piping that subtract from perfectly laminar flow in the systems.

II. Literature Review

Chemical vapor deposition is a process by which matter is is deposited by chemical reaction of gas-phase precursors. Chemical reactions, often endothermic, occur in the gas phase as well as on the surfaces in the reactor. This can result in deposition on surfaces of the reactor itself rather than just on the substrate. Product gasses are vacated from the reactor [27]. The deposition rate and uniformity of a given CVD process are governed by the rate of mass transfer from gas-phase to substrate surface and by the rate of surface reaction. At atmospheric pressures with horizontal substrate surfaces, these two rates usually have a similar order of magnitude and result in fairly uniform deposition. Vertical surfaces will have a lower mass transfer rate, yielding thicker deposits at the edges of a substrate [28]. Since the fibrous and porous substrates required to make CMCs have both vertical and horizontal surfaces, another method must be utilized. At low pressures (~0.001 atm) the mass transfer rate becomes more ideal for vertical surfaces. At such low pressures, in order to keep the same amount of reactants in the gas flow, the amount of carrier gasses can lessened. Without the extra carrier gas species, there is less interference in adsorption of reactants onto the substrate yielding in higher deposition rates [28]. Increased temperature has a tendency to result in smoother, more uniform deposition as well [29]. This leads to a common setup that has an inductive hot plate to heat the substrate. The walls of the reactor can be heated, cooled, or insulated. Hot-wall reactors can aid in reducing the species growth on surfaces other than the substrate [30].

Silicon carbide is a highly variable material. It has more than 170 polytypes, cubic (3C or β) and hexagonal (6H or α, and 4H) being the most common. It is a semiconductor, has high hardness, high thermal conductivity, high thermal stability, and high chemical resistance [31]. Further, as the matrix of a CMC it becomes very fracture resistant. As silicon carbide is such a desirable ceramic material, there has been a great deal of research into finding ways of producing it. Powell and Rowland report on a laundry list of epitaxy methods of producing SiC in addition to CVD [30]. Even using CVD, there are innumerable methods of producing SiC. One can use a single precursor gas that supplies both the silicon and the carbon, or one can use two gasses that each supply one species. Several studies have been done utilizing methyltrichlorosilane (MTS: CH_3SiCl_3) as a precursor [6, 10, 12-14, 32-34]. Other studies explored the use of silicon tetrachloride ($SiCl_4$) and methane (CH_4) or other hydrocarbons as a two-gas precursor system since $SiCl_4$ is cheaper than MTS [9,10, 32, 35, 36]. While the MTS and $SiCl_4/CH_4$ systems were shown to be effective in producing good quality SiC deposits, the inclusion of chlorine into the system was found to have a detrimental effect on growth rates. Chlorine-bearing species are also harder to safely exhaust from the reactors [13, 14]. Removing the chlorine from the reaction, several studies have focused on the use of silane and a simple hydrocarbon, usually methane or propane [5, 7, 8, 10, 31, 37, 38]. The relative low cost of silane and propane, as well as the lack of chlorine to etch surface and cause problems when disposing of exhaust chemicals led to the choice of using them in this model system to generate SiC.

One of the largest problems in modeling any of these methods is the sheer number of reactions that occur, both in gas-phase equilibrium and on the substrate surface. Stephanie de Persis, *et al*. reported a possible 111 species with C-H bonds in 610 irreversible reactions and 20 species with Si-H bonds in 144 irreversible reactions resulting from silane and hydrogen. This did not even include any species with Si-C bonds. (Chlorinated species would result in even more species and reactions, yet another good reason to not use it in an introductory model.) To reduce the computational power needed for these models, certain criteria for a species inclusion must be made. If a species is not consumed in any reactions it can be ignored. If removing a particular species from the model results in less than a 1% deviation in concentration profiles, it can be ignored [7]. The important reactions (17 gas-phase and 15 surface) and species (17) chosen by Blanquet, *et al*. are used in this thesis as they make up a relatively simple model that still has enough complexity to be realistic [5]. Details of the reaction are in the section on methodology.

Even ignoring redundant species and reactions to get a reasonably easy-to-compute model, all one gets is information about reaction rates. To design a true model of a deposition process, one must also include the changes in geometry. William Ros, *et al*. produced a method of simulating the growth of a ceramic that relies on a Monte Carlo random walk algorithm [19]. This is computationally expensive and focused only upon a single species' growth. Ideally, a model should include both detailed chemical data and detailed surface growth.

III. Modeling Chemical Vapor Deposition

When modeling a the chemical vapor deposition process, there are several components that must be included: bulk fluid flow, diffusion, chemistry, thermodynamics, and geometry changes resulting from fiber growth. A preform is placed in a reactor and heated while gas-phase pre-ceramic chemicals are made to flow over and through the fibers. The chemicals react with each other, forming new chemical species that also react. Some species will then adsorb to the surfaces of the preform. Once adsorbed, a species can desorb, stay on the surface but remain inert, or react with the surface to create or remove bulk material. Those species that desorb then continue through the reactor and are pulled out through the exhaust system. As surface reactions occur and build up more bulk material, the available paths of flow change and can even be cut off, resulting in porosity in the bulk material [4, 27, 29]. Each of these behaviors has governing physics behind them that must be understood in order to model them properly. This chapter discusses the background of each area.

Fluid Flow

The fluid flow behavior of a system is dependent on several fluid material properties as well as the geometry in which the fluid moves. The motion of a fluid can be determined using the thermally-decoupled Navier-Stokes Equations. [Equations 1 & 2] They take these particular forms since the gas-phase flow is compressible. Equation 1 represents the conservation of momentum, while Equation 2 shows the conservation of mass.

As can be seen in Equation 1, the viscosity, density, and pressure of a fluid are of great importance towards determining how it will flow through a system. Increasing viscosity creates a more negative value on the right side of the equation, resulting in a lower value for the acceleration of the fluid (the time derivative of the velocity). A similar results come from increasing the density of the fluid.. This is to be expected, as stickier and thicker fluids are harder to get up to speed. The pressure, or more accurately, the gradient of the pressure which can be thought of as pressure difference, causes the fluid to accelerate towards the low pressure regions. And, since pressure is not coupled to a velocity term, it is sufficient that a pressure gradient exists for fluid flow to initiate, even without body forces [39, 40].

$$\rho\frac{\partial\vec{u}}{\partial t}+\rho\vec{u}\cdot\nabla\vec{u}=-\nabla p+\nabla\cdot\left[\mu\left(\nabla\vec{u}+\left(\nabla\vec{u}\right)^{T}\right)-\frac{2}{3}\mu\left(\nabla\cdot\vec{u}\right)\vec{I}\right]+\vec{F}$$

Equation 1

$$\frac{\partial\rho}{\partial t}+\nabla\cdot\left(\rho\vec{u}\right)=0$$

Equation 2

Where:

ρ = fluid density [kg/m^3]
u = velocity [m/s]
t = time [s]
p = pressure [Pa]
μ = viscosity [Pa s]
I = identity matrix
F = body forces [N/m^3]

The flowing that results from pressure gradients and body forces can be, in general, either laminar or turbulent. (There can be flows that exhibit both in a mixed

region.) Laminar flow is characterized by fluid moving in layers without much cross-layer mixing. Turbulent flow is characterized by matter mixing between layers, rapid diffusivity of momentum and heat, and non-zero vorticity (curl of velocity). One method that can be useful in determining what type of flow is present in a system is to calculate the Reynolds number (Re). It is the ratio of inertial forces to viscous forces. While the dividing line is often wide and dependent on the geometry, below Re ~ 1000 flow will typically be laminar; above will typically be turbulent. The Reynolds number is often proportional to fluid velocity, so at the low speeds of chemical inflow that pre-ceramics undergo, flow can be characterized as laminar [40]. Turbulent flow is usually considered to be undesirable when using CVD as the random flow tends to create uneven deposition. If one can set up a procedure where the Reynolds number remains in the laminar region, deposition becomes more reliable. According to Kern and Schnable, an ideal Reynolds number for atmospheric pressure experiments is between 10 and 100, while for low pressure setups it should be closer to 1 [28].

Thermodynamics

Reliable deposition is also affected by the heat flowing through a CVD reactor. The Heat Equation [Equation 3], the third Navier-Stokes equation, is used to model thermal energy flow and conservation in a system in conjunction with Equation 2 (mass is still conserved). Most chemical reaction rates in CVD are temperature dependent and are endothermic, changing the temperature of the system further [29]. The beauty of the Heat Equation is that it works in both fluids (the pre-ceramic gases) and solids (the

preform and the reactor walls). In solids, there is no mass flow, so both the velocity and viscous heating (Q_{vh}) terms are zero [39]. In the case of SiC CVD, there will not be much (if any) viscous heating in the gas phase. Heat sources/sinks include the reactor wall temperature, the heating element for the substrate, and the heat change that results from chemical reaction. There is also an element of heat source and sink in the inflow and exhaust of the gas [41]. In most CVD processes, the preform substrate is heated by either hot plate or inductive heating.

$$\rho C_P \frac{\partial T}{\partial t} + \rho C_P \vec{u} \cdot \nabla T = \nabla \cdot (k \nabla T) + Q + Q_{vh}$$

Equation 3

Where:

ρ = density [kg/m^3]
C_P = heat capacity [J/kg K]
T = temperature [K]
u = fluid velocity [m/s]
k = thermal conductivity [W/m K]
Q = heat sources/sinks [W/m^3]
Q_{vh} = Viscous heating source [W/m^3]

Chemical Reaction and Diffusion

Chemical species move about not only by the convection applied by the general fluid flow, but by the diffusion that results from uneven concentrations. This is the method by which species adsorb to the surface of the substrate. The movement resulting from diffusion is governed by Fick's Law. [Equation 4] The time derivative of the

concentration accounts for accumulation and consumption of the species. The term with the velocity component connects to the convective transport from the fluid flow. Diffusion transport is represented by the third term. The diffusion coefficient is a tensor that accounts for not only the diffusion of the target species on its own, but the interaction it has with each other species. The final term is used as a source/sink term, usually related to the combined rates of all the chemical reactions with which the particular species is involved [39].

$$\frac{\delta c}{\delta t} + \vec{u} \cdot \nabla c = \nabla \cdot (D \nabla c) + r$$

Equation 4

Where:

c = concentration of a species [mol/m^3]
t = time [s]
u = velocity [m/s]
D = diffusion coefficient [m^2/s]
r = Reaction rate expression for species [mol/ m^3 s]

The reaction rate expression in Fick's Law is a function of the individual reactions in which a species occurs. Specific reactions are governed by the modified Arrhenius equation for reaction rates. [Equation 5] It is modified by the explicitness of the temperature dependence of the pre-factor *A*. Each of the terms in the Arrhenius equation must be determined experimentally by measuring reaction rates and plotting their natural logarithms against the inverse of the temperature. The line that results will give -Ea/R as its slope and the natural logarithm of the pre factor as the intercept. The temperature dependance factor β is often viewed as a fudge factor to make data fit a nice line, but a

non-zero value can indicate that the activation energy is ranged. Individual species diffusion data is determined by the calculation of entropy, enthalpy, and heat capacity from the Shomate Equations [Equation 6] [39, 42].

$$r = A\left(T/T_o\right)^{\beta} e^{-E_a/RT}\left[X\right]^n\left[Y\right]^m$$

Equation 5

Where:

r = Reaction rate [mol/ m^3 s]
[X], [Y] = Concentration of reactants [mol/m^3]
n, m = Reaction orders
A = Pre-factor [$mol^{1-(n+m)}L^{(n+m)-1}s^{-1}$]
β = Temperature dependance factor
E_a = Activation energy [J]
R = Gas constant, 8.3145 m^3 Pa/mol K
T = Temperature [K]
T_o = Reference temperature, 298 K

$$C_P^{\circ}\left[\frac{J}{mol\cdot K}\right] = A + Bt + Ct^2 + Dt^3 + Et^{-2}$$
$$H^{\circ}\left[\frac{kJ}{mol}\right] = At + \frac{1}{2}Bt^2 + \frac{1}{3}Ct^3 + \frac{1}{4}Dt^4 - Et^{-1} + F - H$$
$$S^{\circ}\left[\frac{J}{mol\cdot K}\right] = A\ln t + Bt + \frac{1}{2}Ct^2 + \frac{1}{3}Dt^3 - \frac{E}{2t^2} + G$$

Equation 6

Where:

C_p^o = Molar Heat Capacity [J/ mol K]
H^o = Molar Enthalpy [kJ/mol]
S^o = Molar Entropy [J/ mol K]
t = Temperature [K] / 1000K
A, B, C, D, E, F, G, H are cofactors determined by experiment

Deposition Growth

Modeling changes in geometry can be difficult. Random-walk algorithms do a good job, but are computationally expensive [19, 26]. A finite element method can be used to model deposition growth by deforming the mesh itself. This can be treacherous, however. The mesh is what the entire finite element method is built upon. If the movement of the backbone has problems, the whole solution becomes problematic.

The way to use this method is to use a mesh with particularly small elements, especially near the substrate surface. As mass adsorbs onto the surface and reacts, the gaseous products leave behind new surface species of Si and C. Using knowledge of the material density and of the mass flow, retrieved via Fick's Law, it is possible to calculate the velocity at which the surface expands at each mesh element. This velocity can then be fed into the motion of the mesh which indicates the growth of the substrate [39, 43].

Finite Element Method

Many problems are very, very difficult to solve analytically. Fortunately, with the power of modern computing, it is feasible to solve problems numerically. The finite element method of numerical analysis is based upon the idea that continuous domains can be sub-divided into finitely sized, but not necessarily uniform, "elements". Over each part of the mesh of elements, an approximation of the analytical governing equations is solved. These approximations are based upon the integral forms of the partial differential equations rather than a Taylor series expansion for derivatives as used in the finite difference method. Further, there is an assumption that a solution can be determined over

each of these elements that is a linear combination of known functions, often polynomials. The individual solutions of the elements must then be linked by the relationships that these elements have with each other, usually by making them into a piece-wise continuous solution over the whole domain. The finite element method can, however, handle discontinuities with ease [44].

Like any numerical solution, finite element analysis is imperfect. Computers must truncate the numbers stored in memory at some physical limit. Also, the choice of mesh elements can greatly affect the final result. If, for example, the original domain to be solved over is a circle, it will be impossible for a mesh of triangular elements to completely cover the original domain. The size of the elements is also important. If the mesh is small, coverage of the original domain can be made more complete and the solutions from the finite difference calculations will be more accurate. There must be a trade off however; the smaller the mesh size, the more calculations must be performed and computing power has its limits [44]. One of the advantages that COMSOL offers is the ability to customize mesh size in different areas of the domain. Solution parameters often have more complicated and abrupt behaviors around edges and corners than in bulk regions. A smaller mesh can be generated at problem areas to get the fine details; a larger mesh in the bulk areas can help save computational power [39, 45].

IV. Methodology

With an understanding of the underlying mechanism that govern the process of producing SiC by CVD, the actual modeling process could begin. This work was divided

into two separate modeling systems. The first model was intended as a semi-guided exploration into the capabilities of the software used. A simple, supplied model was used as a starting point for exploring how well the multiphysics modules work together and what information can be gleaned from such a model. The second model was aimed toward generating a complete, unified model of both the chemistry and geometry changes that occur when making SiC.

Steam/Propane Reactor Tube

In an effort to start understanding the physics involved with the ceramic production, an example model provided by COMSOL was used as a jumping point. Their model for a steam reformer was used for the physics and chemistry with a geometry closer to the CVD process to be modeled. This model was of gaseous propane and steam water reacting in a tube to create carbon dioxide and hydrogen gas [46]. A complete report of the model will be included in Appendix D.

The model starts with the two-dimensional geometry of the reactor system. The "fibers" of the preform were modeled as an array of circles suspended in a space to be surrounded by the reacting gasses, shown in Figure 1. The offset arrangement of the array of fibers was chosen to more closely resemble the patters of woven fibers in a fabric. The fibers were assumed to be incompressible and completely solid pyrolytic carbon fiber. The area through which the gasses were to flow was rectangular, representing a reactor sitting on a hot plate, having no thermal insulation on the top surface, and having an inlet and outlet that span the complete vertical dimension.

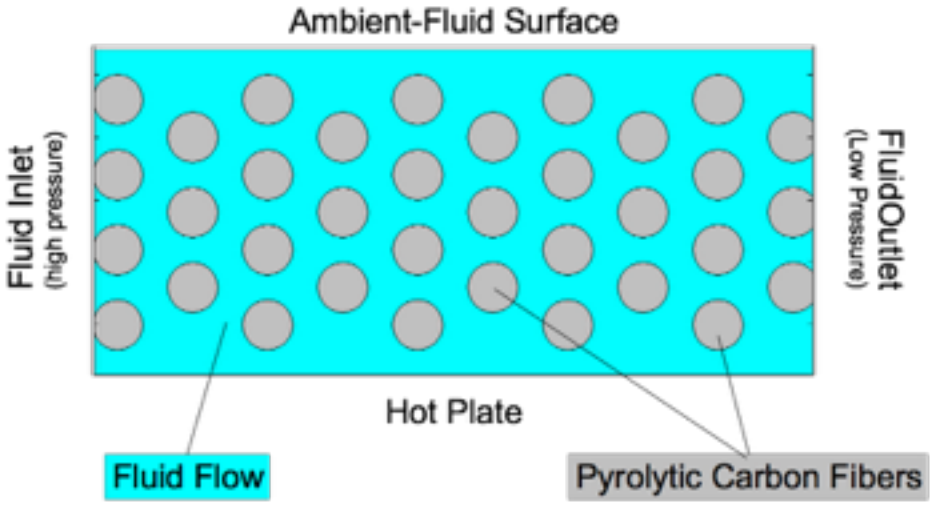

Figure 1, Steam/propane reactor: Geometry and setup of experiment. Fiber radii are 0.002 m.

To this geometry, a simple flow model was added where material flows from the left side, the fluid inlet, to the right, the fluid outlet. The Single Phase Laminar Flow module in COMSOL was appropriate for such flow as the process of impregnating preforms is done at low speeds and pressures. A no-slip boundary condition was applied to the hot plate, ambient-fluid surface, and the fiber walls. A pressure of 10^5 Pa was applied to both inlet and outlet, the inlet having an additional 75 Pa to create a pressure gradient. The model was run to find the steady-state solution. The resulting pressure gradient is shown in Figure 3 with the higher pressure being in red and the lower pressures in green. This pressure gradient was then the cause of the fluid flow that is shown in Figure 4. As the gas flows from high pressure to low pressure, the fibers force it to flow into channels between them, resulting in higher velocity flow (shown in redder tones). Low pressure areas behind each fiber result in small vortices of slower moving (bluer) fluid.

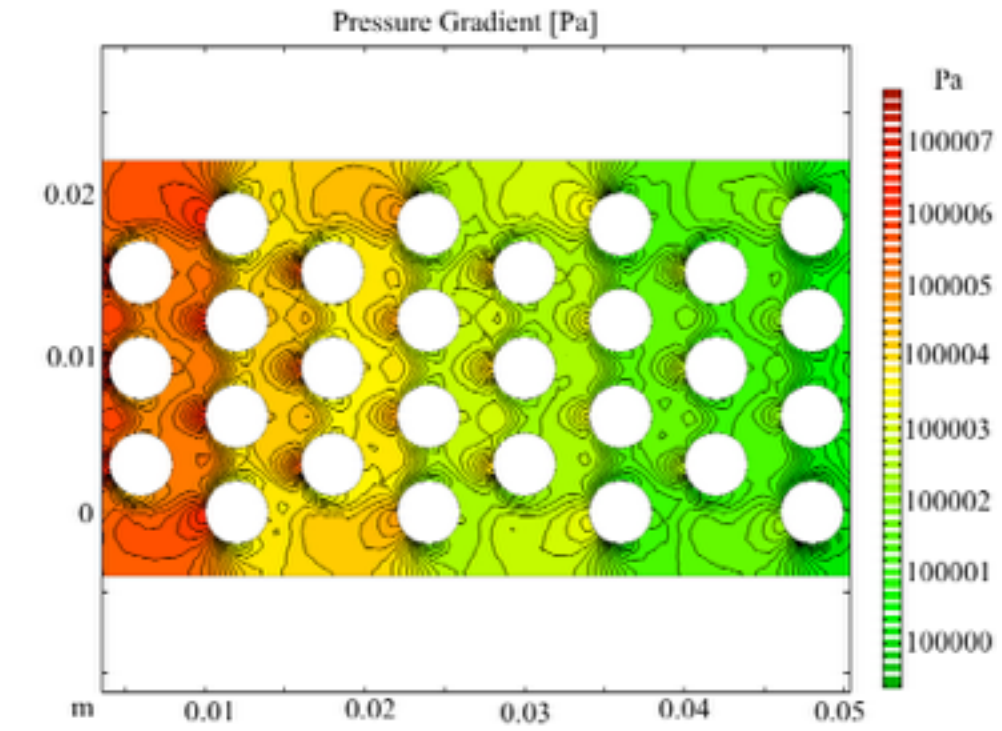

Figure 2, Steam/propane reactor: Steady state pressure gradient [Pa]

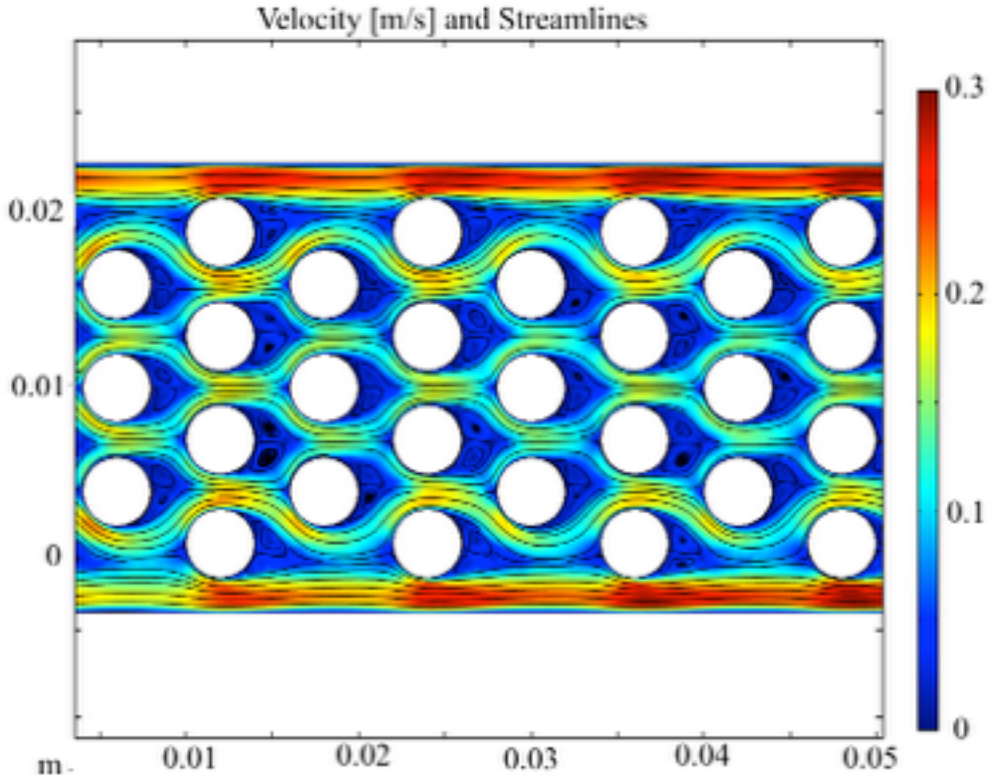

Figure 3, Steam/propane reactor: Steady state velocity magnitude [m/s] and field lines.

Having completed the flow portion of this model, the thermal and chemical portions were added. This utilized the Heat Transfer in Fluids, Heat Transfer in Solids, and Transport of Concentrated Species modules. The starting temperature of the fluid in the reactor and the fibers was 293.15 K. The inflow fluid temperature was taken to be 700 K and the hot plate was assigned an energy output of 3000 W/m^2. There was heat loss into the ambient atmosphere on the top surface and heat was allowed flow out with the fluid. The reaction $C_3H_8 + H_2O \rightarrow H_2 + CO_2$ was entered into the system along with initial mass fractions for each species (0.28, 0.50, 0.01, and 0.01 respectively). The heat of the reaction was also included into the Heat Transfer module. These updates to the model resulted in the steady-state solutions for temperature and the mass-fraction of propane shown in Figures 4 and 5. Figure 4 shows a temperature gradient with red being the hottest and blue being the coolest. As could be expected, the cooler temperatures were along the ambient-fluid boundary where heat is lost as well as towards the outlet. This also makes sense as the reaction was endothermic and had a fairly high activation energy resulting in much of the heat energy available being used. This also corresponded to the mass fraction of propane map in Figure 5. At the onset (near the inlet) there was a higher ratio of propane in the system as its had not has the opportunity of react. There was also a higher ratio at the fluid-ambient surface as there was not as much of the heat that was needed to activate the reaction. The low pressure vortices seen in Figure 3 held the fluid for more time, giving the chemicals more chance to react. This lead to the lower mass fraction of propane behind each fiber. Similar data for the other chemical species,

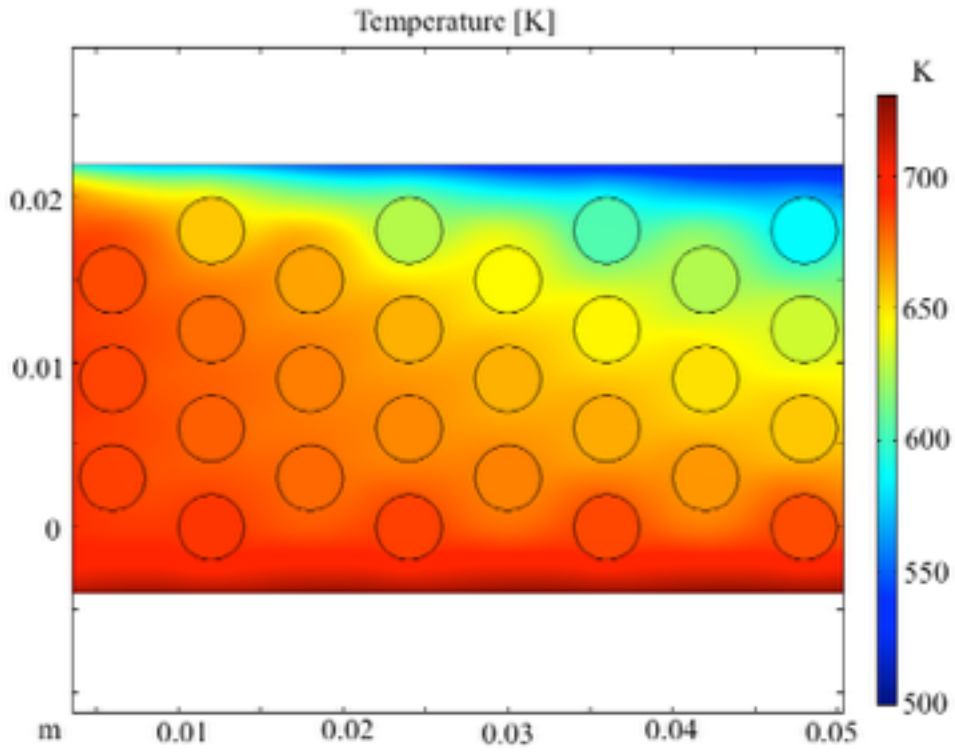

Figure 4, Steam/propane reactor: Steady state temperature [K]

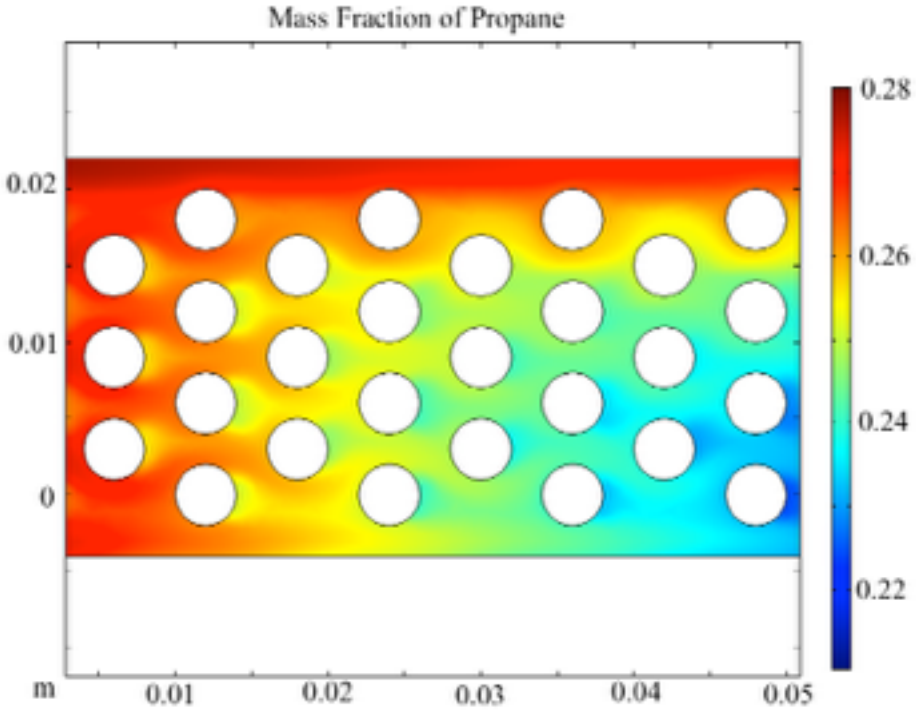

Figure 5, Steam/propane reactor: Steady state mass fraction of C3H8

though not shown, can be drawn out the model with ease. In a SiC deposition system, these type of features in the flow may cause nonuniform deposition on the substrates. This shows how important it is to optimize the system parameters.

This initial exploration into the capability that COMSOL offered was quite revealing. COMSOL was able to track a great many physical characteristics (i.e. temperature, velocity, and concentration) simultaneously and was able to report back on each at any given point or average across a surface. This shows good promise for being able to generate the desired complete SiC model.

Silicon Carbide Model System in 2-D

After exploring the simple propane and steam system, the more complex silicon carbide deposition process was tackled. The new phase of exploration was done in three disparate parts: a flow model, a chemical reaction model, and a moving mesh model. With each part, an overly-simplified model was used in order to understand the way that COMSOL models the physics and what kinds of effects various changes in the initial settings can have.

Flow Model

The flow model started out with a very similar geometry to the initial exploration model. An off-set array of circular "fibers" around which gas-phase fluid flows was generated as in Figure 6. Each fiber was taken to have a radius of 0.002 m. A rectangular area surrounds the fibers as a model of the reactor. An additional rectangle was placed in between the inlet and the fibers to start including larger, more complex

geometries. The Single-Phase Laminar Flow module was used. The inlet is the left-most edge and the outlet, the right-most. A fluid pressure difference was applied between inlet and outlet to cause flow. At the onset, the same fluid properties were used as in the previous model. Thermodynamics were ignored for this portion of the model, so there exists no hot plate or ambient heat loss.

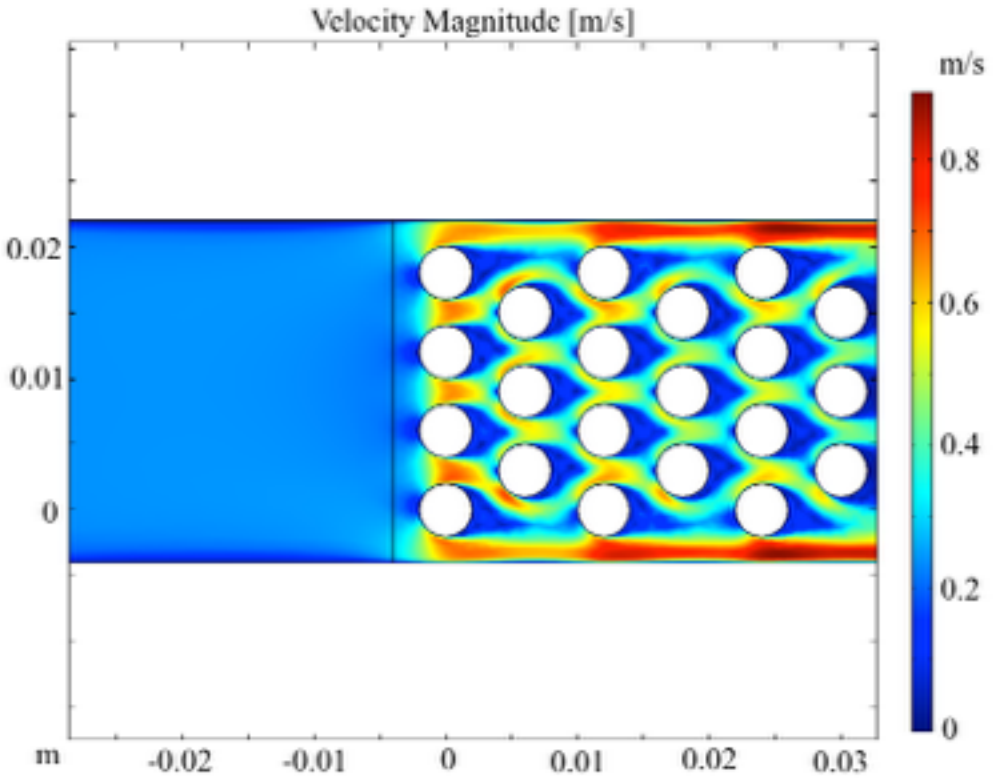

Figure 6, Flow model: Geometry (distances in [m]) and velocity magnitude (color gradient) [m/s]. Pressure difference of 491 Pa and X, Y fiber distance of thrice the radius.

Since the introductory exploration of steam and propane was only looking at a static model, and understanding how optimization of said model works is part of the goal in this endeavor, the parameterization of variables in the model was investigate. In this flow portion of the model, there are only a few things that can be parameterized: the

pressure difference between inlet and outlet, the geometry, and the fluid properties. The fluid properties are to be controlled by the chemistry and thermodynamics, so the pressure and geometry were focused on. In this first case, given a geometry with each fiber being separated in X and Y direction by thrice the fiber radius, the pressure difference was parameterized from 0.1 to 50 Pa. The average fluid velocity taken across the outlet edge was calculated [Figure 7]. The maximum Reynolds number taken from every finite element mesh cell was also calculated [Figure 8]. As long as the fluid remains in the laminar flow region, the deposition should be fairly stable. The Reynolds number is useful in helping to determine how turbulent the flow was.

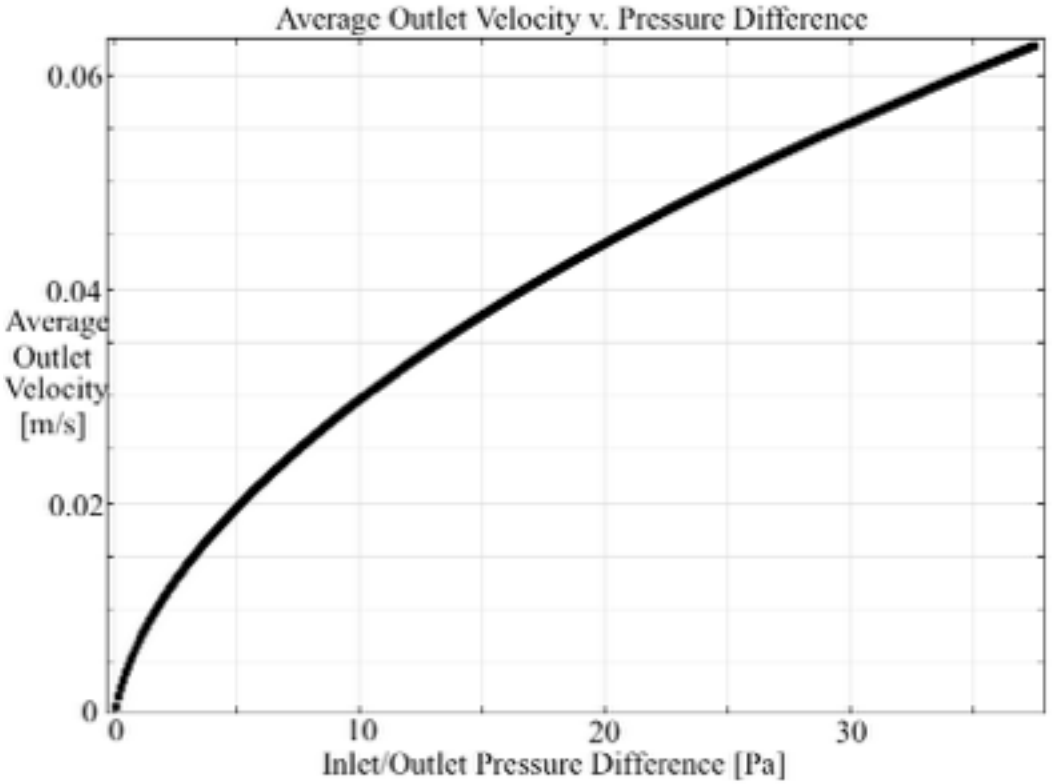

Figure 7, Flow model: Average outlet velocity [m/s] for pressure differences from 0.1 to 50 Pa and X,Y separation of thrice fiber radius

As the geometries used in this thesis were deliberately simplified, it was not of great importance to investigate the effects of differences of geometry in detail, but in the future, such investigation could be most helpful. One example was investigated: changing the X-directional separation of the fibers with a constant difference of inflow pressure to outflow pressure of 3 Pa. The separation ranged from twice the fiber radius (fibers almost touching) to twenty times the radius. This modeled the differences between tighter and looser weaves of fabric. As with pressure differences, average outlet velocity and maximum Reynolds number were calculated [Figures 9 and 10].

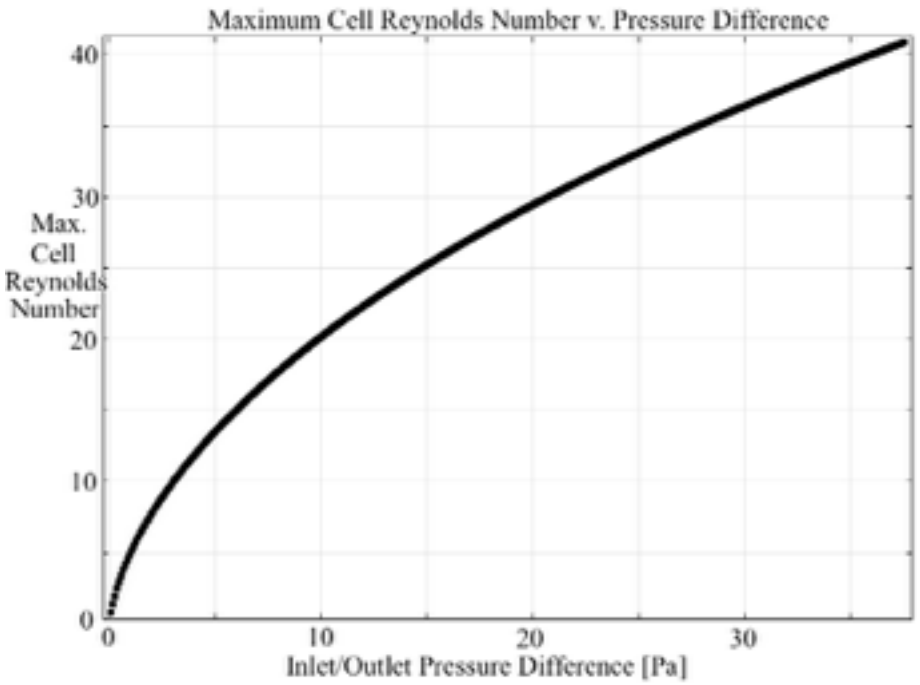

Figure 8, Flow model: Maximum Reynolds number for pressure differences from 0.1 to 50 Pa and X, Y separation of thrice fiber radius.

Figure 9 shows that a maximum average output flow rate can be found when the horizontal separation of fibers is between 0.006 and 0.008 m. Since in this model the fibers are of radius 0.002 m, the maximum average output flow rate is found when the

fiber centers are separated at a distance between 3 and 4 times the fiber radius. While the Reynolds number seems to be somewhat random at first look, it only ranges from 9.4 to 12.2. When the pressure was varied, the Reynolds number ranged from 0 to more than 40 [Figure 8]. This would suggest that the tightness of fabric weave does not have as great an effect on fluid turbulence as the pressure difference from inlet to outlet does. This would further indicate that while the choice of fabric style will matter to the final material characteristics, it will not have great effect on the production characteristics.

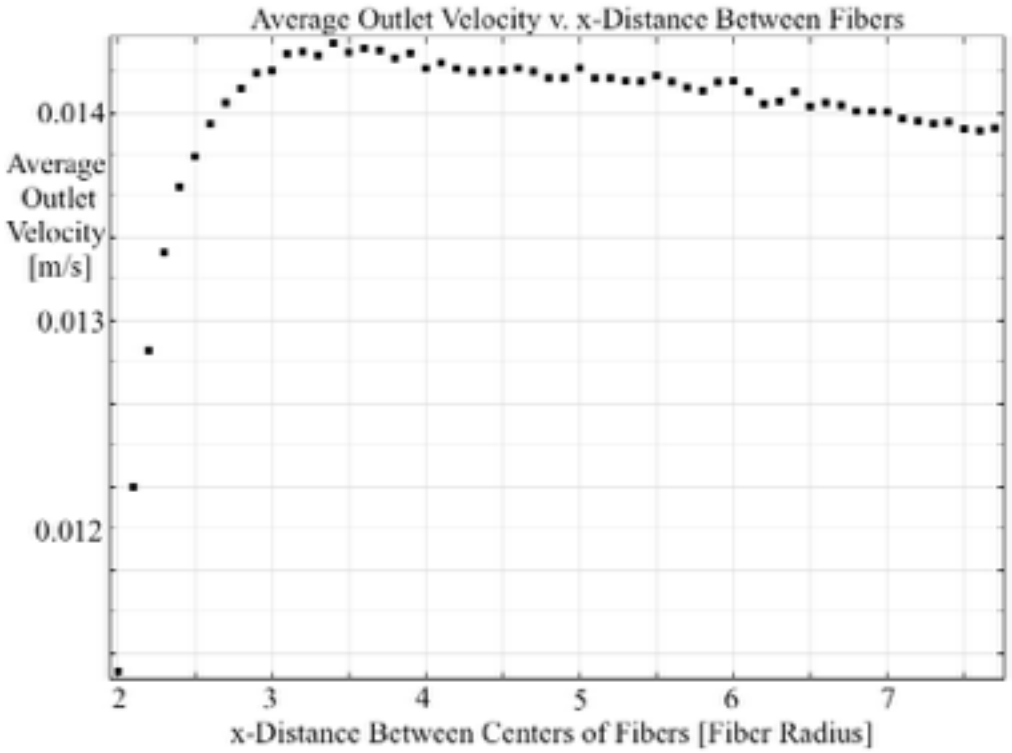

Figure 9, Flow model: Average outlet velocity for fiber x-distance from 2-20 fiber radii and pressure difference of 3 Pa.

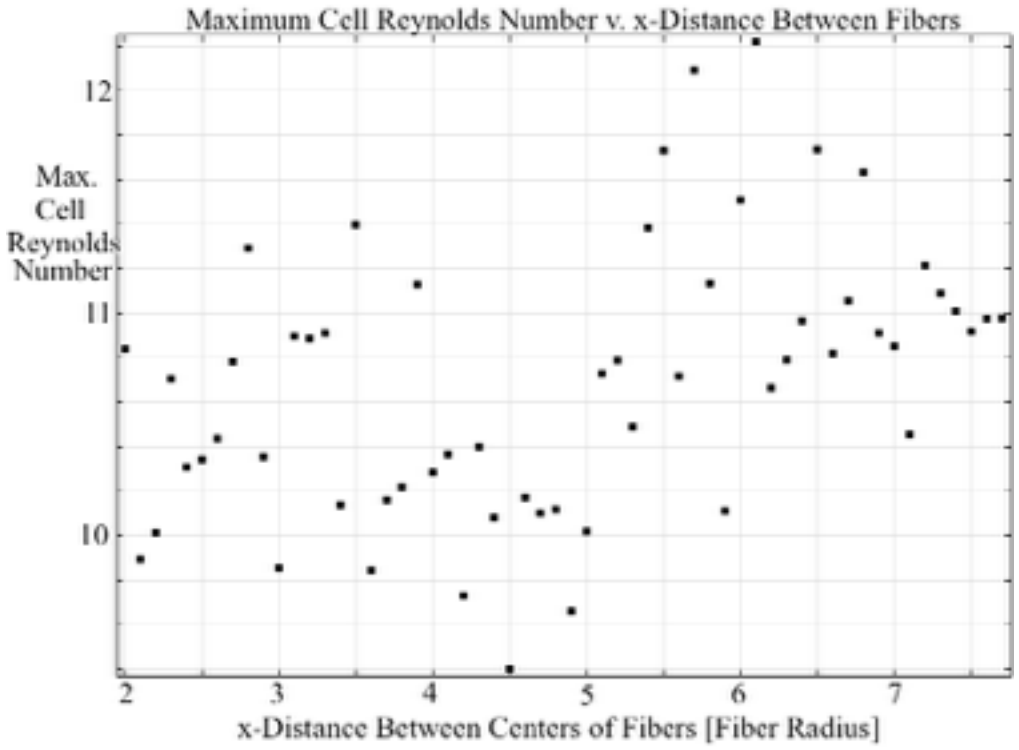

Figure 10, Flow model: Maximum Reynolds number for fiber x-distance from 2-20 fiber radii and pressure difference of 3 Pa.

Chemical Reaction Model

The second model required for this project was the of chemical reactions and their associated thermodynamics. The process of converting silane and propane to silicon carbide in a hydrogen environment is complex and involves well over 600 reactions [7, 8]. A reduced model was used as reported by Blanquet, *et al*. with 32 reactions shown in Tables 1 and 2[5]. The first two reactions in Table 2 indicate that hydrogen can etch the surface. Reaction 11 in Table 1 is incompletely reported. Since Reaction 12 from Table 1 and Reaction 10 from Table 2 are both tied to it, and both silicon and carbon are deposited without them, all three were ignored in this model building process. This was not thought to be too egregious as Dollet reported that

H_3SiCH_3 and similar species were not created in large amounts (at 1573 K and 5332 Pa) [8]. It was reported that Si_2C and C_2H_2 were the main gas species that were involved with the deposition of SiC directly when performed at a pressure of 250 mbar and temperatures from 1600 to 2000°C. At higher temperature and lower pressure, SiC_2 replaces C_2H_2 as one of the top contributing elements [5].

The Chemical Reaction Engineering module was used in a non-dimensional, time-dependent study. The fifteen reactions of the gas phase were entered into the model in the form of coefficients of the rate equation [Equation 5]. The coefficients of the Shomate Equations [Equation 6] for each species were also entered. While Blanquet, *et al*. reported the forward reaction rate coefficients they used in their models, there were no reverse reaction coefficients [5]. It was decided to search for all coefficients to all equations in the Chemistry WebBook posted by the National Institute for Standards and Technology (NIST) [42]. These values are reported in Appendix A for the species data and Appendix B for the reaction data. The initial ratio of Silane/Propane/Hydrogen was 3/1/8. Running the model for from (0 to 10)*10^{-7} s at a temperature of 2073 K resulted in the concentrations of gaseous species shown in Figure 11. Figure 12 shows the same, but zoomed in to see the lower concentration species. Hydrogen gas, H_2 remains near a concentration of 0.5 mol/m^3, so it was not shown on the figures. Silane comes to a steady state of about 0.12 mol/m^3, while the propane is used up entirely. Hydrogen atoms, methane, silylene, and atomic silicon make up the bulk of the remaining gas phase species.

Table 1, Gas phase reactions and their Arrhenius equation parameters [5].

Homogeneous Model				
Reactions		A	β	E/R
1.	$SiH_4 \Leftrightarrow SiH_2 + H_2$	6.671×10^{29}	-4.795	31946
2.	$Si_2H_6 \Leftrightarrow SiH_2 + SiH_4$	3.240×10^{29}	-4.24	29202
3.	$SiH_2 \Leftrightarrow Si + H_2$	1.060×10^{14}	-0.88	22657
4.	$2H + H_2 \Leftrightarrow 2H_2$	9.200×10^{16}	-0.6	0
5.	$C_3H_8 \Leftrightarrow CH_3 + C_2H_5$	1.698×10^{16}	0	42715
6.	$CH_4 + H \Leftrightarrow CH_3 + H_2$	2.200×10^{4}	3	4406
7.	$C_2H_5 + H \Leftrightarrow 2CH_3$	1.000×10^{14}	0	13350
8.	$2CH_3 \Leftrightarrow C_2H_6$	9.030×10^{16}	-1.18	330
9.	$C_2H_4 + H \Leftrightarrow C_2H_5$	2.210×10^{13}	0	1040
10.	$C_2H_4 \Leftrightarrow C_2H_2 + H_2$	1.500×10^{15}	0	41467
11.	$H_3SiCH_3 \Leftrightarrow SiH_2 + H_2$	2.000×10^{14}	0	36413
12.	$H_3SiCH_3 \Leftrightarrow HSiCH_3 + H_2$	1.000×10^{14}	0	32033
13.	$Si_2 \Leftrightarrow 2Si$	1.000×10^{15}	0	37460
14.	$Si_2 + CH_4 \Leftrightarrow Si_2C + 2H_2$	3.011×10^{15}	0	10000
15.	$SiH_2 + Si \Leftrightarrow Si_2 + H_2$	1.500×10^{14}	0	0
16.	$CH_3 + Si \Leftrightarrow SiCH_2 + H$	1.390×10^{12}	0.5	0
17.	$SiCH_2 + SiH_2 \Leftrightarrow Si_2C + 2H_2$	1.000×10^{15}	0	0

Table 2, Surface reactions and their Arrhenius equation parameters [5].

Heterogeneous Model				
Reactions		A	β	E/R
1.	**$C_{vol} + Si_{surf} + H_2 \rightarrow SiH_2 + C_{surf}$**	**$2.200x10^{18}$**	**0**	**52786**
2.	**$2Si_{vol} + 2C_{surf} + H_2 \rightarrow C_2H_2 + 2Si_{surf}$**	**$2.200x10^{32}$**	**0**	**52786**
3.	$SiH_4 + C_{surf} \rightarrow SiH_{2surf} + H_2 + C_{vol}$	$1.592x10^{10}$	0	9401
4.	$SiH_{2surf} \rightarrow H_2 + Si_{surf}$	$2.912x10^{14}$	0	4527
5.	$SiH_2 + C_{surf} \rightarrow SiH_{2surf} + C_{vol}$	$3.060x10^{11}$	0.5	0
6.	$Si + C_{surf} \rightarrow Si_{surf} + C_{vol}$	$3.167x10^{11}$	0.5	0
7.	$C_2H_2 + Si_{surf} \rightarrow 2C_{surf} + H_2 + 2Si_{vol}$	$3.040x10^{18}$	0.5	0
8.	$C_2H_4 + 2Si_{surf} \rightarrow 2C_{surf} + 2H_2 + 2Si_{vol}$	$2.342x10^{16}$	0.5	0
9.	$CH_4 + Si_{surf} \rightarrow C_{surf} + 2H_2 + Si_{vol}$	$2.098x10^{5}$	0.5	0
10.	$HSiCH_3 + C_{surf} \rightarrow Si_{surf} + H + CH_3 + C_{vol}$	$2.490x10^{11}$	0.5	0
11.	$CH_3 + Si_{surf} \rightarrow C_{surf} + 1.5H_2 + Si_{vol}$	$4.270x10^{11}$	0.5	0
12.	$Si_2 + 2C_{surf} \rightarrow 2Si_{surf} + 2C_{vol}$	$1.000x10^{20}$	0.5	0
13.	$Si_2C + Si_{surf} \rightarrow Si_2 + C_{surf} + Si_{vol}$	$1.000x10^{11}$	0.5	0
14.	$SiCH_2 + C_{surf} \rightarrow Si_{surf} + CH_2 + C_{vol}$	$2.550x10^{11}$	0.5	0
15.	$CH_2 + Si_{surf} \rightarrow C_{surf} + H_2 + Si_{vol}$	$4.419x10^{11}$	0.5	0

There was difficulty in getting the Reaction Engineering module to work smoothly. The built-in versions for the Shomate equations [Equation 6] were different than the ones reported by NIST. The cofactors, thus, could not be entered in without errors. A work-around was attempted, but time constraints prevented the finished model from being built. Had this been completed, experiments would have been done where temperature would be parameterized as well as initial concentrations of species.

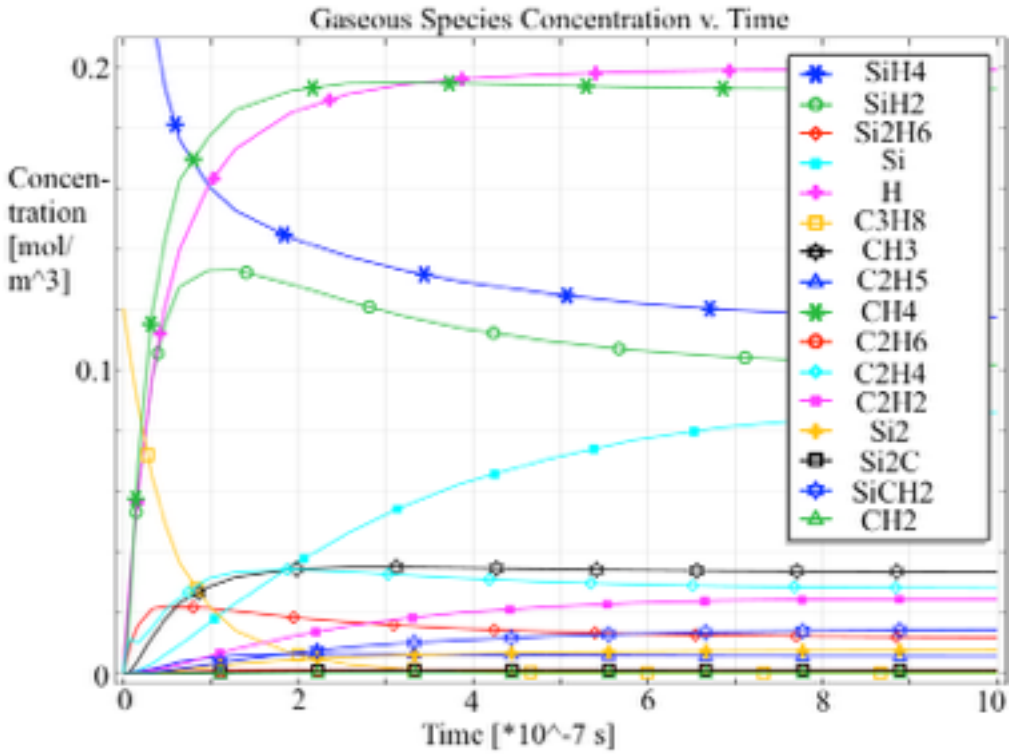

Figure 11: Chemistry model: Molar concentrations [mol/m^3] of gas-phase species as a function of time [10^{-7} s].

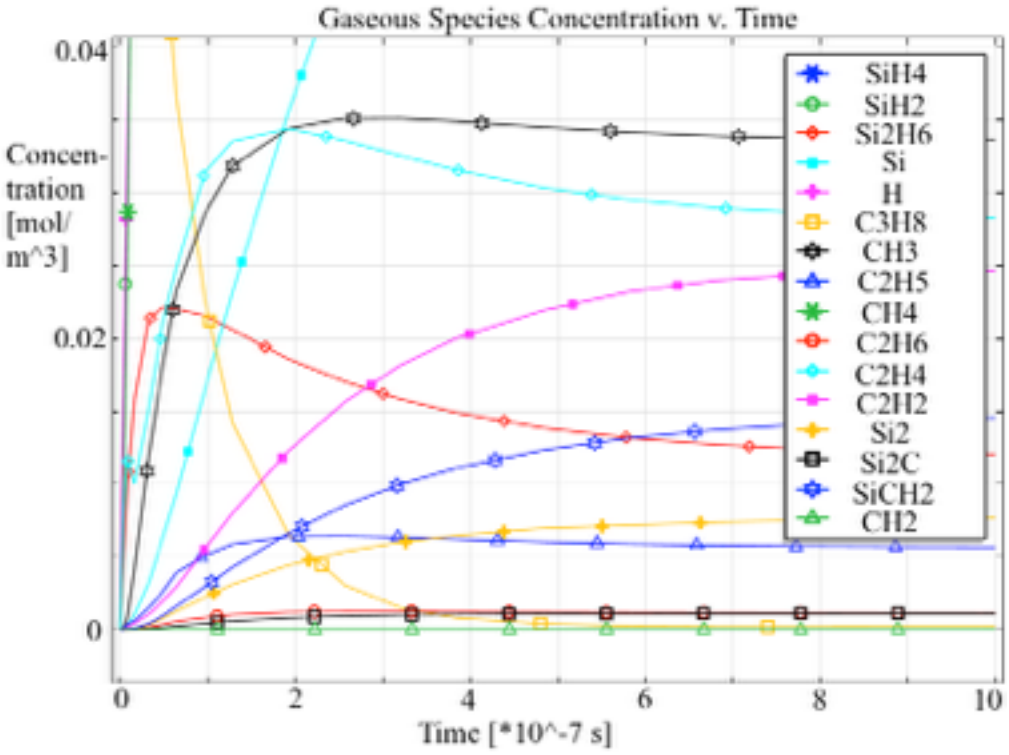

Figure 12, Chemistry model: Molar concentrations [mol/m^3] of gas-phase species as a function of time [10^{-7} s], zoomed in.

Moving Mesh

The next modeling step was to create a model that would include the deformation of the geometry of the system as chemical reactions deposit more silicon carbide on the surfaces. A combination of the Transport of Diluted Species and Deformed Geometry modules was used. To give a proof of concept, rather than the complex chemistry from the previous model, as simple single species model was created. The geometry was of a square of 0.1 m for the matrix area and four circular fibers of radius 0.005 m, shown in Figure 13. An ideal gas with an initial concentration of 20 mol/m^3, a diffusion coefficient of 10^{-9} m^2/s, and a density of 10 mol/m^3 when in solid form was used. The concentration of the gas phase was contained to be always zero at the boundaries of the fibers. In a

more true-to-life model, the concentration of the species at the boundaries would be determined by the chemical reaction rates that produce SiC using Fick's Law.

The mesh used for the finite element analysis has to have constraints put upon it for the deformation to occur. The mesh of the matrix area was given the freedom to move without any constraint. The mesh along outer boundaries on left and right edges was constrained to only move in vertical directions. Similarly, the top and bottom edges had a mesh constrained to only move horizontally. Edges, after all, cannot move outward in an enclosed volume. The boundaries of the fibers were constrained to a velocity that results from flow rates as determined by Fick's Law for diffusion and by material density.

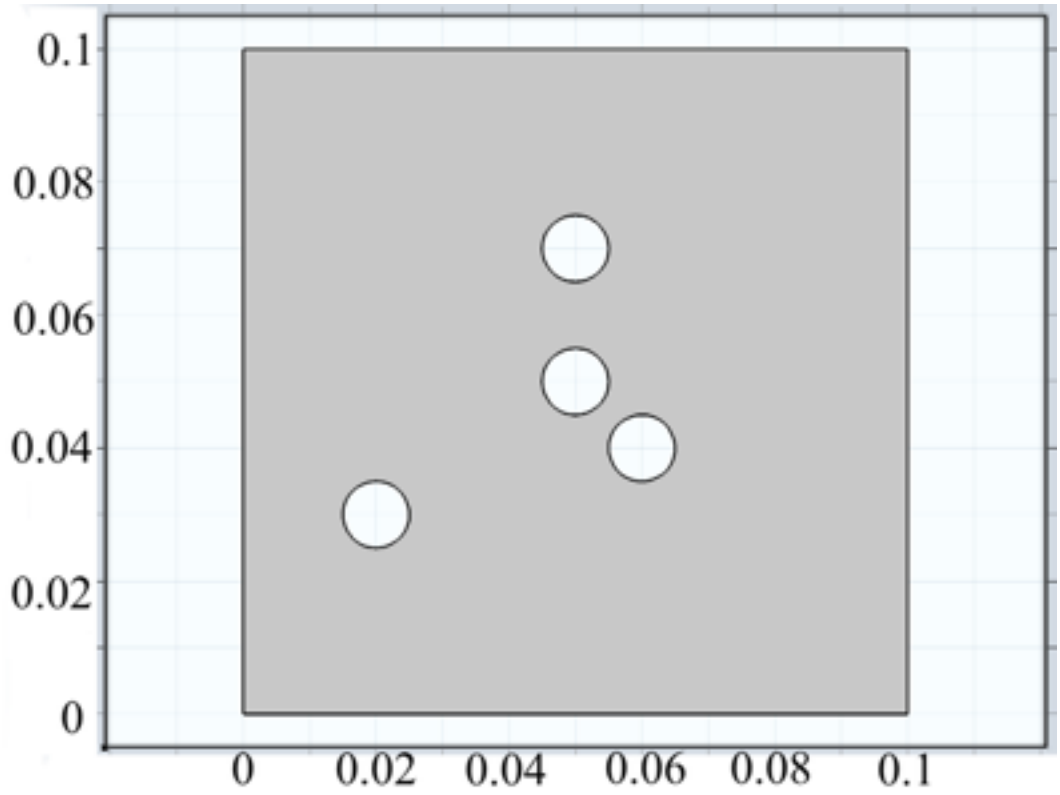

Figure 13, Moving mesh model: Geometry. Sides are 0.1 m, circle radii are 0.005 m.

The model was then run as a time dependent study in steps of 100 s for 10^6 s. The results are shown in Figure 14. The white circles are the original fiber positions and sizes. The grey areas being the accumulated bulk material. The colored areas show the concentration of the remaining gas species. One problem with this method is that the mesh tends to become so deformed that the mesh elements will invert and start modeling unreal physics. To combat this, the model has to occasionally be stopped, a new mesh set to the new geometry, and started up again. An automatic re-meshing can be set up, but it tends to keep odd artifacts from the previous mesh.

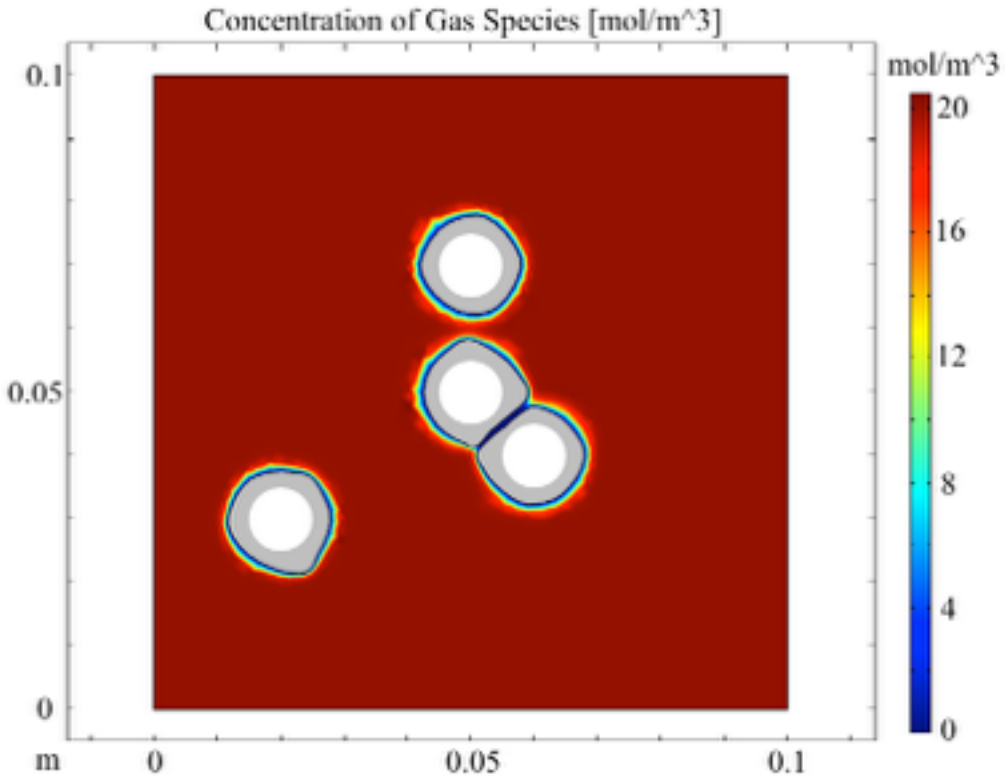

Figure 14, Moving mesh model: Surface growth model after time lapse. White is original geometry, grey deposited material, color scale remaining species concentration [mol/m^3].

V. Conclusions and Recommendations

Conclusions of Research

This research project investigated the creation of a series of models that would build towards a unified chemical and geometric model of a SiC CVD process. This was done to gain a better understanding of how the CVD process works and how the given parameters affect the final product. This was also done in an effort to find a modeling software package that can handle rigors of modeling the complex process that results in such desirable materials.

The first model, that of a steam and propane reactor tube, showed how well COMSOL software is at pulling out material information from the model at all times and positions. Velocity, pressure, mass fraction, and temperature were all very easy to attain. The second model helped to showed some of the effects of changes in pressure and geometry. The third model was unfortunately not completed due to time constraints. It was, however, able to at least verify that propane, as the carbon source and limiting factor in deposition rate, is consumed very quickly [33]. The final model showed the feasibility of using a finite element method for modeling deposition growth without the expense that comes from random walk algorithms.

Significance of Research

This thesis was a preliminary study into using COMSOL as a method for modelingSiC CVD production. It showed that the software is capable, even if occasionally problematic (like with the Shomate equation parameters). The various

parameters that are given as input into the model have different levels of effect on the resulting simulations. Fluid pressure is a major component of determining how uniform the flow is. Lower pressure results in more uniform (laminar) flow. Even with laminar flow, vortices of low pressure can form. This leads to uneven reaction rates and species concentrations across the substrate surfaces. This can strongly affect the uniformity of the deposition of SiC on the substrate. Temperature has a large effect on deposition rates, but as the chemical reaction model was unable to be finished, it was unable to be verified numerically. Changes in initial geometry did not have much effect on flow characteristics.

Recommendations for Future Research

A completely integrated model is within reach, it was only time constraints that prevent its inclusion in this thesis. Once a complete model for SiC/substrate production via CVD is complete, it would be advantageous to compare the model to actual experiment to see how well it correlates with reality and what changes might need to be made. Additionally, more complex (and therefor realistic) geometries should be used. (An example three-dimensional geometry is included in Appendix C.)

It is possible for users to build their own modules for use in COMSOL. If the time and expertise can be applied to the work, a specialized module for modeling the CVD process could be created. Furthermore, it would be entirely feasible to generate similar modules for other forms of CMC production, such as polymer liquid infiltration.

.

Appendix A: Chemical Species Data

This section lists the data of individual species as taken from the NIST Chemistry WebBook. Species name, formula, and molecular mass is given on the first line for each species. The ranges of temperatures (in Kelvin) over which the Shomate parameters (A-H) are valid are given in the second line. Shomate parameter units are as follows: A [J/mol K], B [J/mol K^2], C [J/mol K^3], D [J/mol K^4], E [J K/mol], F [J/mol], G [J/mol K], H [J/mol]. [30]

Table 3, Properties of individual chemical species. Includes name, formula, molecular mass, and Shomate parameters with the temperatures over which they are valid.

Silane	SiH	32.1173	
	298. - 1300. K	1300. - 6000. K	
A [J/mol K]	6.060189	99.84949	
B [J/mol K	139.9632	4.251530	
C [J/mol K	-77.88474	-0.809269	
D [J/mol K	16.24095	0.053437	
E [J K/mol]	0.135509	-20.39005	
F [J/mol]	27.39081	-40.54016	
G [J/mol K]	174.3351	266.8015	
H [J/mol]	34.30905	34.30905	
Silylene	:SiH2	30.1014	
A [J/mol K]			
B [J/mol K			
C [J/mol K			
D [J/mol K			
E [J K/mol]			

F [J/mol]			
G [J/mol K]			
H [J/mol]			
Hydrogen	H	2.01588	
Gas	298. - 1000 K.	1000. - 2500. K	2500. - 6000. K
A [J/mol K]	33.066178	18.563083	43.413560
B [J/mol K	-11.363417	12.257357	-4.293079
C [J/mol K	11.432816	-2.859786	1.272428
D [J/mol K	-2.772874	0.268238	-0.096876
E [J K/mol]	-0.158558	1.977990	-20.533862
F [J/mol]	-9.980797	-1.147438	-38.515158
G [J/mol K]	172.707974	156.288133	162.081354
H [J/mol]	0.0	0.0	0.0
Disilane	Si	62.2186	
A [J/mol K]			
B [J/mol K			
C [J/mol K			
D [J/mol K			
E [J K/mol]			
F [J/mol]			
G [J/mol K]			
H [J/mol]			
Silicon	Si	28.0855	
	298. - 1685 K.	1685. - 3505. K	3505. - 6000. K
A [J/mol K]	22.81719	27.19604	14.59321
B [J/mol K	3.899510	-1.198306×10	5.224644
C [J/mol K	-0.082885	5.353262×10	-1.078879
D [J/mol K	0.042111	-6.956612×10	0.074000
E [J K/mol]	-0.354063	-4.294375×10	2.309405

F [J/mol]	-8.163946	40.36163	450.3365
G [J/mol K]	43.27846	77.37178	190.2494
H [J/mol]	0.000000	48.46997	450.0018
Hydrogen	*H	1.00794	
Elemental	298. - 6000. K		
A [J/mol K]	20.78603		
B [J/mol K	4.850638×10		
C [J/mol K	-1.582916×10		
D [J/mol K	1.525102×10		
E [J K/mol]	3.196347×10		
F [J/mol]	211.8020		
G [J/mol K]	139.8711		
H [J/mol]	217.9994		
Propane	C	44.0956	
A [J/mol K]			
B [J/mol K			
C [J/mol K			
D [J/mol K			
E [J K/mol]			
F [J/mol]			
G [J/mol K]			
H [J/mol]			
Methyl Radical	*CH	15.0345	
	298. - 1400. K	1400. - 6000. K	
A [J/mol K]	28.13786	67.18081	
B [J/mol K	36.74736	7.846423	
C [J/mol K	-4.347218	-1.440899	
D [J/mol K	-1.595673	0.092685	
E [J K/mol]	0.001860	-17.66133	

F [J/mol]	135.7118	92.47100	
G [J/mol K]	217.4814	235.9023	
H [J/mol]	145.6873	145.6873	
Ethyl Radical	*C	29.0611	
A [J/mol K]			
B [J/mol K			
C [J/mol K			
D [J/mol K			
E [J K/mol]			
F [J/mol]			
G [J/mol K]			
H [J/mol]			
Methane	CH	16.0425	
A [J/mol K]			
B [J/mol K			
C [J/mol K			
D [J/mol K			
E [J K/mol]			
F [J/mol]			
G [J/mol K]			
H [J/mol]			
Ethane	C	30.069	
A [J/mol K]			
B [J/mol K			
C [J/mol K			
D [J/mol K			
E [J K/mol]			

F [J/mol]			
G [J/mol K]			
H [J/mol]			
Ethylene	C	28.0532	
	298. - 1200. K	1200. - 6000. K	
A [J/mol K]	-6.387880	106.5104	
B [J/mol K	184.4019	13.73260	
C [J/mol K	-112.9718	-2.628481	
D [J/mol K	28.49593	0.174595	
E [J K/mol]	0.315540	-26.14469	
F [J/mol]	48.17332	-35.36237	
G [J/mol K]	163.1568	275.0424	
H [J/mol]	52.46694	52.46694	
Acetylene	C	26.0373	
A [J/mol K]			
B [J/mol K			
C [J/mol K			
D [J/mol K			
E [J K/mol]			
F [J/mol]			
G [J/mol K]			
H [J/mol]			
Silicon dimer	*Si	56.171	
	298. - 1100. K	1100. - 6000. K	
A [J/mol K]	24.19988	47.92605	
B [J/mol K	31.58280	-4.345921	
C [J/mol K	-8.262313	1.037265	
D [J/mol K	-3.875582	-0.072474	
E [J K/mol]	0.150614	-0.208383	

F [J/mol]	581.9149	571.7143	
G [J/mol K]	250.9182	280.7259	
H [J/mol]	589.9440	589.9440	
Disilicon Carbide	Si	68.1817	
	298. - 1200. K	1200. - 6000. K	
A [J/mol K]	38.96220	62.75874	
B [J/mol K	41.84126	-7.005439	
C [J/mol K	-29.86230	4.097706	
D [J/mol K	7.853285	-0.425546	
E [J K/mol]	-0.139347	0.696590	
F [J/mol]	521.8578	513.9207	
G [J/mol K]	277.4360	312.3410	
H [J/mol]	535.5520	535.5520	
	SiCH	42.1121	
A [J/mol K]			
B [J/mol K			
C [J/mol K			
D [J/mol K			
E [J K/mol]			
F [J/mol]			
G [J/mol K]			
H [J/mol]			
Methylene	:CH	14.0266	
	298. - 1400. K	1400. - 6000. K	
A [J/mol K]	31.96823	51.55901	
B [J/mol K	6.783603	3.876975	
C [J/mol K	12.51890	-0.649608	
D [J/mol K	-5.696265	0.037901	
E [J K/mol]	-0.031115	-10.72589	

F [J/mol]	376.3558	350.6715	
G [J/mol K]	229.9150	232.3212	
H [J/mol]	386.3924	386.3924	
Carbon	C	12.0107	
Elemental	298. - 6000. K		
A [J/mol K]	21.17510		
B [J/mol K	-0.812428		
C [J/mol K	0.448537		
D [J/mol K	-0.043256		
E [J K/mol]	-0.013103		
F [J/mol]	710.3470		
G [J/mol K]	183.8734		
H [J/mol]	716.6690		
Silicon Carbide	SiC	40.0962	
Gas Phase	298. - 1000. K	1000. - 6000. K	
A [J/mol K]	60.32180	33.36570	
B [J/mol K	4.423940	4.437140	
C [J/mol K	-61.79470	-0.865113	
D [J/mol K	39.06140	0.057726	
E [J K/mol]	-1.675991	3.073291	
F [J/mol]	696.3070	717.4580	
G [J/mol K]	277.6700	262.5750	
H [J/mol]	719.6480	719.6480	
Silicon Carbide alpha	298. - 1000. K	1000. - 4000. K	
A [J/mol K]	20.55859	46.90222	
B [J/mol K	64.57962	5.845968	
C [J/mol K	-52.98827	-1.085410	
D [J/mol K	16.95813	0.093021	
E [J K/mol]	-0.781847	-3.448876	
F [J/mol]	-82.73693	-95.46716	

G [J/mol K]	19.90848	56.97520	
H [J/mol]	-71.54598	-71.54598	
Silicon Carbide beta	298. - 1100.	1100. - 4000.	
A [J/mol K]	20.50009	48.22227	
B [J/mol K	63.37170	5.004148	
C [J/mol K	-49.54023	-1.037594	
D [J/mol K	14.82801	0.086339	
E [J K/mol]	-0.759969	-3.912333	
F [J/mol]	-84.29337	-98.46542	
G [J/mol K]	20.30926	57.76221	
H [J/mol]	-73.22000	-73.22000	

Appendix B: Chemical Reaction Data

The following tables list the coefficients for the Arrhenius equations (Equation #) for each homogenous reaction supplied by Blanquet, *et al*. (Table 1) The coefficients were taken from the NIST Chemistry WebBook. The units for the reaction rate coefficient k change with the order of the reaction, thus the units for the Arrhenius pre-factor (A) change as well. A is in units of [s^{-1}] for reactions of order 1, [cm^3 mol^{-1} s^{-1}] for reactions of order 2, and [cm^6 mol^{-2} s^{-1}] for reactions of order 3. For those reactions where NIST was not able to supply data, the forward reaction cofactors were used from Blanquet, *et al*. The reverse reaction cofactors were calculated based upon the thermochemistry of the individual species. [2, 30]

Table 4, Homogeneous reaction forward reaction rate equation parameters. Reaction numbers correspond to those in Table 1. Values retrieved from NIST Chemical Kinetics Database. Units of A are [s^{-1}] for reactions of order 1, [cm^3 mol^{-1} s^{-1}] for reactions of order 2, and [cm^6 mol^{-2} s^{-1}] for reactions of order 3. The reference temperature is 298 K.

Forward Reaction	Reaction Order	A	n	Ea [J]
1	1	4.92E+28	-15.9	3.42E+04
	2	1.67E-06	18.2	-6.26E+04
2	1	8.96E+22	-9.7	2.62E+05
3	1	9.73E+08	0.0	2.61E+05
	2	3.90E+28	-12.5	2.87E+05
4				
5	1	5.42E+18	-2.3	3.71E+05

	2	2.26E+30	-11.2	3.66E+05
6	2	6.56E+11	2.7	3.73E+04
7	2	2.82E+13	0.1	-3.27E+02
8	2	3.27E+13	-0.5	-1.67E+02
	3	1.40E+24	-7.1	1.32E+04
9	2	2.43E+13	0.1	9.03E+03
	3	5.64E+18	-0.2	4.65E+03
10	1	7.50E+06	5.0	2.41E+05
	2	3.61E+24	-6.2	4.08E+05
11				
12				
13				
14				
15				
16				
17				

Table 5, Homogeneous reaction reverse reaction rate equation parameters. Reaction numbers correspond to those in Table 1. Values retrieved from NIST Chemical Kinetics Database. Units of A are [s^{-1}] for reactions of order 1, [cm^3 mol^{-1} s^{-1}] for reactions of order 2, and [cm^6 mol^{-2} s^{-1}] for reactions of order 3. The reference temperature is 298 K.

Reverse Reaction	Reaction Order	A	n	Ea [J]
1	2	2.17E+08	3.1	-1.06E+04
2	2	3.13E+14	-1.1	3.45E+02
3				
4				

5	2	1.72E+13	-0.2	-9.81E+02
	3	4.25E+27	-16.1	1.58E+04
6	2	2.46E+11	1.6	4.22E+04
7	2	4.03E+12	0.6	4.26E+04
8	1	6.92E+18	-2.7	3.86E+05
	2	4.28E+17	1.5	3.78E+05
9	1	5.85E+12	0.6	1.60E+05
	2	7.06E+18	-0.8	1.54E+05
10	2	3.01E+11	0.0	1.63E+05
11				
12				
13	3	5.94E+14	0.0	1.97E+03
14				
15				
16				
17				

Appendix C: 3-D Fabric Preform Model

After completing the two dimensional model, it would be considered ideal to extend into three dimensions. This would result in a more realistic geometry, and thus a more realistic model. The geometry of this models was chosen to be layers of simple square-woven fabric.

Modeling the fabric started with a single fiber. It was modeled as the sweep of a circular face along a sinusoidal backbone. The fiber was then replicated thrice. Each replica was then translated, flipped, and/or rotated until there were four fiber, two in the warp and two in the weft, in the beginning of a square-weave. The warp and weft fibers were then replicated horizontally until the desired size of the fabric was reached. Then, the resulting single layer of fabric was then replicated vertically to create the complete preform as shown in Figure 15. A COMSOL model report follows.

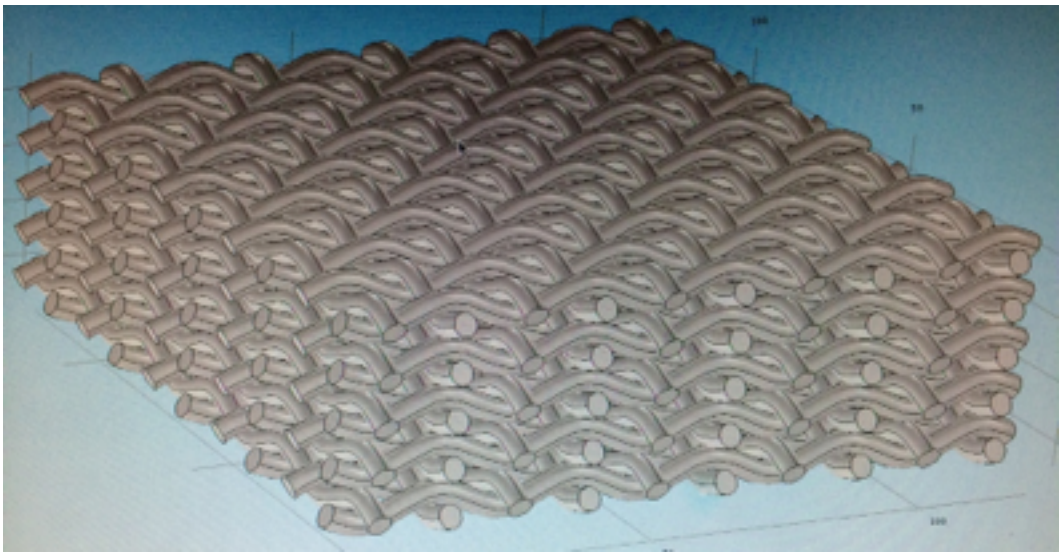

Figure 15, 3-D fabric preform model.

1. Global Definitions

1.1. Parameters 1

Parameters

Name	Expression	Description
R_fib	2	Radius of fiber
nx_fib	10	number of fibers in x direction
n_layer	5	number of layers
ny_fib	12	number of fibers in y direction

2. Model 1 (mod1)

2.1. Definitions

2.1.1. Selections

Fibers

Selection type
Explicit

Selection
Domains 2–111

Fiber Boundaries

Selection type
Explicit

Selection
Boundaries 6–665

2.1.2. Coordinate Systems

Boundary System 1

Coordinate system type	Boundary system
Identifier	sys1

Settings

Name	Value
Coordinate names	{t1, t2, n}
Create first tangent direction from	Global Cartesian

2.2. Geometry 1

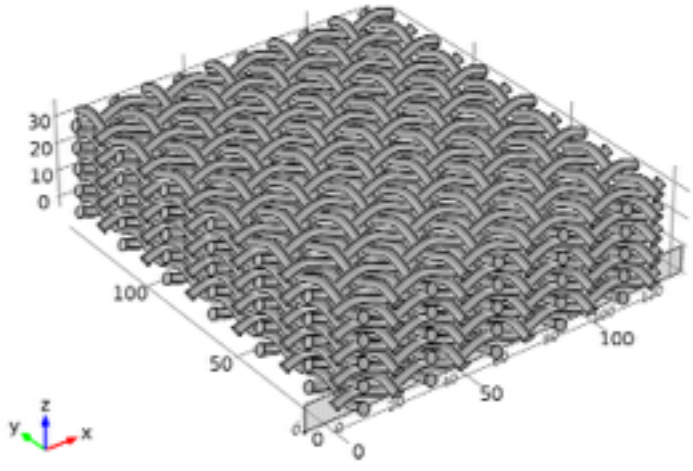

Geometry 1

Units

Length unit	m
Angular unit	deg

Geometry statistics

Property	Value
Space dimension	3
Number of domains	111
Number of boundaries	666
Number of edges	1472
Number of vertices	958

2.2.1. Warp Spine (wp1)

Plane Geometry (wp1)

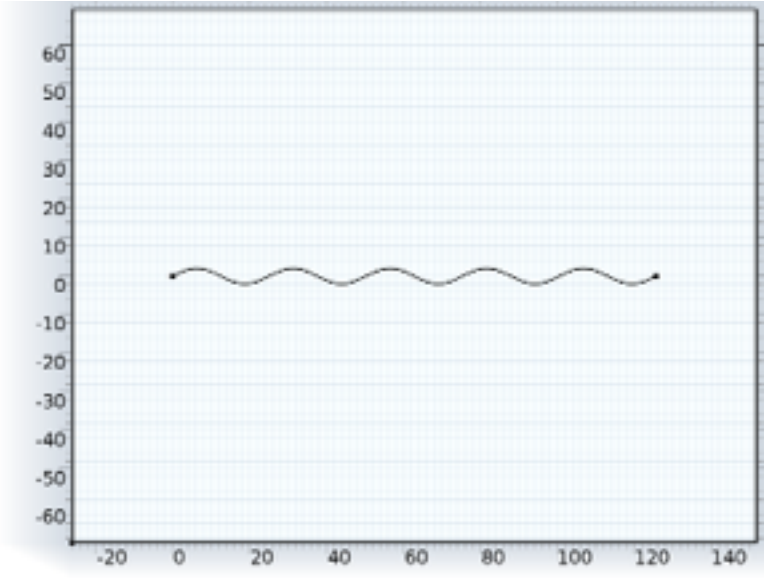

Plane Geometry

Units

Length unit	m
Angular unit	deg

Geometry statistics

Property	Value
Space dimension	2
Number of domains	0
Number of boundaries	0

Center Line (pc1)

Position

Name	Value
Position	{0, 0}

Rotation angle

Name	Value
Maximum	nx_fib*R_fib*2*pi
Expressions	{s, R_fib*sin(s/(2*R_fib))}

2.2.2. Warp Face (wp2)

Selections of resulting entities

Name	Value
Plane type	General
Points	{{0, 0, 0}, {0, 1, 0}, {-0.5, 0, 1}}
Draw on work plane in 3D	On

Plane Geometry (wp2)

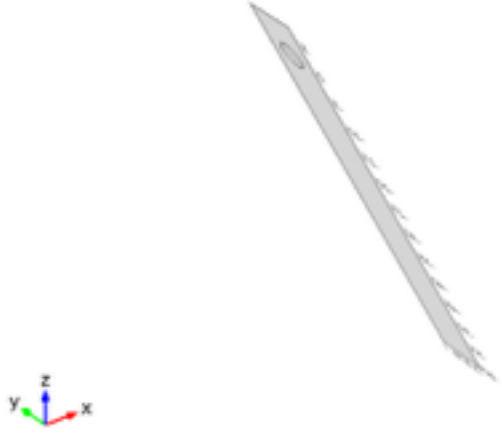

Plane Geometry

Units

Length unit	m
Angular unit	deg

Geometry statistics

Property	Value
Space dimension	2
Number of domains	0
Number of boundaries	0

Circle 1 (c1)

Position

Name	Value
Position	{0, 0}
Radius	R_fib

2.2.3. Weft Spine (wp3)

Selections of resulting entities

Name	Value
Draw on work plane in 3D	On

Plane Geometry (wp3)

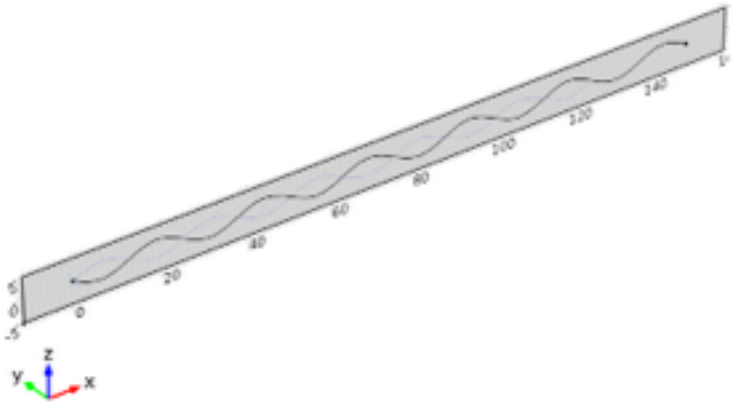

Plane Geometry

Units

Length unit	m
Angular unit	deg

Geometry statistics

Property	Value
Space dimension	2
Number of domains	0
Number of boundaries	0

Center Line (pc1)

Position

Name	Value
Position	{0, 0}

Rotation angle

Name	Value
Maximum	ny_fib*R_fib*2*pi
Expressions	{s, -R_fib*sin(s/(2*R_fib))}

2.2.4. Weft Face (wp4)

Selections of resulting entities

Name	Value
Plane type	General
Points	{{0, 0, 0}, {0, 1, 0}, {0.5, 0, 1}}
Draw on work plane in 3D	On

Plane Geometry (wp4)

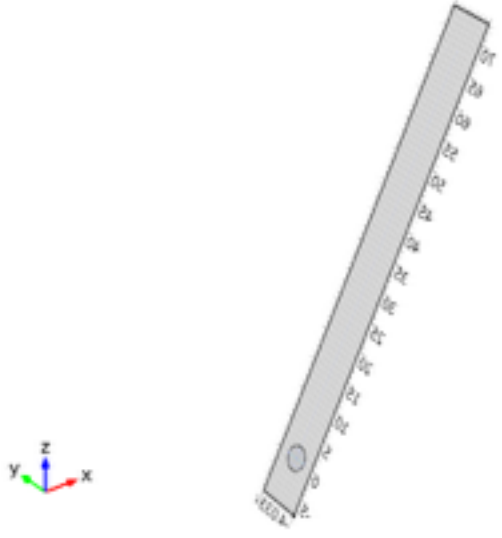

Plane Geometry

Units

Length unit	m

Angular unit	deg

Geometry statistics

Property	Value
Space dimension	2
Number of domains	0
Number of boundaries	0

Circle 1 (c1)

Position

Name	Value
Position	{0, 0}
Radius	R_fib

2.2.5. Warp Fiber 1 (swe1)

Selections of resulting entities

Name	Value
Keep input objects	Off
Include all inputs in finalize operation	Off

2.2.6. Weft Fiber 1 (swe2)

Selections of resulting entities

Name	Value
Keep input objects	Off
Include all inputs in finalize operation	Off
Face-spine alignment	Adjust spine

2.2.7. Rotate Weft Fiber 1 (rot2)

Selections of resulting entities

Name	Value
Rotation	90
Point on axis of rotation	{2*R_fib*pi/2, 0, 0}
Axis type	z - axis

2.2.8. Warp Fiber 2 (copy1)

Selections of resulting entities

Name	Value
Keep input objects	On
x	0
y	12.566370614359172
z	0

2.2.9. Flip Warp Fiber 2 (rot1)

Selections of resulting entities

Name	Value
Rotation	180
Point on axis of rotation	{0, 2*R_fib*pi, 0}
Axis type	x - axis

2.2.10. Weft Fiber 2 (copy3)

Selections of resulting entities

Name	Value
Keep input objects	On
x	12.566370614359172
y	0
z	0

2.2.11. Flip Weft Fiber 1 (rot3)

Selections of resulting entities

Name	Value
Rotation	180
Point on axis of rotation	{3*R_fib*pi, 0, 0}
Axis type	y - axis

2.2.12. Warp (arr1)

Selections of resulting entities

Name	Value
Array type	Linear
Size	ny_fib/2
Displacement	{0, 4*R_fib*pi, 0}

2.2.13. Weft (arr2)

Selections of resulting entities

Name	Value
Array type	Linear
Size	nx_fib/2
Displacement	{4*R_fib*pi, 0, 0}

2.2.14. Fabric Layers (arr3)

Selections of resulting entities

Name	Value
Array type	Linear
Size	n_layer
Displacement	{0, 0, 4*R_fib}

2.2.15. Polymer Matrix (blk1)

Position

Name	Value
Position	{0 - (2*R_fib), -(R_fib*pi) - (2*R_fib), -(2*R_fib) - (2*R_fib)}

Size and shape

Name	Value
Size	{2*pi*nx_fib*R_fib + (4*R_fib), 2*pi*ny_fib*R_fib + (4*R_fib), 4*R_fib*n_layer + (4*R_fib)}

Appendix D: COMSOL Model Reports

There are four COMSOL-generated model reports given. One for the Steam/ Propane Reactor Tube model and one each for the three parts of the SiC CVD model: Flow Model, Chemical Reaction Model, and Moving Mesh Model.

1. Global Definitions

1.1. Parameters 1

Parameters

Name	Expression	Description
R_fib	.002	fiber radius [m]
N_fib	10	number of fibers per layer
L_fib	4	number of layers
u_in	.05[m/s]	inflow velocity [m/s]
p_in	75[Pa]	Pressure difference
p_ref	1e5[Pa]	Reference pressure
T_in	700[K]	Inlet temperature
ht	100[W/m^2/K]	Heat transfer coefficient
D_H2_C3H8	2.7e-5[m^2/s]	Binary diffusion coefficient
D_CO2_C3H8	5.1e-6[m^2/s]	Binary diffusion coefficient
D_C3H8_H2O	8.4e-6[m^2/s]	Binary diffusion coefficient
D_CO2_H2	3.6e-5[m^2/s]	Binary diffusion coefficient
D_H2_H2O	4.9e-5[m^2/s]	Binary diffusion coefficient
D_CO2_H2O	1.1e-5[m^2/s]	Binary diffusion coefficient
M_C3H8	44.1e-3[kg/mol]	Molar mass
M_H2	2.016e-3[kg/mol]	Molar mass
M_CO2	44.01e-3[kg/mol]	Molar mass
M_H2O	18.016e-3[kg/mol]	Molar mass
w_C3H8_in	0.28[1]	Initial weight fraction
w_H2_in	0.01[1]	Initial weight fraction
w_CO2_in	0.01[1]	Initial weight fraction
H_sr	410e3[J/mol]	Enthalpy of reaction
Cp	2800[J/kg/K]	Heat capacity, fluid

2. Model 1 (mod1)

2.1. Definitions

2.1.1. Variables

Variables

Selection

Geometric entity level	Entire model

Name	Expression	Description
T_out	aveop1(T2)	Average outlet temperature
rate	chcs.x_w_C3H8*p/T2/R_const*7e5[1/s]*exp(-83.14e3[J/mol]/R_const/T2)	Reaction rate
dens_sr	p/T2/R_const*(chcs.x_w_C3H8*M_C3H8 + chcs.x_w_H2*M_H2 + chcs.x_w_CO2*M_CO2 + chcs.x_w_H2O*M_H2O)	Density, fluid

2.1.2. Model Couplings

Average 1

Coupling type	Average
Operator name	aveop1

Source selection

Geometric entity level	Boundary
Selection	Boundary 4

2.1.3. Coordinate Systems

Boundary System 1

Coordinate system type	Boundary system
Identifier	sys1

Settings

Name	Value
Coordinate names	{t1, n, to}
Create first tangent direction from	Global Cartesian

2.2. Geometry 1

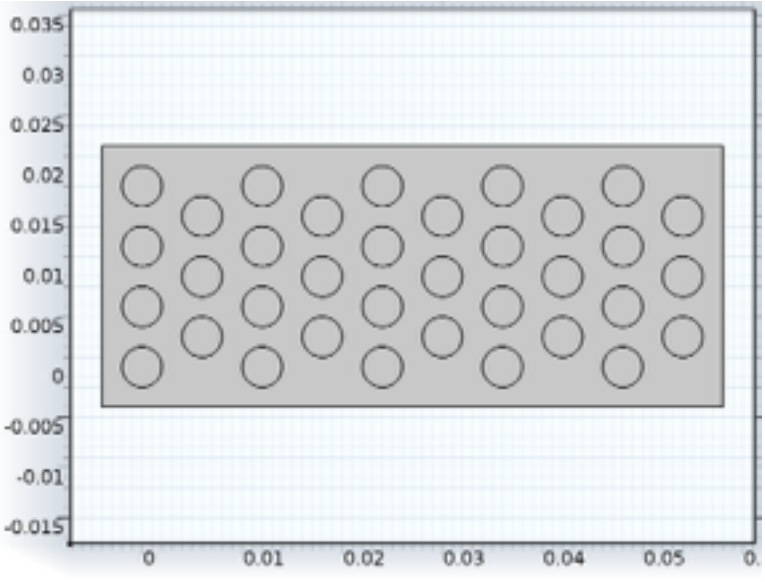

Geometry 1

Units

Length unit	m
Angular unit	deg

Geometry statistics

Property	Value
Space dimension	2
Number of domains	36
Number of boundaries	144

2.2.1. Circle 1 (c1)

Position

Name	Value
Position	{0, 0}
Radius	R_fib

2.2.2. Array 1 (arr1)

Selections of resulting entities

Name	Value
Create selections	On
Size	{N_fib/2, L_fib}
Displacement	{6*R_fib, 3*R_fib}

2.2.3. Copy 1 (copy1)

Selections of resulting entities

Name	Value
Keep input objects	On
x	0.0060
y	0.0030

2.2.4. Array 2 (arr2)

Selections of resulting entities

Name	Value
Size	{N_fib/2, L_fib - 1}
Displacement	{6*R_fib, 3*R_fib}

2.2.5. Rectangle 1 (r1)

Position

Name	Value
Position	{-2*R_fib, -2*R_fib}
Width	N_fib*3*R_fib + R_fib
Height	3*R_fib*L_fib + R_fib
Size	{N_fib*3*R_fib + R_fib, 3*R_fib*L_fib + R_fib}

2.3. Materials

2.3.1. Pyrolytic graphite [solid,as deposited]

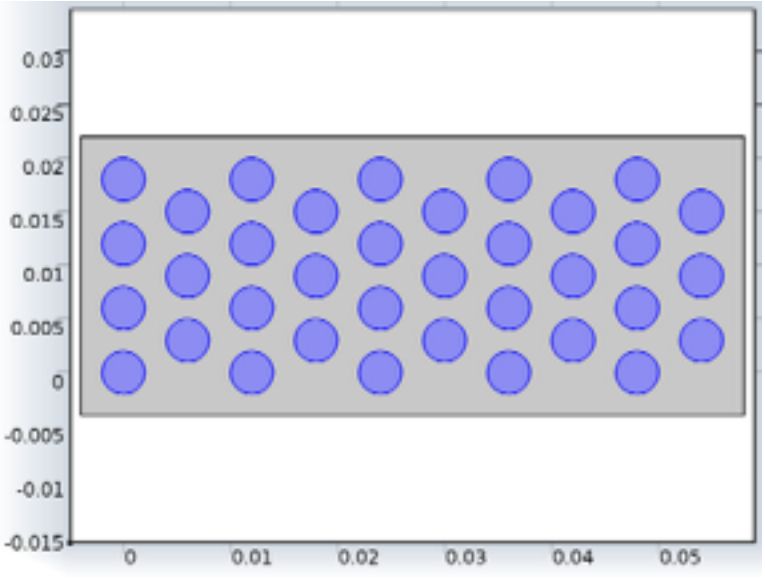

Pyrolytic graphite [solid,as deposited]

Selection

Geometric entity level	Domain
Selection	Domains 2–36

2.4. Laminar Flow (spf)

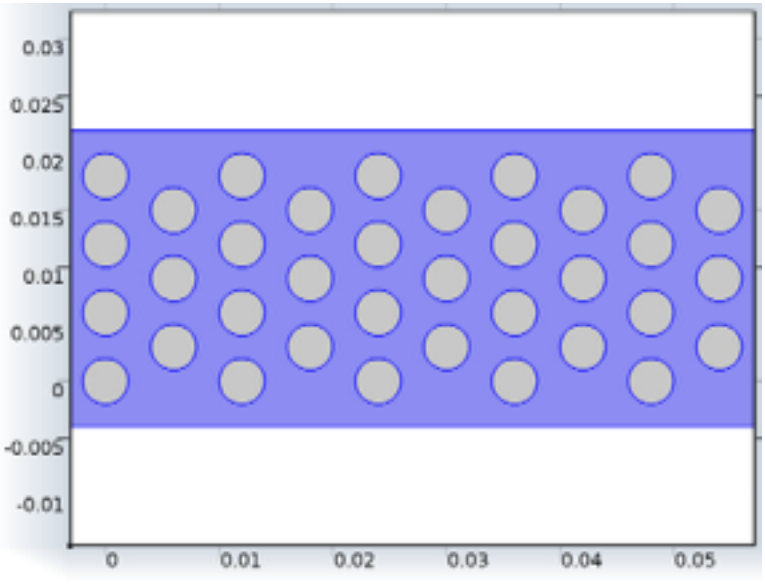

Laminar Flow

Selection

Geometric entity level	Domain
Selection	Domain 1

Settings

Description	Value
Discretization of fluids	P1 + P1
Value type when using splitting of complex variables	{Real, Real, Real, Real, Real, Real, Real, Real, Real}
Equation form	Study controlled
Compressibility	Compressible flow (Ma<0.3)
Neglect inertial term (Stokes flow)	Off
Use shallow channel approximation	Off
Allow out of plane properties	1

Description	Value
Allow radiation properties	1
Allow stokes properties	1
Allow turbulence properties	1
Allow MaxwellStefan diffusion	1
Use pseudo time stepping for stationary equation form	0
Local CFL number	1.3^min(niterCMP, 9) + if(niterCMP>=25, 9*1.3^min(niterCMP - 25, 9), 0) + if(niterCMP>=45, 90*1.3^min(niterCMP - 45, 9), 0)
Streamline diffusion	1
Crosswind diffusion	1
Isotropic diffusion	0
Turbulence model type	None
Smoothing parameter	0.1
Show equation assuming	std1/stat

2.4.1. Fluid Properties 1

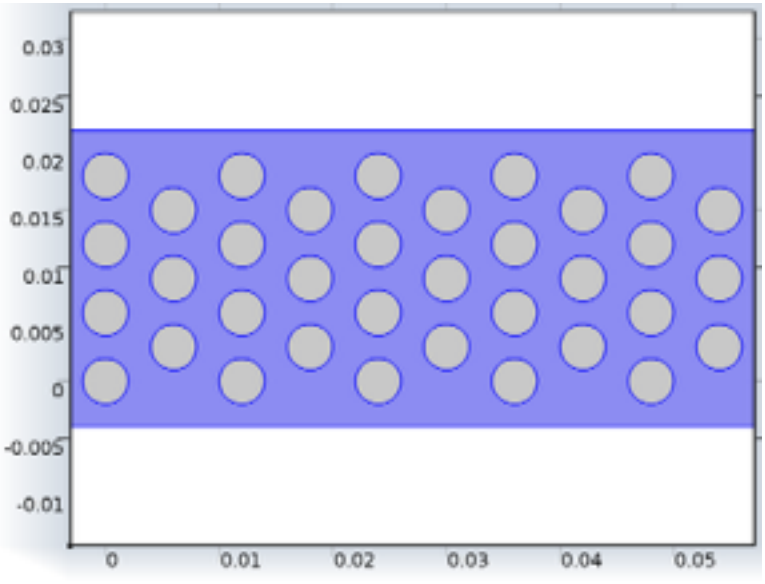

Fluid Properties 1

Selection

Geometric entity level	Domain
Selection	Domain 1

Settings

Description	Value
Density	User defined
Density	1
Dynamic viscosity	User defined
Dynamic viscosity	1
Reference length	1
Reference length scale	Automatic
Mixing length limit	Automatic

2.4.2. Wall 1

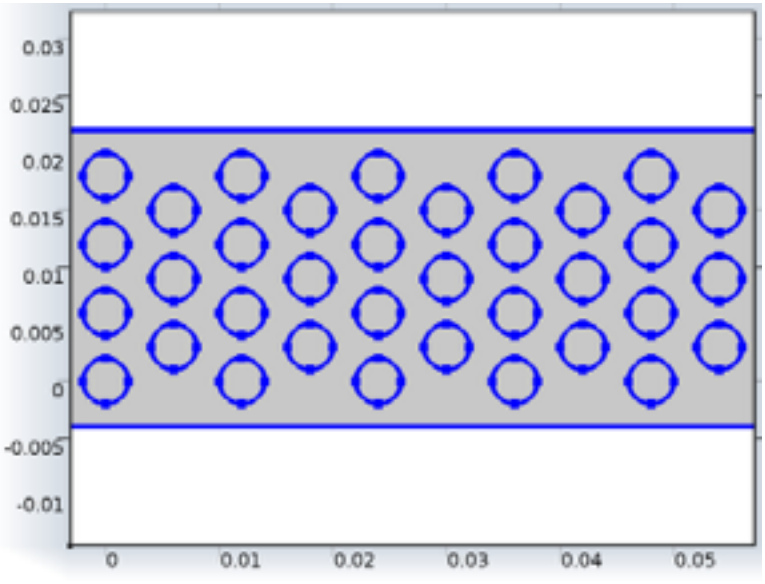

Wall 1

Selection

Geometric entity level	Boundary
Selection	Boundaries 2–3, 5–144

Settings

Description	Value
Temperature	User defined
Temperature	293.15[K]
Electric field	User defined
Electric field	{0, 0, 0}
Boundary condition	No slip
Apply reaction terms on	Individual dependent variables
Use weak constraints	0

2.4.3. Initial Values 1

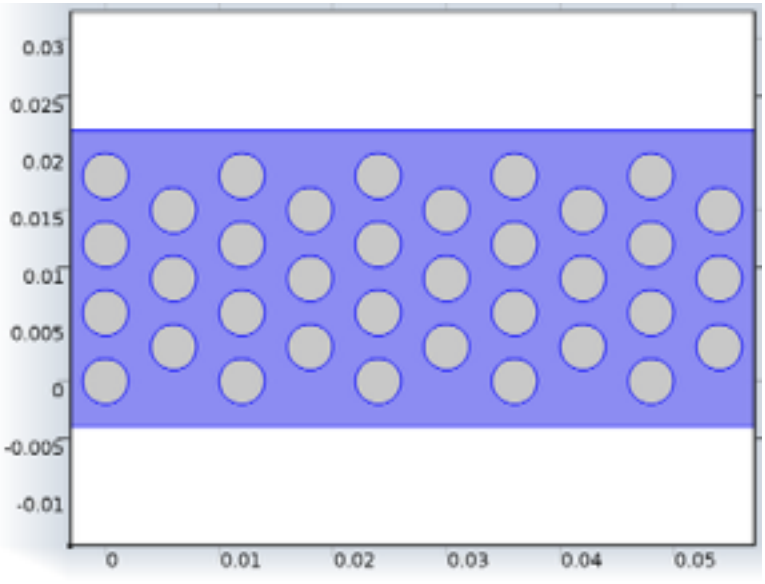

Initial Values 1

Selection

Geometric entity level	Domain
Selection	Domain 1

Settings

Description	Value
Velocity field	{0, 0, 0}
Pressure	p_ref

2.4.4. Inlet 1

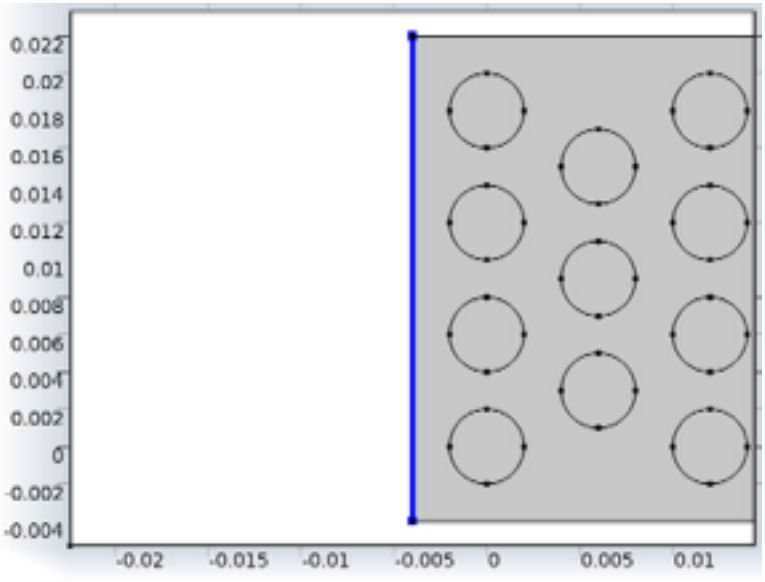

Inlet 1

Selection

Geometric entity level	Boundary
Selection	Boundary 1

Settings

Description	Value
Apply reaction terms on	All physics (symmetric)
Use weak constraints	0
Boundary condition	Pressure, no viscous stress
Pressure	p_in + p_ref
Standard pressure	1[atm]
Standard molar volume	0.0224136[m^3/mol]
Normal mass flow rate	1e-5[kg/s]

Description	Value
Mass flow type	Mass flow rate
Standard flow rate defined by	Standard density
Channel thickness	1.0[m]

2.4.5. Outlet 1

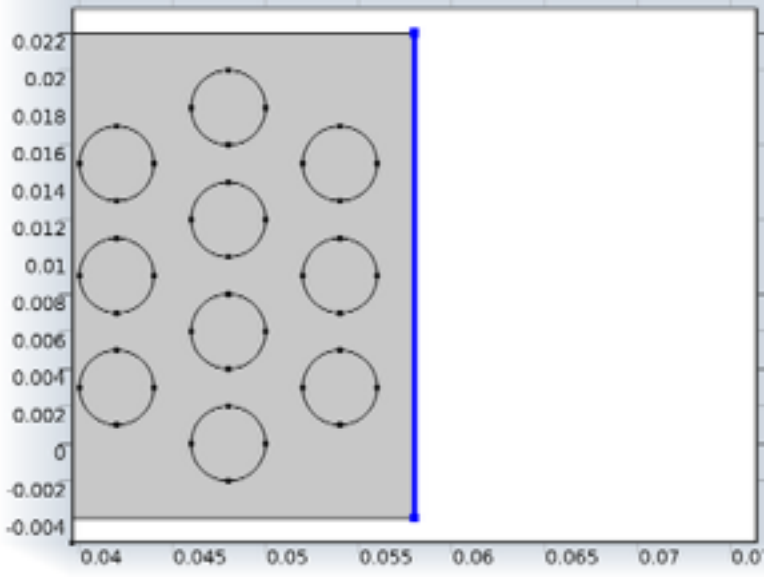

Outlet 1

Selection

Geometric entity level	Boundary
Selection	Boundary 4

Settings

Description	Value
Apply reaction terms on	All physics (symmetric)
Use weak constraints	0
Boundary condition	Pressure, no viscous stress
Pressure	p_ref

2.5. Heat Transfer in Fluids 2 (ht2)

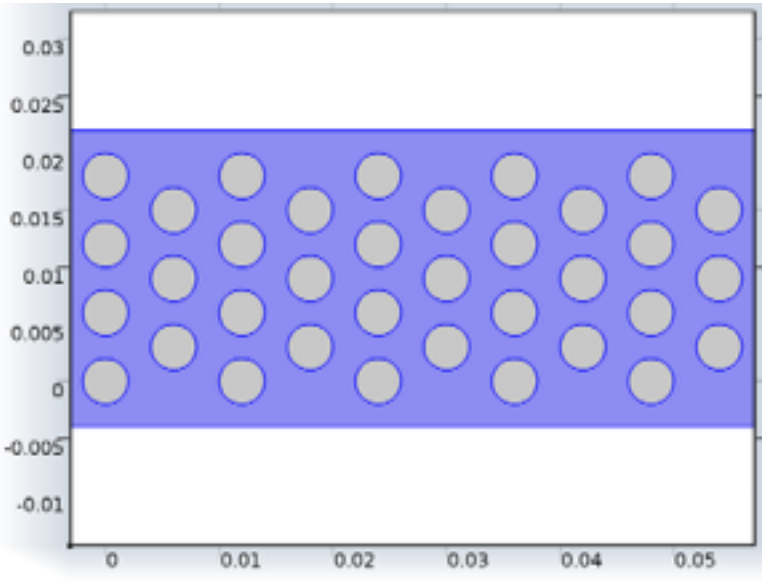

Heat Transfer in Fluids 2

Selection

Geometric entity level	Domain
Selection	Domain 1

Settings

Description	Value
Temperature	Linear
Compute boundary fluxes	1
Apply smoothing to boundary fluxes	1
Value type when using splitting of complex variables	Real
Equation form	Study controlled
Out-of-plane heat transfer	0
Surface-to-surface radiation	0
Radiation in participating media	0

Description	Value
Heat transfer in biological tissue	0
Heat transfer in porous media	0
Moving frame	Moving frame flag (false)
Streamline diffusion	1
Crosswind diffusion	1
Isotropic diffusion	0
Show equation assuming	std1/stat

2.5.1. Heat Transfer in Fluids 1

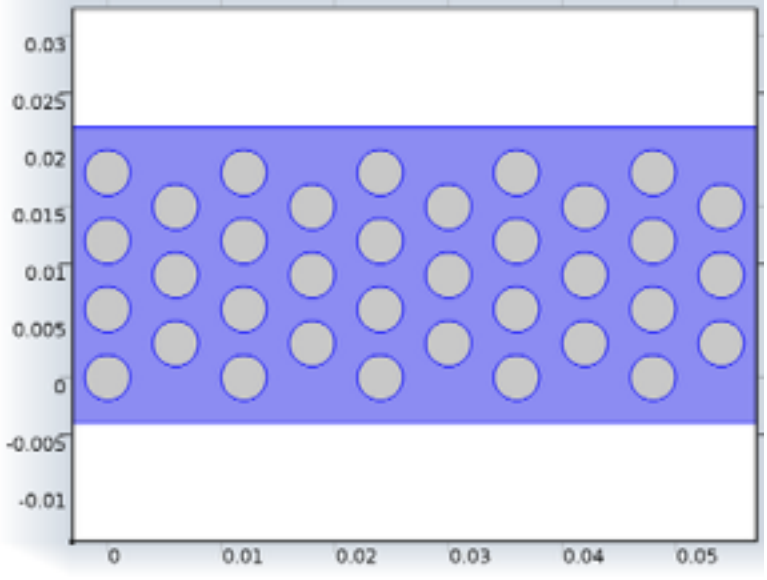

Heat Transfer in Fluids 1

Selection

Geometric entity level	Domain
Selection	Domain 1

Settings

Description	Value
Fluid type	Gas/Liquid
Thermal conductivity	User defined
Thermal conductivity	{{k_sr, 0, 0}, {0, k_sr, 0}, {0, 0, k_sr}}
Density	User defined
Density	1
Heat capacity at constant pressure	User defined
Heat capacity at constant pressure	Cp
Ratio of specific heats	User defined
Ratio of specific heats	1.5

2.5.2. Thermal Insulation 1

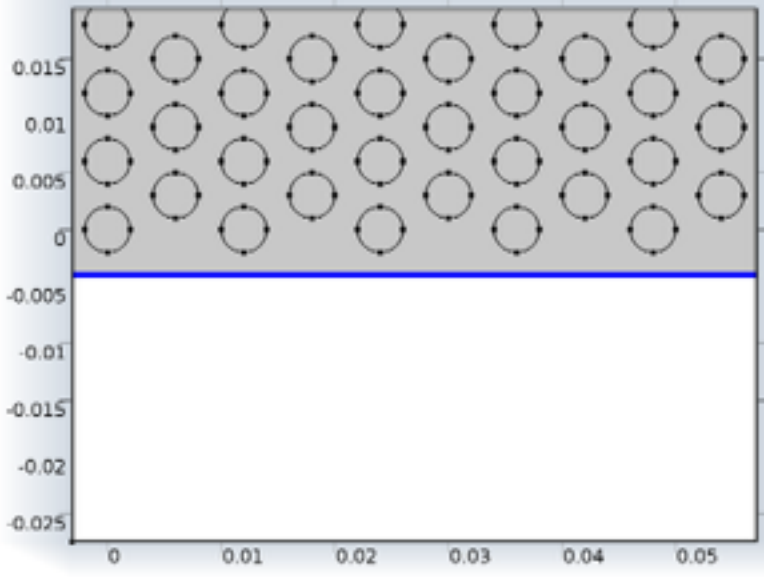

Thermal Insulation 1

Selection

Geometric entity level	Boundary

Selection	Boundary 2

2.5.3. Initial Values 1

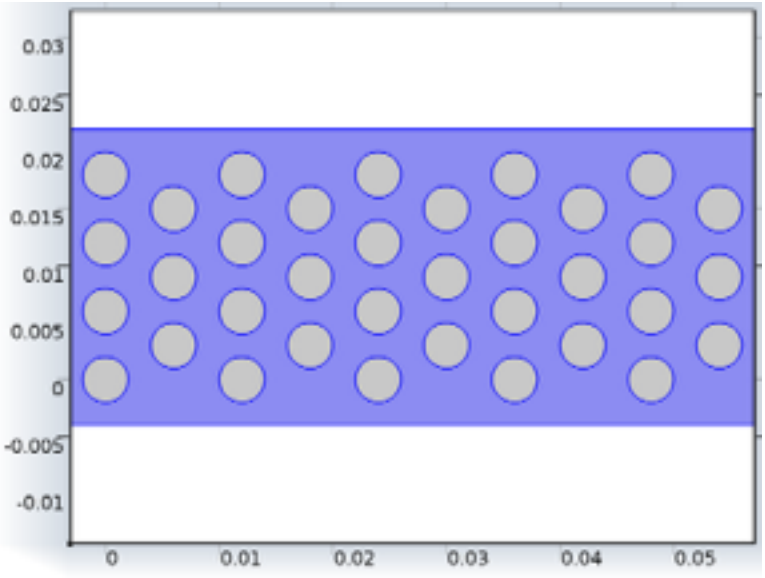

Initial Values 1

Selection

Geometric entity level	Domain
Selection	Domain 1

Settings

Description	Value
Temperature	293.15[K]

2.5.4. Surface-to-Ambient Radiation 1

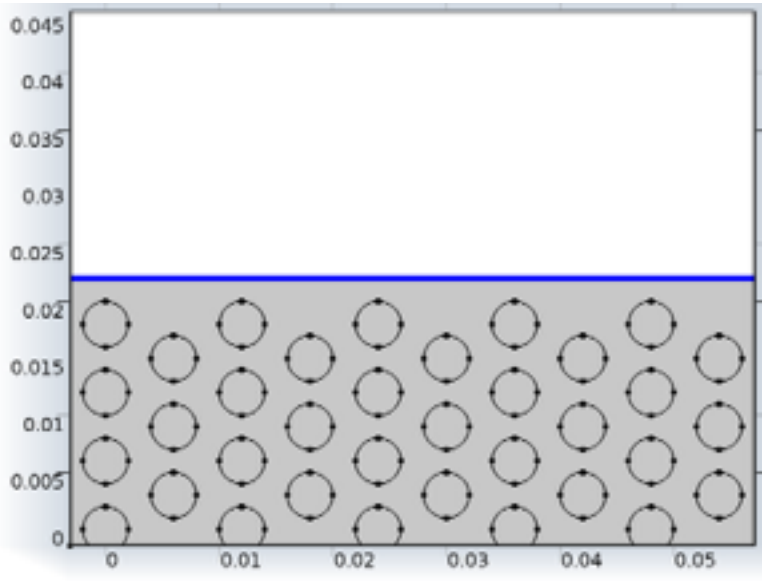

Surface-to-Ambient Radiation 1

Selection

Geometric entity level	Boundary
Selection	Boundary 3

Settings

Description	Value
Ambient temperature	293.15[K]
Surface emissivity	User defined
Surface emissivity	.998

2.5.5. Outflow 1

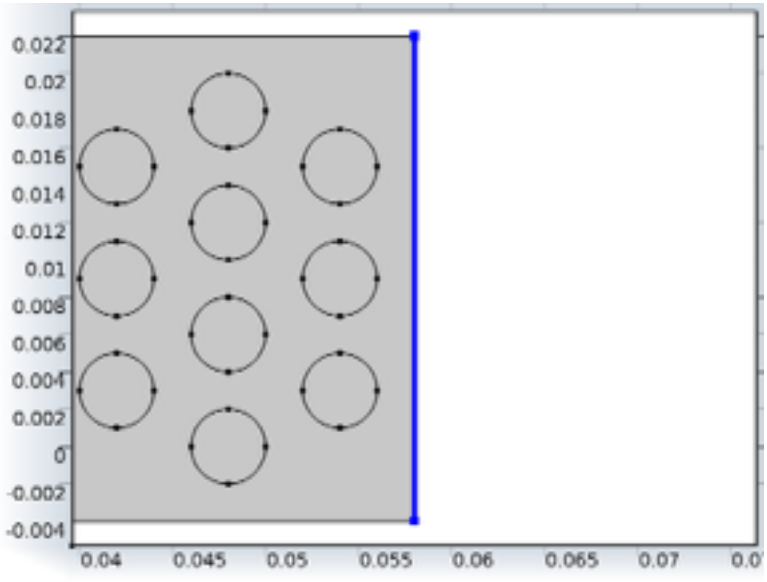

Outflow 1

Selection

Geometric entity level	Boundary
Selection	Boundary 4

2.5.6. Boundary Heat Source 1

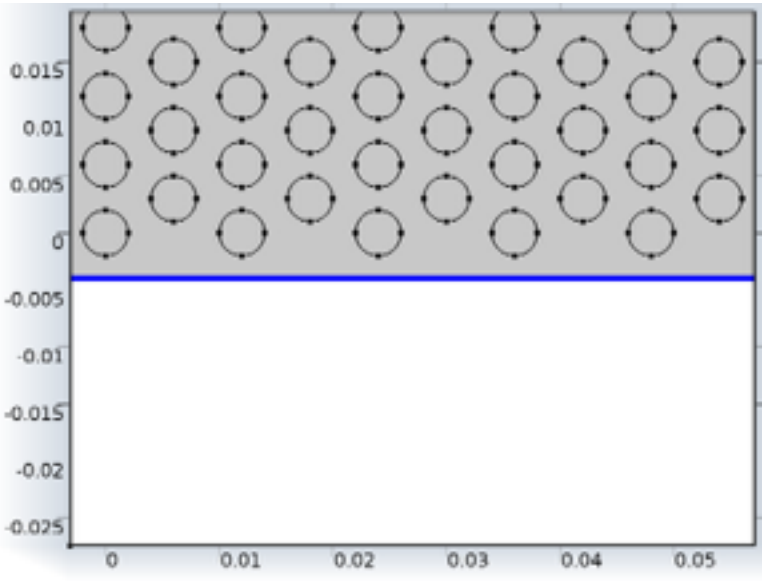

Boundary Heat Source 1

Selection

Geometric entity level	Boundary
Selection	Boundary 2

Settings

Description	Value
Heat source	General source
Boundary heat source	User defined
Boundary heat source	1000

2.5.7. Heat Flux 1

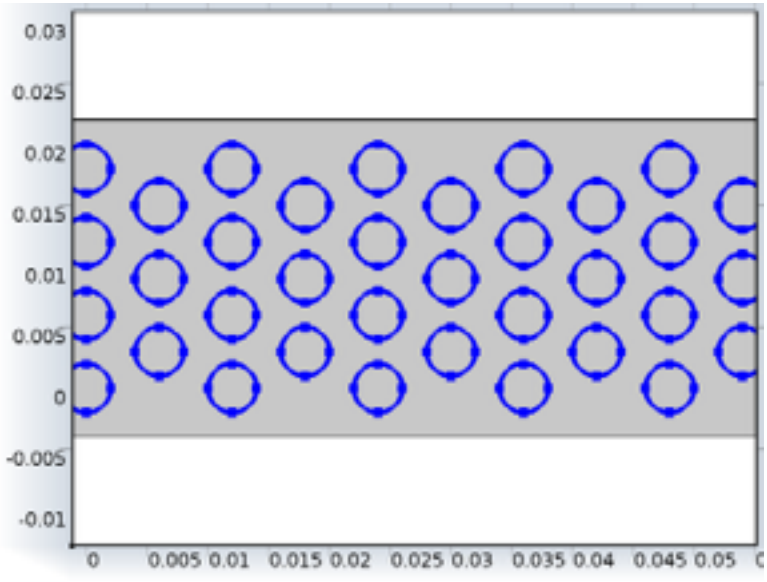

Heat Flux 1

Selection

Geometric entity level	Boundary
Selection	Boundaries 5–144

Settings

Description	Value
Heat flux	General inward heat flux
Inward heat flux	ht*(T1 - T2)
Heat transfer coefficient	-5
External temperature	T1

2.5.8. Heat Source 1

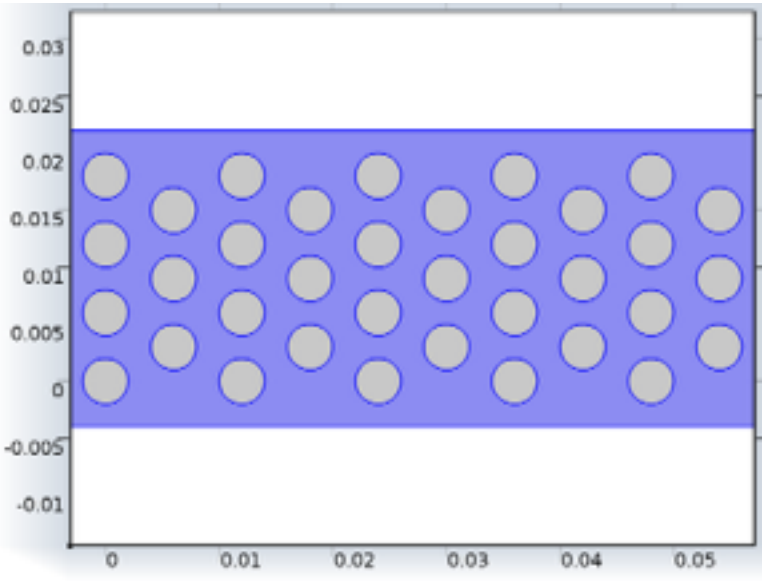

Heat Source 1

Selection

Geometric entity level	Domain
Selection	Domain 1

Settings

Description	Value
Heat source	General source
Heat source	User defined
Heat source	-rate*H_sr

2.5.9. Temperature 1

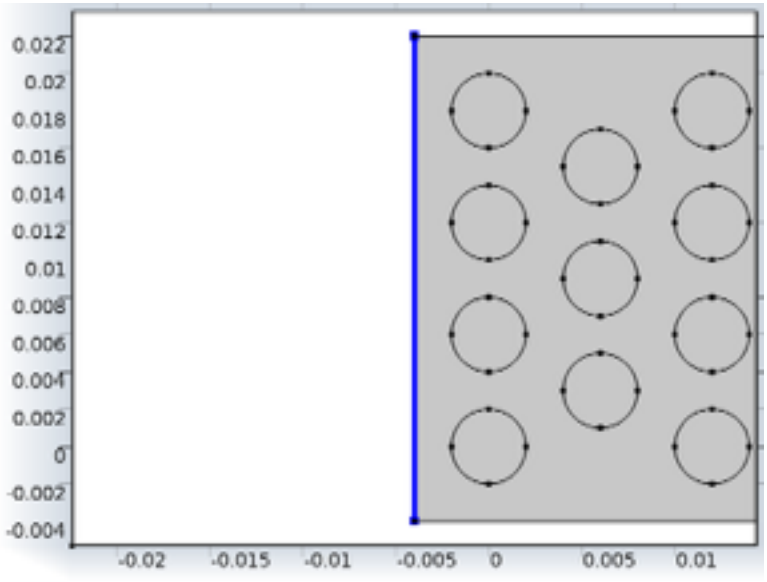

Temperature 1

Selection

Geometric entity level	Boundary
Selection	Boundary 1

Settings

Description	Value
Temperature	600
	Classic constraints
Apply reaction terms on	All physics (symmetric)
Use weak constraints	0

2.6. Heat Transfer in Solids (ht)

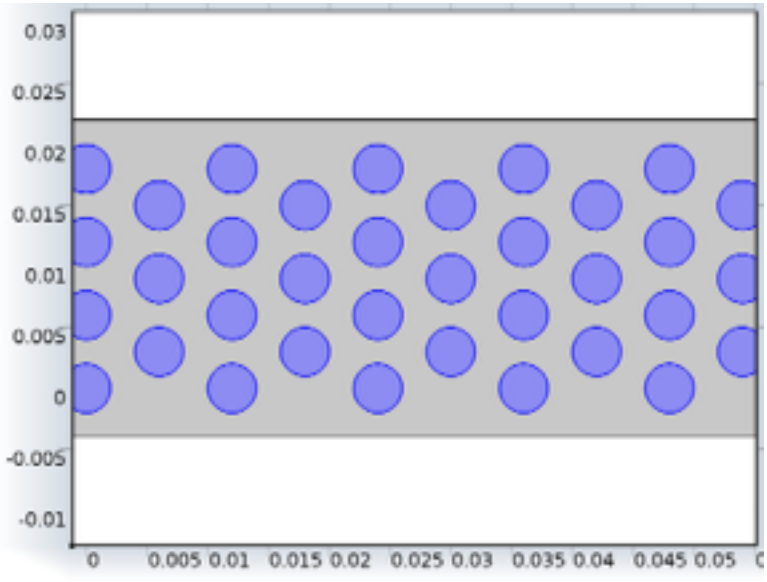

Heat Transfer in Solids

Selection

Geometric entity level	Domain
Selection	Domains 2–36

Settings

Description	Value
Temperature	Quadratic
Compute boundary fluxes	1
Apply smoothing to boundary fluxes	1
Value type when using splitting of complex variables	Real
Equation form	Study controlled
Out-of-plane heat transfer	0
Surface-to-surface radiation	0

Description	Value
Radiation in participating media	0
Heat transfer in biological tissue	0
Heat transfer in porous media	0
Moving frame	Moving frame flag (false)
Streamline diffusion	1
Crosswind diffusion	1
Isotropic diffusion	0
Show equation assuming	std1/stat

2.6.1. Heat Transfer in Solids 1

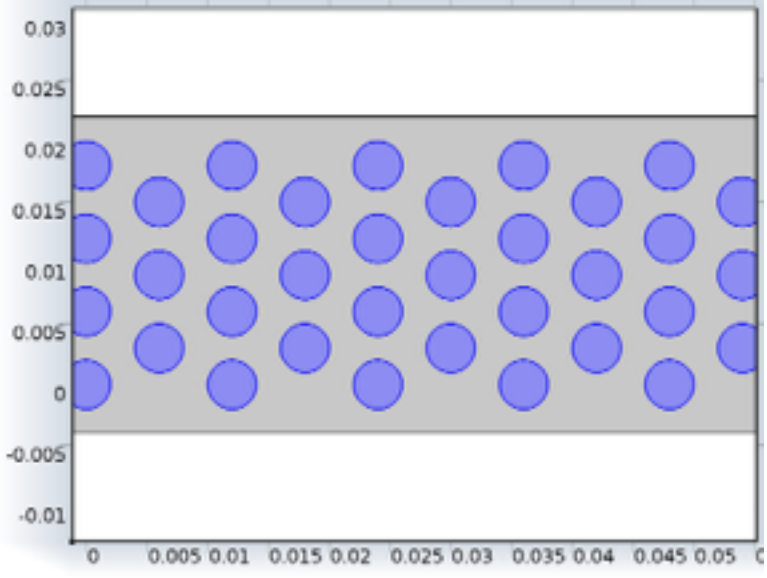

Heat Transfer in Solids 1

Selection

Geometric entity level	Domain
Selection	Domains 2–36

Settings

Description	Value
Thermal conductivity	From material
Thermal conductivity	{{0, 0, 0}, {0, 0, 0}, {0, 0, 0}}
Density	From material
Heat capacity at constant pressure	From material

Properties from material

Property	Material	Property group
Thermal conductivity	Pyrolytic graphite [solid,as deposited]	Basic
Density	Pyrolytic graphite [solid,as deposited]	Basic
Heat capacity at constant pressure	Pyrolytic graphite [solid,as deposited]	Basic

2.6.2. Thermal Insulation 1

Selection

Geometric entity level	Boundary
Selection	No boundaries

2.6.3. Initial Values 1

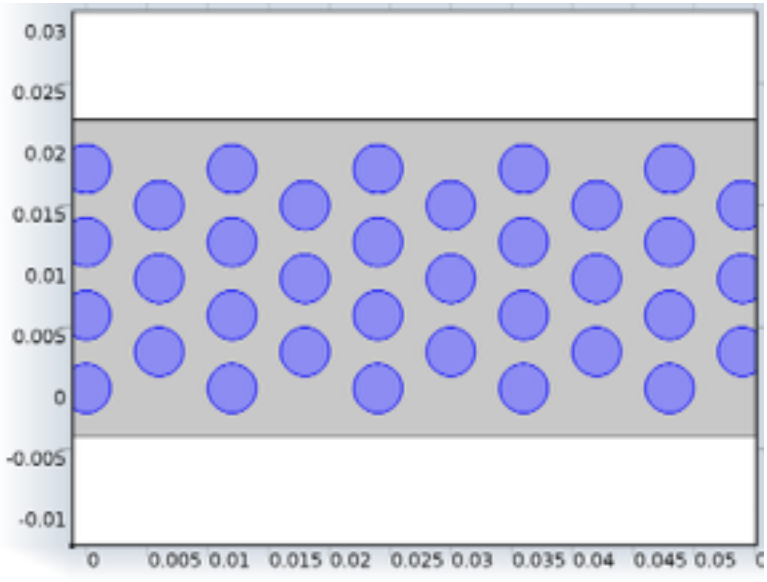

Initial Values 1

Selection

Geometric entity level	Domain
Selection	Domains 2–36

Settings

Description	Value
Temperature	293.15[K]

2.6.4. Heat Flux 1

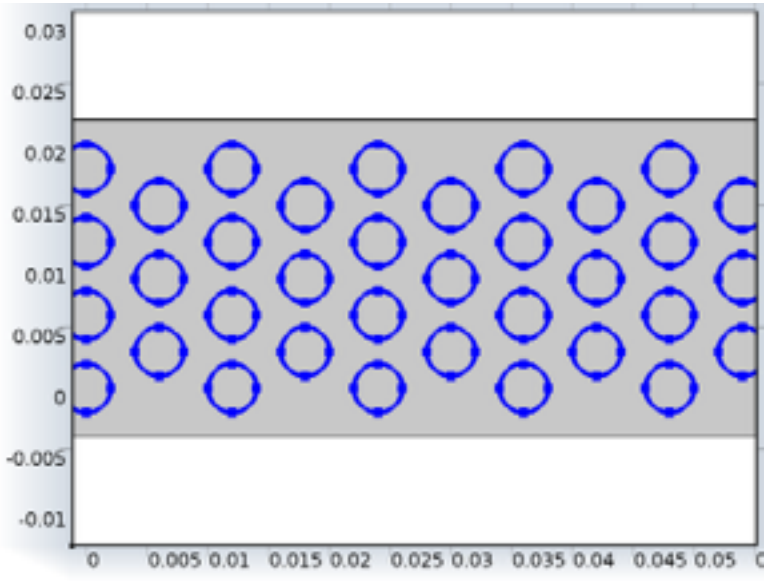

Heat Flux 1

Selection

Geometric entity level	Boundary
Selection	Boundaries 5–144

Settings

Description	Value
Heat flux	General inward heat flux
Inward heat flux	-ht*(T1 - T2)
Heat transfer coefficient	5
External temperature	T2

2.7. Transport of Concentrated Species (chcs)

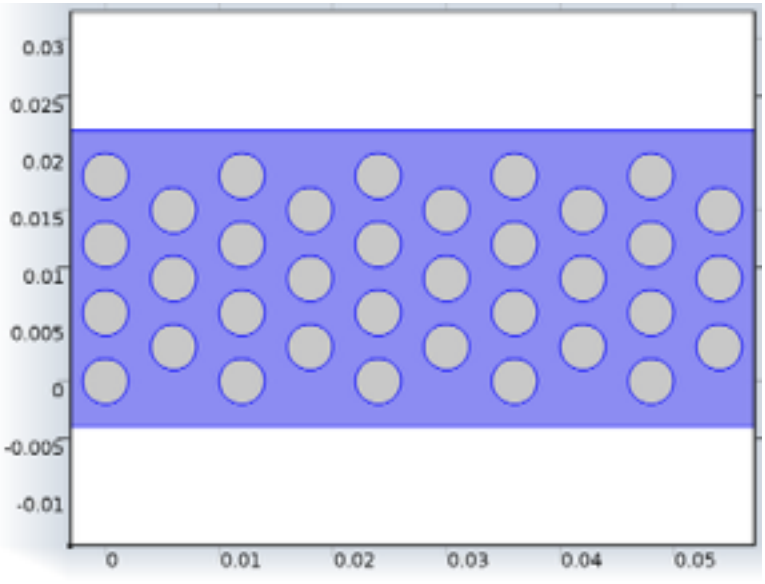

Transport of Concentrated Species

Selection

Geometric entity level	Domain
Selection	Domain 1

Settings

Description	Value
Mass fraction	Linear
Compute boundary fluxes	1
Apply smoothing to boundary fluxes	1
Value type when using splitting of complex variables	Real
Equation form	Study controlled
Migration in electric field	0
Convection	1

Description	Value
Diffusion model	Mixture-averaged
Residual	Approximate residual
From mass constraint	w H2O
Streamline diffusion	1
Crosswind diffusion	1
Crosswind diffusion type	Do Carmo and Galeão
Isotropic diffusion	0
Regularization	On
Enable space-dependent physics interfaces	0
Synchronize with COMSOL Multiphysics	
Show equation assuming	std1/stat

2.7.1. Convection and Diffusion

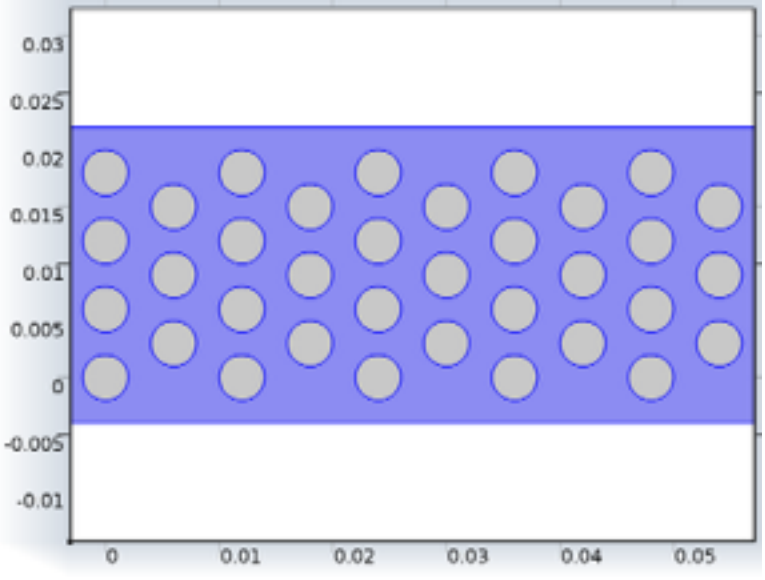

Convection and Diffusion

Selection

Geometric entity level	Domain
Selection	Domain 1

Settings

Description	Value
Velocity field	Velocity field (spf/fp1)
Electric potential	User defined
Electric potential	0
Thermal diffusion coefficient	{0, 0, 0, 0}
Molar mass	{M_H2O, M_C3H8, M_H2, M_CO2}
Density	dens_sr
Mixture density	User defined
Maxwell-Stefan diffusivity matrix	{{1, D_C3H8_H2O, D_H2_H2O, D_CO2_H2O}, {D_C3H8_H2O, 1, D_H2_C3H8, D_CO2_C3H8}, {D_H2_H2O, D_H2_C3H8, 1, D_CO2_H2}, {D_CO2_H2O, D_CO2_C3H8, D_CO2_H2, 1}}
Diffusion coefficient	{{{1e-5[m^2/s], 0, 0}, {0, 1e-5[m^2/s], 0}, {0, 0, 1e-5[m^2/s]}}, {{1e-5[m^2/s], 0, 0}, {0, 1e-5[m^2/s], 0}, {0, 0, 1e-5[m^2/s]}}, {{1e-5[m^2/s], 0, 0}, {0, 1e-5[m^2/s], 0}, {0, 0, 1e-5[m^2/s]}}, {{1e-5[m^2/s], 0, 0}, {0, 1e-5[m^2/s], 0}, {0, 0, 1e-5[m^2/s]}}}

2.7.2. No Flux 1

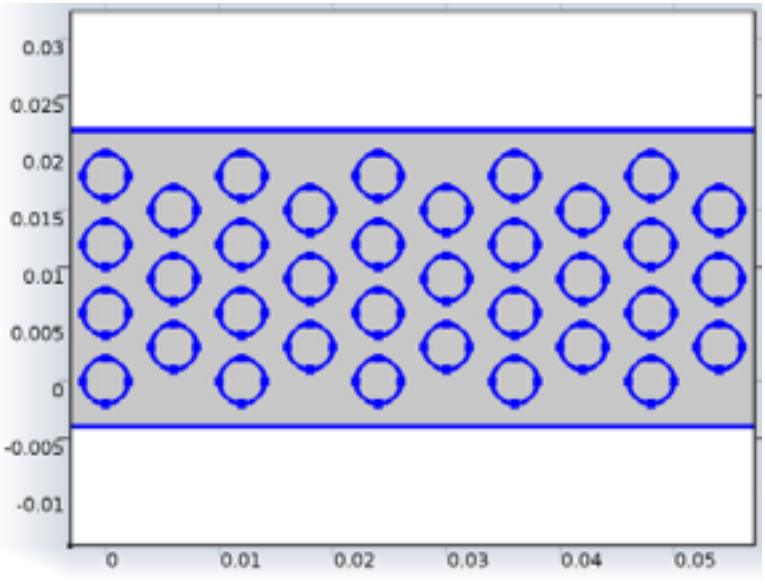

No Flux 1

Selection

Geometric entity level	Boundary
Selection	Boundaries 2–3, 5–144

Settings

Description	Value
Apply for all species	Apply for all species

2.7.3. Initial Values 1

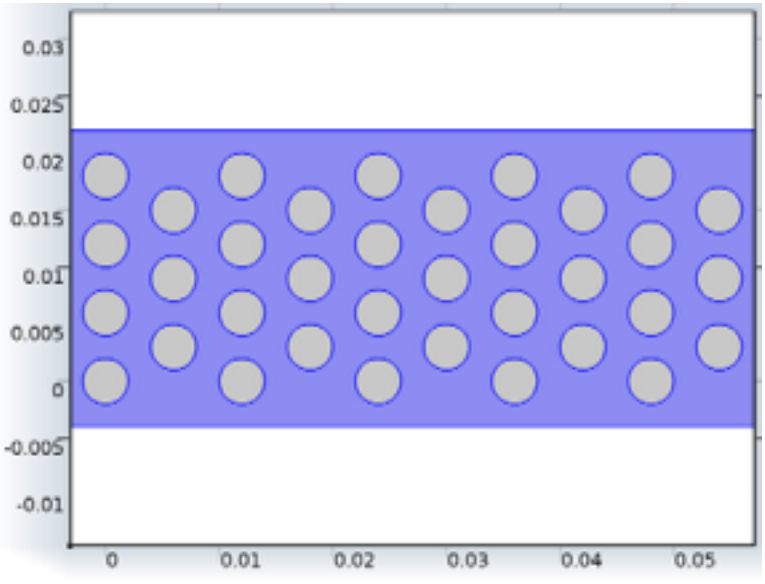

Initial Values 1

Selection

Geometric entity level	Domain
Selection	Domain 1

Settings

Description	Value
Mass fraction	w_C3H8_in
Mass fraction	1/2
Mass fraction	w_H2_in
Mass fraction	w_CO2_in

2.7.4. Reactions 1

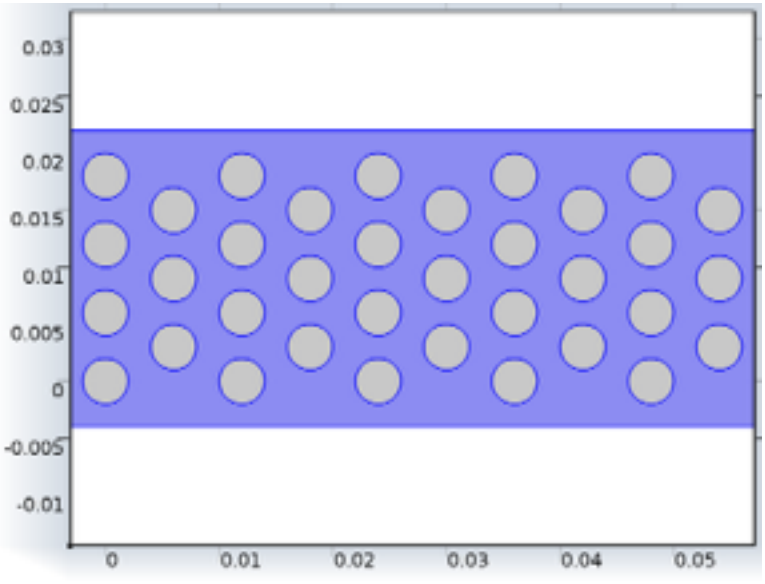

Reactions 1

Selection

Geometric entity level	Domain
Selection	Domain 1

Settings

Description	Value
Total rate expression	{0, -M_C3H8*rate, 10*M_H2*rate, 3*M_CO2*rate}
Mass transfer to other phases	0

2.7.5. Inflow 1

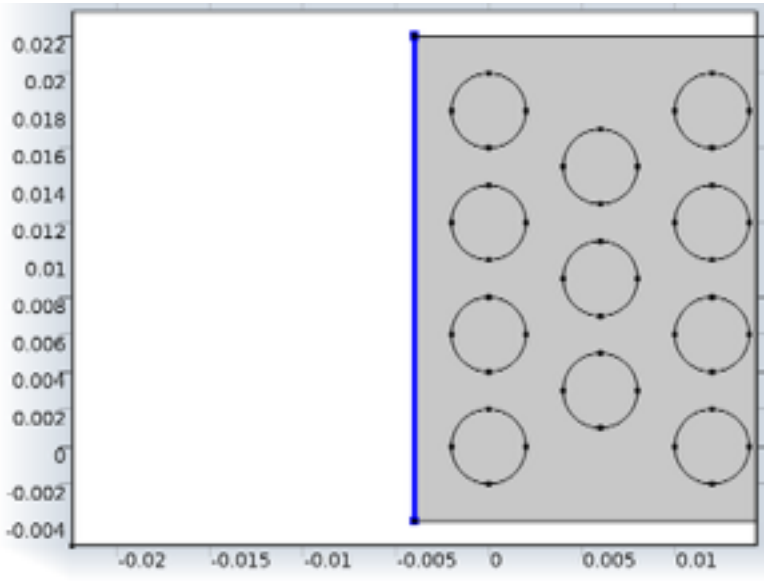

Inflow 1

Selection

Geometric entity level	Boundary
Selection	Boundary 1

Settings

Description	Value
Mixture specification	Mass fractions
Mass fraction	{0, w_C3H8_in, w_H2_in, w_CO2_in}
Apply reaction terms on	All physics (symmetric)
Use weak constraints	0

2.7.6. Outflow 1

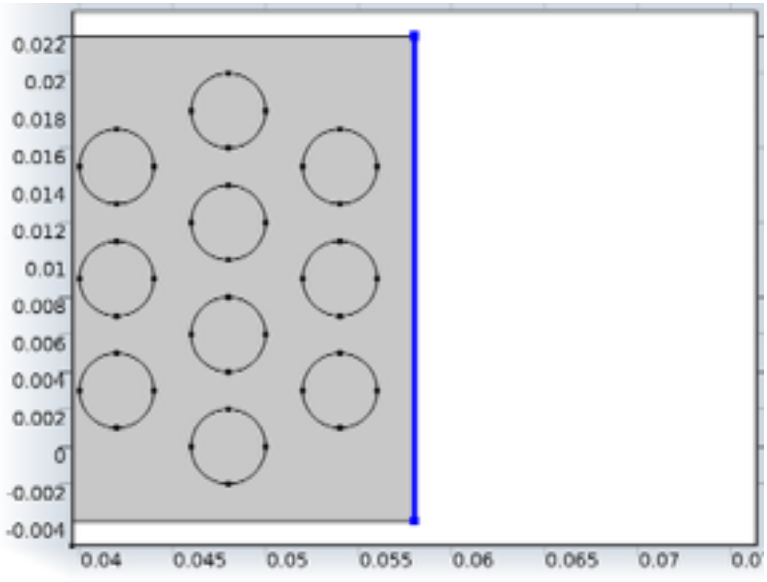

Outflow 1

Selection

Geometric entity level	Boundary
Selection	Boundary 4

2.8. Mesh 1

Mesh statistics

Property	Value
Minimum element quality	0.6495
Average element quality	0.9241
Triangular elements	6484
Edge elements	666
Vertex elements	144

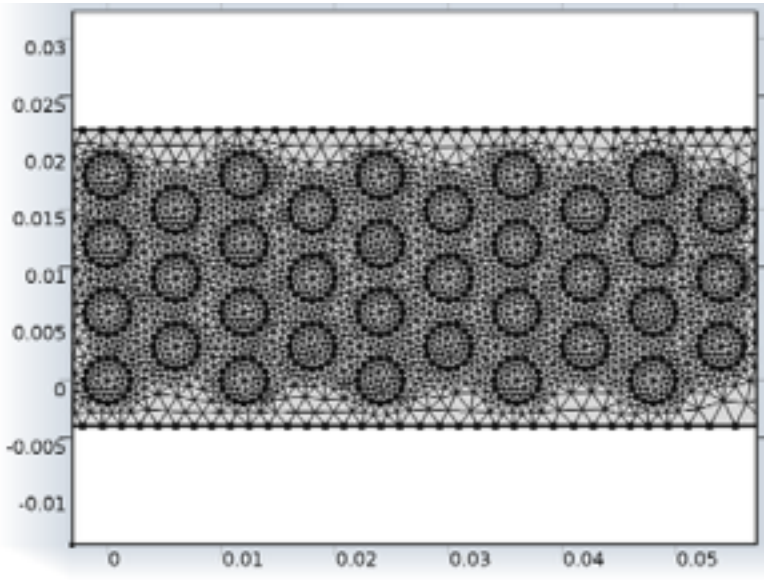

Mesh 1

2.8.1. Size (size)

Settings

Name	Value
Maximum element size	0.0062
Minimum element size	1.24E-4
Resolution of curvature	0.4
Maximum element growth rate	1.4
Predefined size	Coarse

2.8.2. Free Triangular 3 (ftri3)

Selection

Geometric entity level	Remaining

3. Study 1

3.1. Stationary

Study settings

Property	Value
Include geometric nonlinearity	Off

Mesh selection

Geometry	Mesh
Geometry 1 (geom1)	mesh1

Physics selection

Physics	Discretization
Laminar Flow (spf)	physics
Heat Transfer in Fluids 2 (ht2)	physics
Heat Transfer in Solids (ht)	physics
Transport of Concentrated Species (chcs)	physics

3.2. Solver Configurations

3.2.1. Solver 1

Compile Equations: Stationary (st1)

Study and step

Name	Value
Use study	Study 1
Use study step	Stationary

Dependent Variables 1 (v1)

General

Name	Value
Defined by study step	Stationary

Initial values of variables solved for

Name	Value
Solution	Zero

Values of variables not solved for

Name	Value
Solution	Zero

Temperature (mod1.T2) (mod1_T2)

General

Name	Value
Field components	mod1.T2

Velocity field (mod1.u) (mod1_u)

General

Name	Value
Field components	{mod1.u, mod1.v}

Temperature (mod1.T1) (mod1_T1)

General

Name	Value
Field components	mod1.T1

Mass fraction (mod1.w_C3H8) (mod1_w_C3H8)

General

Name	Value
Field components	mod1.w_C3H8

Pressure (mod1.p) (mod1_p)

General

Name	Value
Field components	mod1.p

Mass fraction (mod1.w_CO2) (mod1_w_CO2)

General

Name	Value
Field components	mod1.w_CO2

Mass fraction (mod1.w_H2) (mod1_w_H2)

General

Name	Value
Field components	mod1.w_H2

Stationary Solver 1 (s1)

General

Name	Value
Defined by study step	Stationary

Fully Coupled 1 (fc1)

General

Name	Value
Linear solver	Direct 1

Direct 1 (d1)

General

Name	Value
Solver	PARDISO

4. Results

4.1. Data Sets

4.1.1. Solution 1

Selection

Geometric entity level	Domain
Selection	Geometry geom1

Solution

Name	Value
Solution	Solver 1
Model	Save Point Geometry 1

4.2. Plot Groups

4.2.1. Velocity (spf)

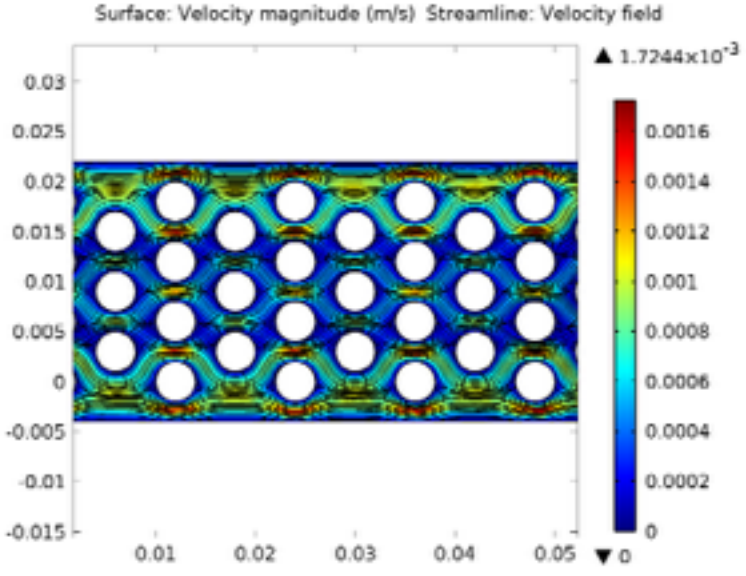

Surface: Velocity magnitude (m/s) Streamline: Velocity field

4.2.2. Pressure (spf)

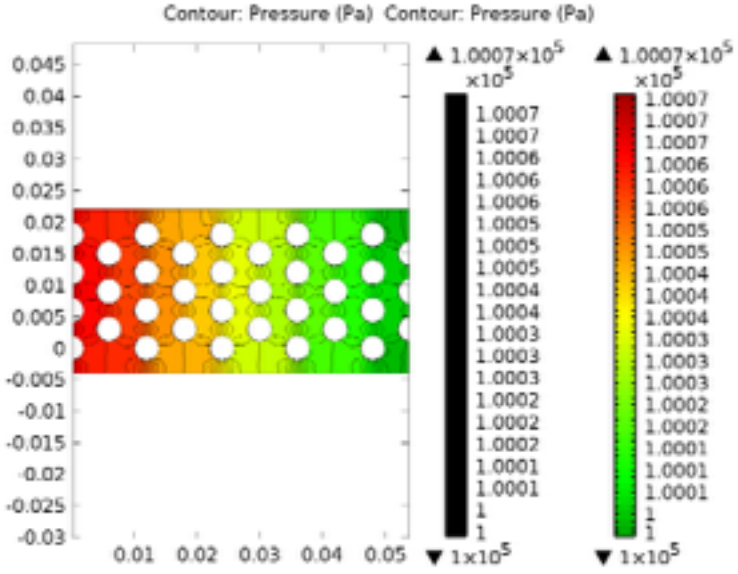

Contour: Pressure (Pa) Contour: Pressure (Pa)

4.2.3. Temperature

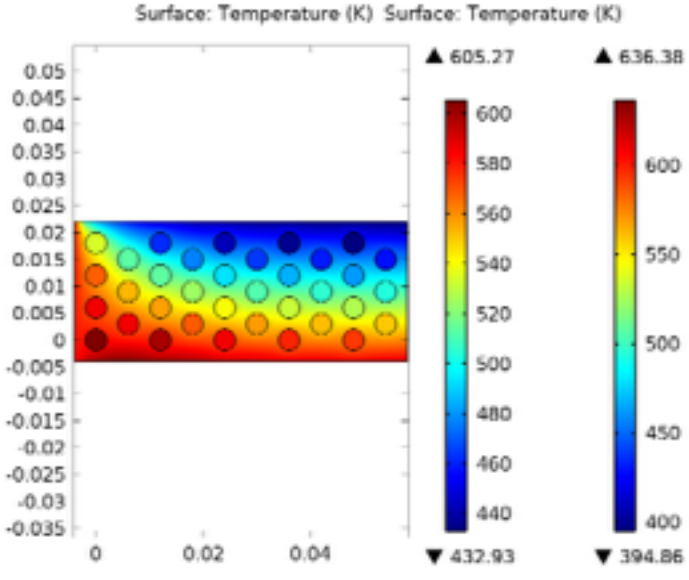

Surface: Temperature (K) Surface: Temperature (K)

4.2.4. Mass Fractions

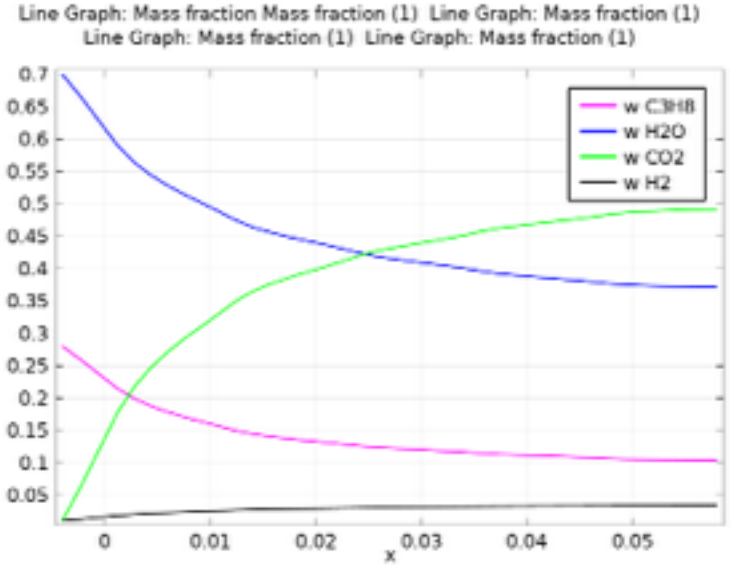

Line Graph: Mass fraction Mass fraction (1) Line Graph: Mass fraction (1) Line Graph: Mass fraction (1) Line Graph: Mass fraction (1)

1. Global Definitions

1.1. Parameters 1

Parameters

Name	Expression	Description
R_fib	.002	fiber radius [m]
N_fib	6	number of fibers per layer
L_fib	4	number of layers
u_in	.05[m/s]	inflow velocity [m/s]
p_in	3[Pa]	Pressure difference
p_ref	1e5[Pa]	Reference pressure
T_in	700[K]	Inlet temperature, reformer bed
ht	100[W/m^2/K]	Heat transfer coefficient, heating tubes
D_H2_C3H8	2.7e-5[m^2/s]	Binary diffusion coefficient
D_CO2_C3H8	5.1e-6[m^2/s]	Binary diffusion coefficient
D_C3H8_H2O	8.4e-6[m^2/s]	Binary diffusion coefficient
D_CO2_H2	3.6e-5[m^2/s]	Binary diffusion coefficient
D_H2_H2O	4.9e-5[m^2/s]	Binary diffusion coefficient
D_CO2_H2O	1.1e-5[m^2/s]	Binary diffusion coefficient
M_C3H8	44.1e-3[kg/mol]	Molar mass
M_H2	2.016e-3[kg/mol]	Molar mass
M_CO2	44.01e-3[kg/mol]	Molar mass
M_H2O	18.016e-3[kg/mol]	Molar mass
w_C3H8_in	0.28[1]	Initial weight fraction
w_H2_in	0.01[1]	Initial weight fraction
w_CO2_in	0.01[1]	Initial weight fraction
H_sr	410e3[J/mol]	Enthalpy of reaction
Cp	2800[J/kg/K]	Heat capacity, fluid
k_sr	0.1[W/m/K]	Thermal conductivity, reformer bed

Name	Expression	Description
visc_sr	2.7e-5[Pa*s]	Viscosity, reformer bed
X_disp	3*R_fib	displacement in x direction between fiber centers
Y_disp	3*R_fib	displacement in y direction between fiber centers

2. Model 1 (mod1)

2.1. Definitions

2.1.1. Variables

Variables

Selection

Geometric entity level	Entire model

Name	Expression	Description
T_out	aveop(T2)	Average outlet temperature
rate	chcs.x_w_C3H8*p/T2/R_const*7e5[1/s]*exp(-83.14e3[J/mol]/R_const/T2)	Reaction rate
dens_sr	p/T2/R_const*(chcs.x_w_C3H8*M_C3H8 + chcs.x_w_H2*M_H2 + chcs.x_w_CO2*M_CO2 + chcs.x_w_H2O*M_H2O)	Density, reformer bed
U_out	aveop(u)	Average outlet velocity
Re_max	maxop1(spf.cellRe)	Maximum Cell Reynolds number

2.1.2. Model Couplings

Average

Coupling type	Average
Operator name	aveop

Source selection

Geometric entity level	Boundary
Selection	Boundary 7

Maximum 1

Coupling type	Maximum
Operator name	maxop1

Source selection

Geometric entity level	Domain
Selection	Domain 2

2.1.3. Selections

Carbon Fibers

Selection type
Explicit

Selection
Domains 3–23

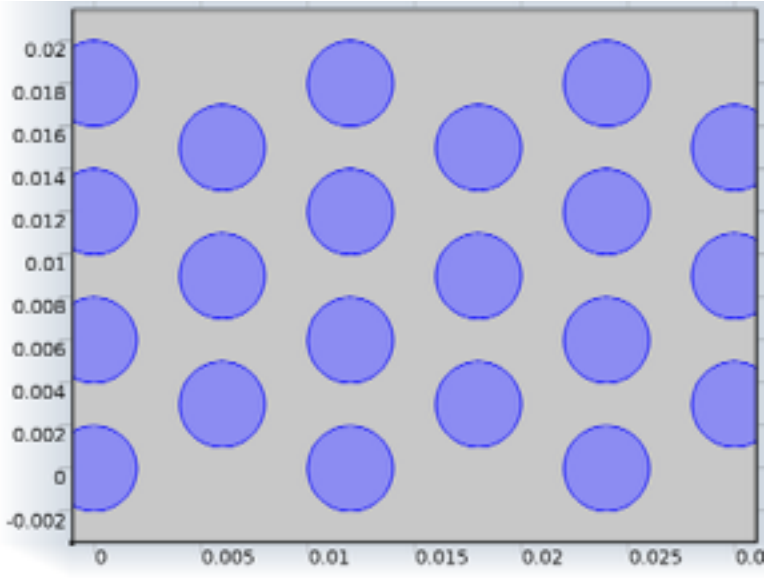

Carbon Fibers

Flow Model

Fluid Matrix

Selection type
Explicit

Selection
No domains

Inlet

Selection type
Explicit

Selection
Boundary 7

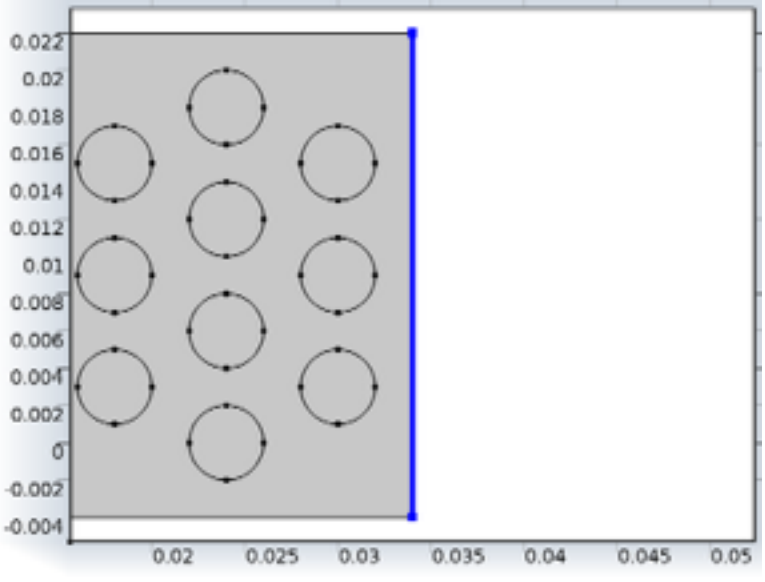

Inlet

Outlet

Selection type
Explicit

Selection
No boundaries

Air Boundary

Selection type
Explicit

Selection
No boundaries

Hot Plate

Selection type
Explicit

Selection
No boundaries

2.1.4. Coordinate Systems

Boundary System 1

Coordinate system type	Boundary system
Identifier	sys1

Settings

Name	Value
Coordinate names	{t1, n, to}
Create first tangent direction from	Global Cartesian

2.2. Geometry 1

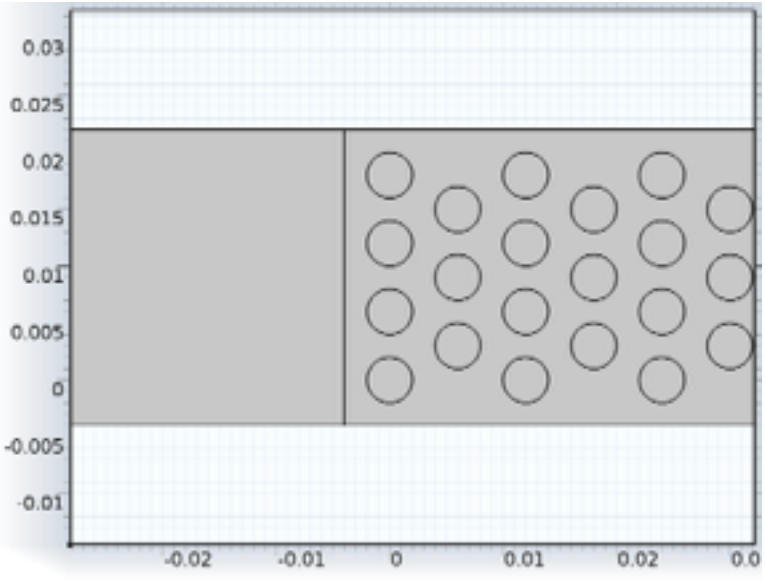

Geometry 1

Units

Length unit	m
Angular unit	deg

Geometry statistics

Property	Value
Space dimension	2
Number of domains	23
Number of boundaries	91

2.2.1. Circle 1 (c1)

Position

Name	Value
Position	{0, 0}
Radius	R_fib

2.2.2. Array 1 (arr1)

Selections of resulting entities

Name	Value
Create selections	On
Size	{N_fib/2, L_fib}
Displacement	{2*X_disp, Y_disp}

2.2.3. Copy 1 (copy1)

Selections of resulting entities

Name	Value
Keep input objects	On
x	0.0060
y	0.0030

2.2.4. Array 2 (arr2)

Selections of resulting entities

Name	Value
Size	{N_fib/2, L_fib - 1}
Displacement	{2*X_disp, Y_disp}

2.2.5. Rectangle 1 (r1)

Position

Name	Value
Position	{-2*R_fib, -2*R_fib}
Width	N_fib*X_disp + R_fib
Height	L_fib*Y_disp + R_fib
Size	{N_fib*X_disp + R_fib, L_fib*Y_disp + R_fib}

2.2.6. Rectangle 2 (r2)

Position

Name	Value
Position	{-.03, -2*R_fib}
Width	(N_fib*X_disp - R_fib) + 0.03
Height	L_fib*Y_disp + R_fib
Size	{(N_fib*X_disp - R_fib) + 0.03, L_fib*Y_disp + R_fib}

2.3. Materials

2.3.1. Pyrolytic graphite [solid,as deposited]

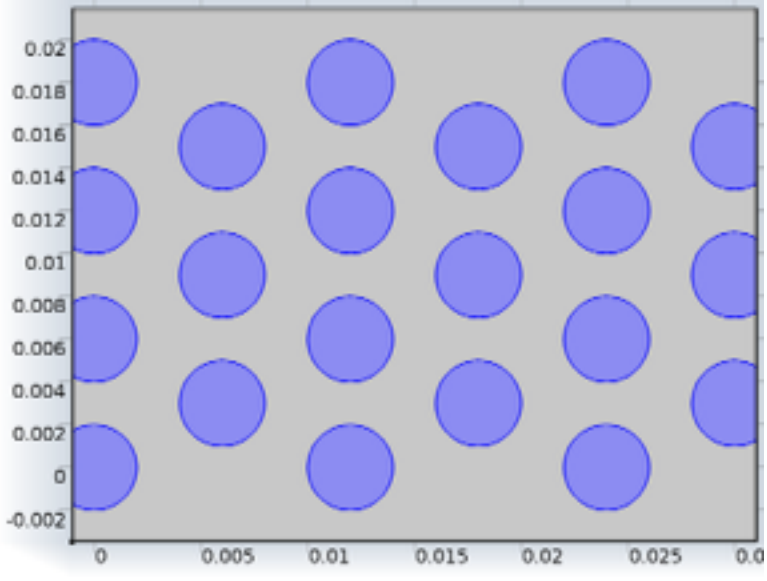

Pyrolytic graphite [solid,as deposited]

Selection

Geometric entity level	Domain
Selection	Domains 3–23

2.4. Laminar Flow (spf)

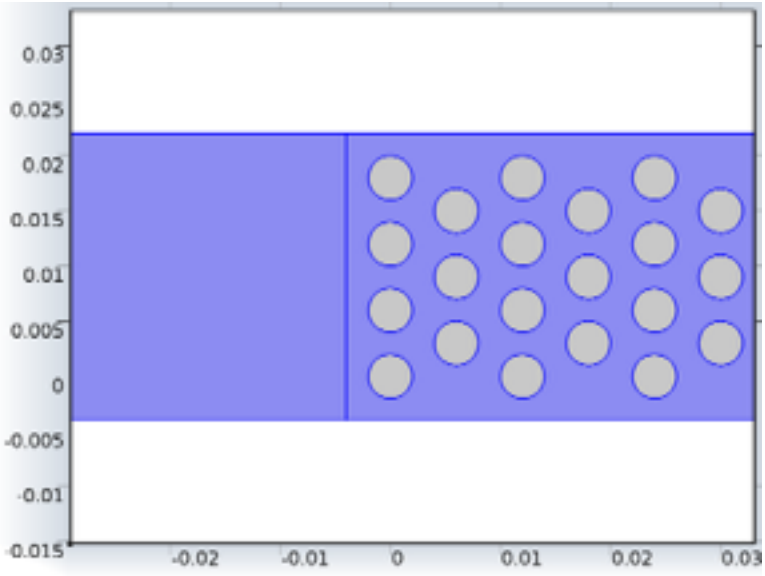

Laminar Flow

Selection

Geometric entity level	Domain
Selection	Domains 1–2

Settings

Description	Value
Discretization of fluids	P1 + P1
Value type when using splitting of complex variables	{Real, Real, Real, Real, Real, Real, Real, Real, Real}
Equation form	Study controlled

Flow Model

Description	Value
Compressibility	Compressible flow (Ma<0.3)
Neglect inertial term (Stokes flow)	Off
Use shallow channel approximation	Off
Allow out of plane properties	1
Allow radiation properties	1
Allow stokes properties	1
Allow turbulence properties	1
Allow MaxwellStefan diffusion	1
Use pseudo time stepping for stationary equation form	0
Local CFL number	1.3^min(niterCMP, 9) + if(niterCMP>=25, 9*1.3^min(niterCMP - 25, 9), 0) + if(niterCMP>=45, 90*1.3^min(niterCMP - 45, 9), 0)
Streamline diffusion	1
Crosswind diffusion	1
Isotropic diffusion	0
Turbulence model type	None
Smoothing parameter	0.1
Show equation assuming	std1/stat

2.4.1. Fluid Properties 1

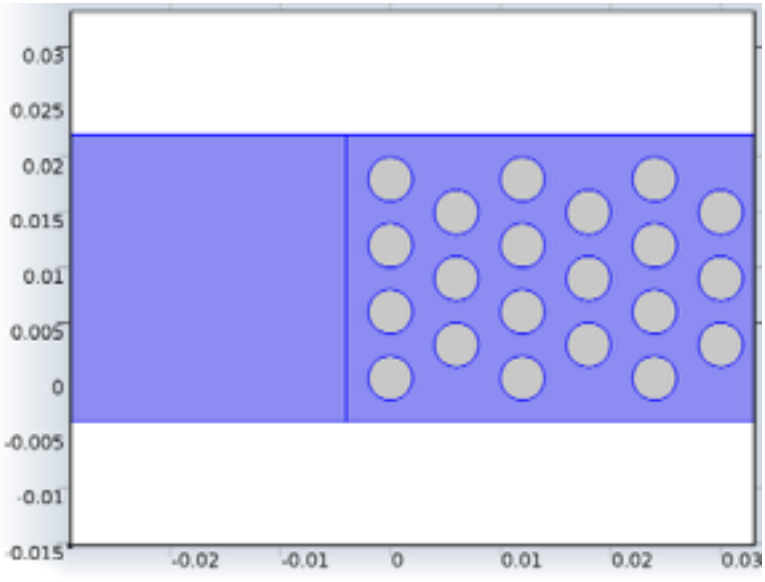

Fluid Properties 1

Selection

Geometric entity level	Domain
Selection	Domains 1–2

Settings

Description	Value
Density	User defined
Density	1000
Dynamic viscosity	User defined
Dynamic viscosity	8.9e-4
Reference length	1
Reference length scale	Automatic
Mixing length limit	Automatic

2.4.2. Wall 1

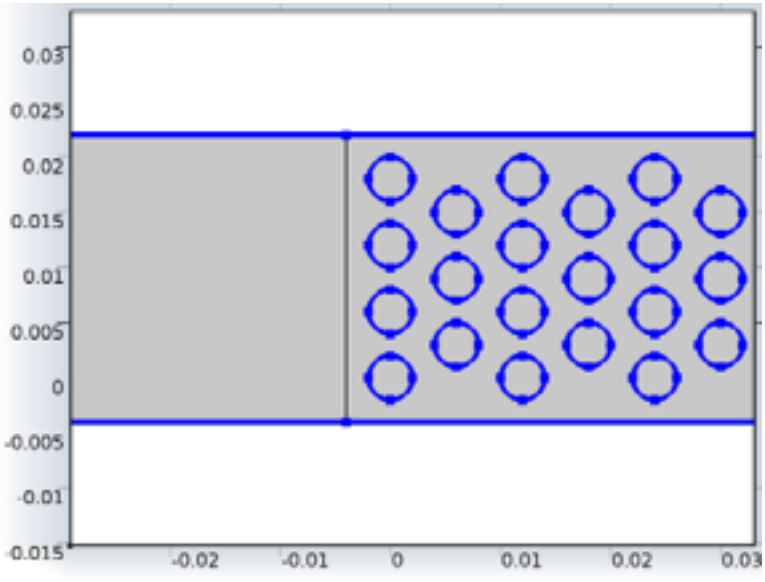

Wall 1

Selection

Geometric entity level	Boundary
Selection	Boundaries 2–3, 5–6, 8–91

Settings

Description	Value
Temperature	User defined
Temperature	293.15[K]
Electric field	User defined
Electric field	{0, 0, 0}
Boundary condition	No slip
Apply reaction terms on	Individual dependent variables
Use weak constraints	0

2.4.3. Initial Values 1

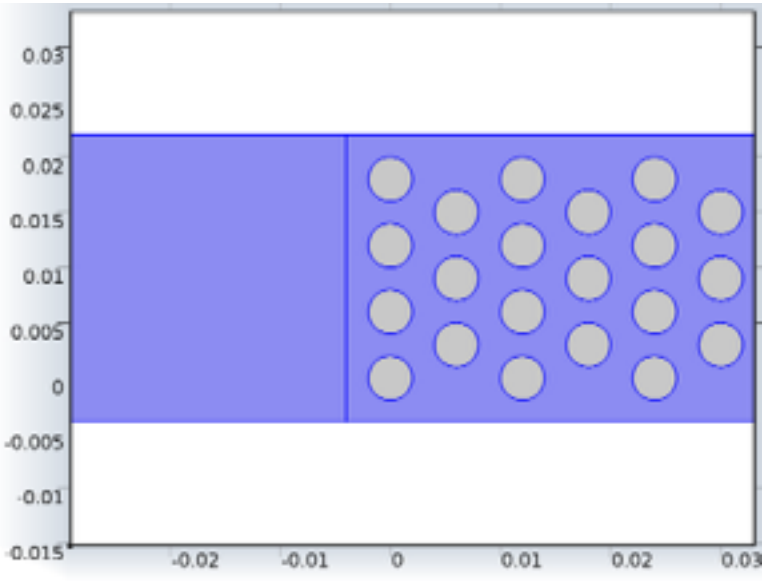

Initial Values 1

Selection

Geometric entity level	Domain
Selection	Domains 1–2

Settings

Description	Value
Velocity field	{0, 0, 0}
Pressure	p_ref

2.4.4. Inlet 1

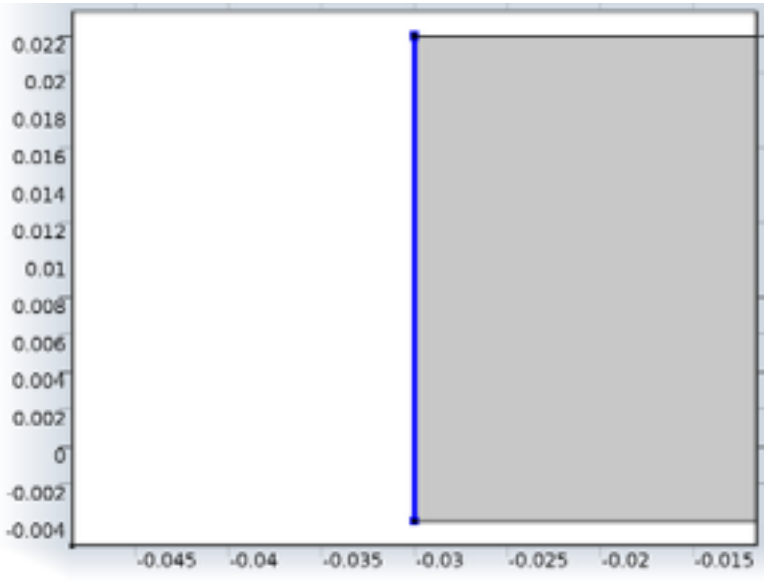

Inlet 1

Selection

Geometric entity level	Boundary
Selection	Boundary 1

Settings

Description	Value
Apply reaction terms on	All physics (symmetric)
Use weak constraints	0
Boundary condition	Pressure, no viscous stress
Pressure	p_in + p_ref
Standard pressure	1[atm]
Standard molar volume	0.0224136[m^3/mol]
Normal mass flow rate	1e-5[kg/s]

Description	Value
Mass flow type	Mass flow rate
Standard flow rate defined by	Standard density
Channel thickness	1.0[m]

2.4.5. Outlet 1

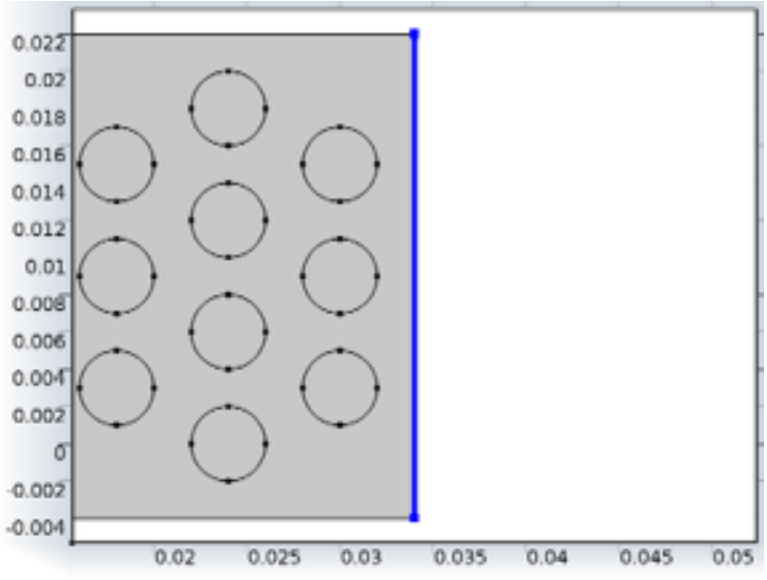

Outlet 1

Selection

Geometric entity level	Boundary
Selection	Boundary 7

Settings

Description	Value
Apply reaction terms on	All physics (symmetric)
Use weak constraints	0
Boundary condition	Pressure, no viscous stress

Description	Value
Pressure	p_ref

2.5. Mesh 1

Mesh statistics

Property	Value
Minimum element quality	0.1701
Average element quality	0.8061
Triangular elements	8963
Quadrilateral elements	1260
Edge elements	716
Vertex elements	90

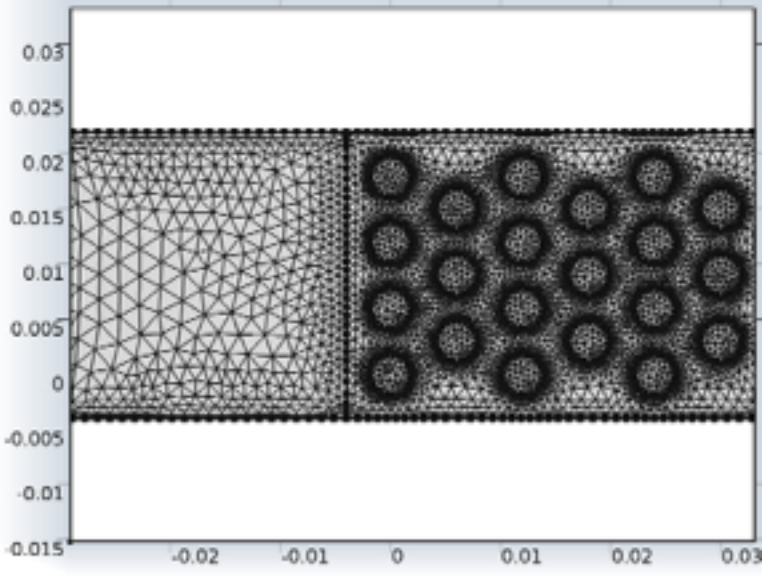

Mesh 1

2.5.1. Size (size)

Settings

Name	Value
Maximum element size	0.0064
Minimum element size	1.28E-4
Resolution of curvature	0.4
Maximum element growth rate	1.4
Predefined size	Coarse

2.5.2. Size 1 (size1)

Selection

Geometric entity level	Domain
Selection	Domains 1–2

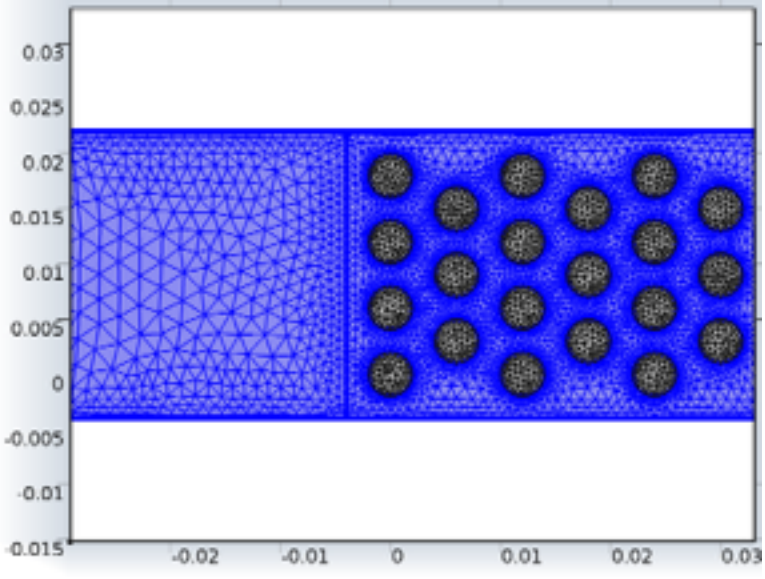

Size 1

Settings

Name	Value
Calibrate for	Fluid dynamics
Maximum element size	0.00226
Minimum element size	1.04E-4
Resolution of curvature	0.6
Maximum element growth rate	1.25
Predefined size	Coarser

2.5.3. Size 2 (size2)

Selection

Geometric entity level	Boundary
Selection	Boundaries 2–3, 5–6, 8–91

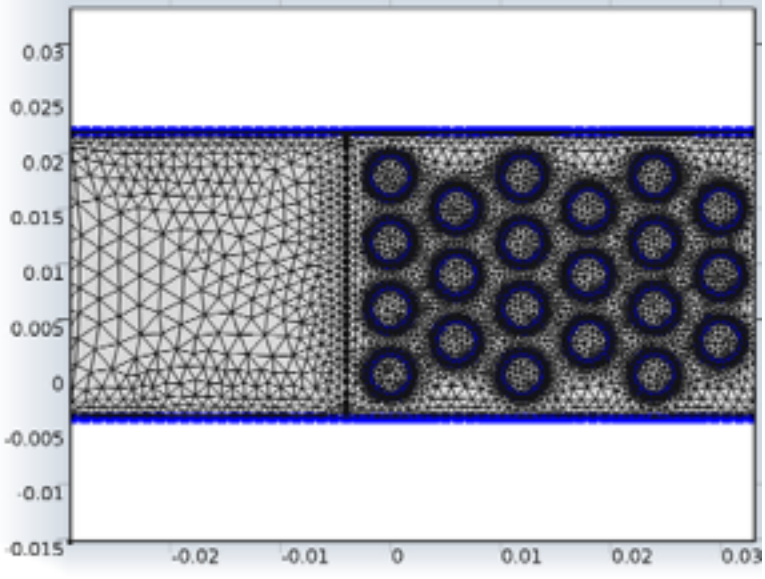

Size 2

Settings

Name	Value
Calibrate for	Fluid dynamics
Maximum element size	0.00117
Minimum element size	5.2E-5
Resolution of curvature	0.3
Maximum element growth rate	1.15

2.5.4. Corner Refinement 1 (cr1)

Selection

Geometric entity level	Domain
Selection	Domains 1–2

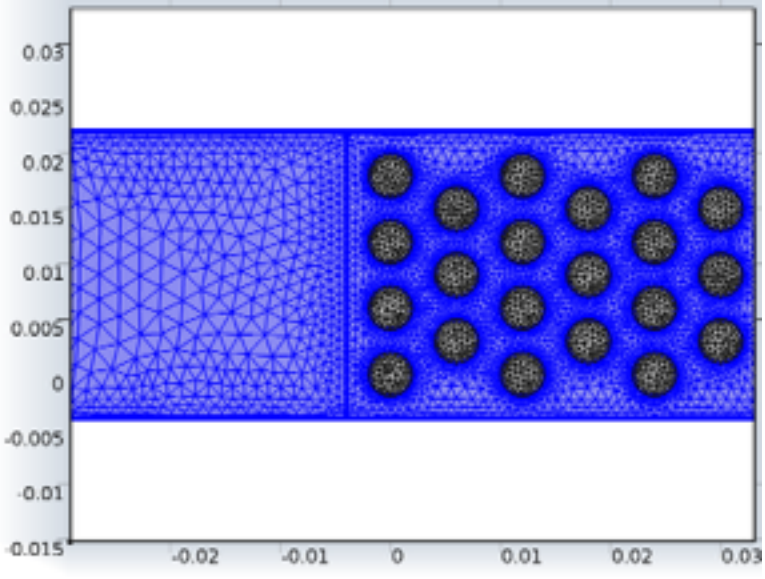

Corner Refinement 1

2.5.5. Free Triangular 1 (ftri1)

Selection

Geometric entity level	Domain

Selection	Domains 1–2

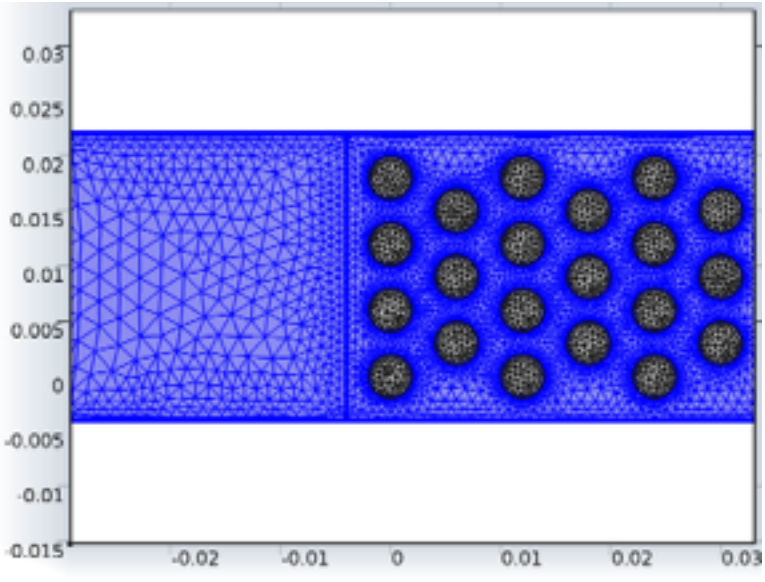

Free Triangular 1

2.5.6. Boundary Layers 1 (bl1)

Selection

Geometric entity level	Domain
Selection	Domains 1–2

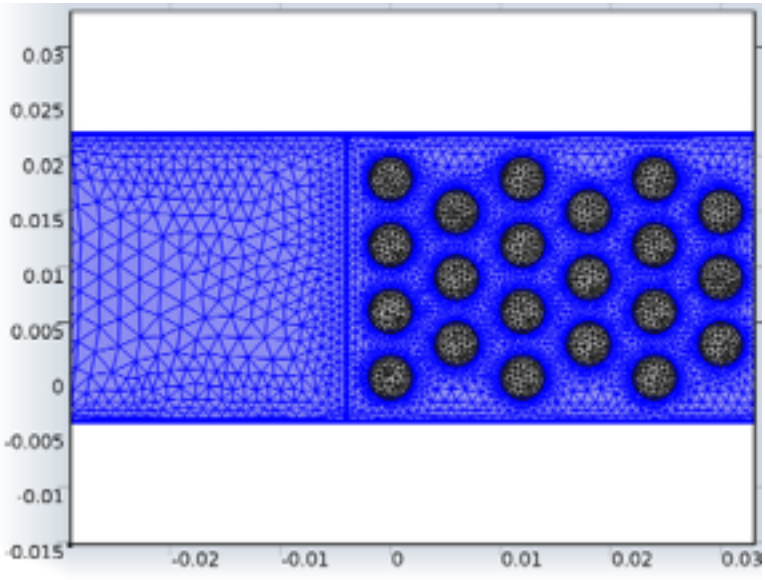

Boundary Layers 1

Settings

Name	Value
Handling of sharp corners	Trimming

Boundary Layer Properties 1 (blp1)

Selection

Geometric entity level	Boundary
Selection	Boundaries 2–3, 5–6, 8–91

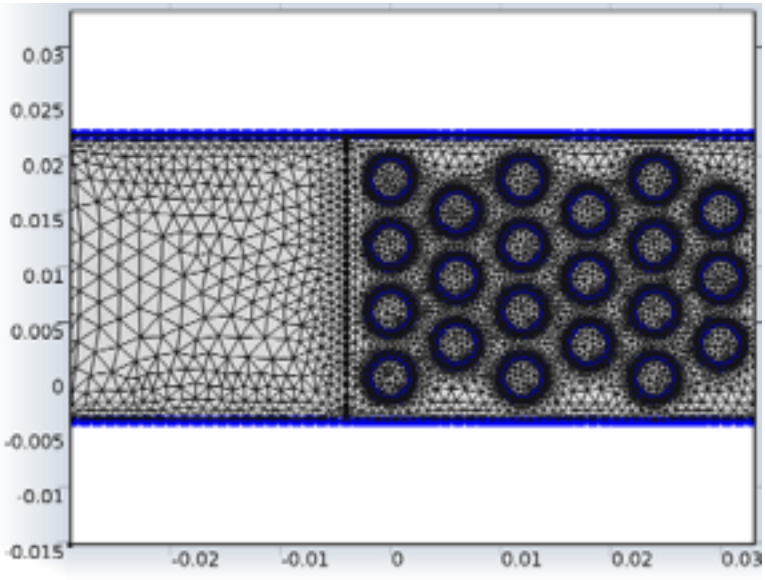

Boundary Layer Properties 1

Settings

Name	Value
Number of boundary layers	2

2.5.7. Free Triangular 2 (ftri2)

Selection

Geometric entity level	Remaining

3. Study 1

3.1. Parametric Sweep

Parameter name: p_in

Parameters:

3.2. Stationary

Study settings

Property	Value
Include geometric nonlinearity	Off

Mesh selection

Geometry	Mesh
Geometry 1 (geom1)	mesh1

Physics selection

Physics	Discretization
Laminar Flow (spf)	physics

3.3. Solver Configurations

3.3.1. Solver 1

Compile Equations: Stationary (st1)

Study and step

Name	Value
Use study	Study 1
Use study step	Stationary

Dependent Variables 1 (v1)

General

Name	Value
Defined by study step	Stationary

Initial values of variables solved for

Name	Value
Solution	Zero

Values of variables not solved for

Name	Value
Solution	Zero

Velocity field (mod1.u) (mod1_u)

General

Name	Value
Field components	{mod1.u, mod1.v}

Pressure (mod1.p) (mod1_p)

General

Name	Value
Field components	mod1.p

Stationary Solver 1 (s1)

General

Name	Value
Defined by study step	Stationary

General

Name	Value
Defined by study step	Parametric Sweep
Parameter value list	range(0.01, 0.01, 0.5)

Fully Coupled 1 (fc1)

General

Name	Value
Linear solver	Direct 1

4. Results

4.1. Data Sets

4.1.1. Solution 1

Selection

Geometric entity level	Domain
Selection	Geometry geom1

Solution

Name	Value
Solution	Solver 1
Model	Save Point Geometry 1

4.1.2. Solution 2

Selection

Geometric entity level	Domain
Selection	Geometry geom1

Solution

Name	Value
Solution	Parametric 2
Model	Save Point Geometry 1

4.2. Tables

4.2.1. Evaluation 2D

Interactive 2D values

Evaluation 2D

x	y	Value
0.01189	0.01756	656.48334

4.3. Plot Groups

4.3.1. Velocity (spf)

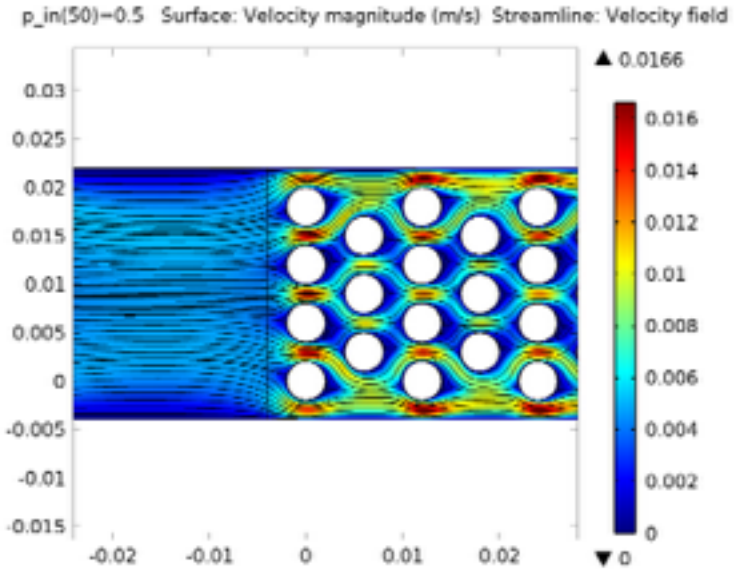

p_in(50)=0.5 Surface: Velocity magnitude (m/s) Streamline: Velocity field

4.3.2. Pressure (spf)

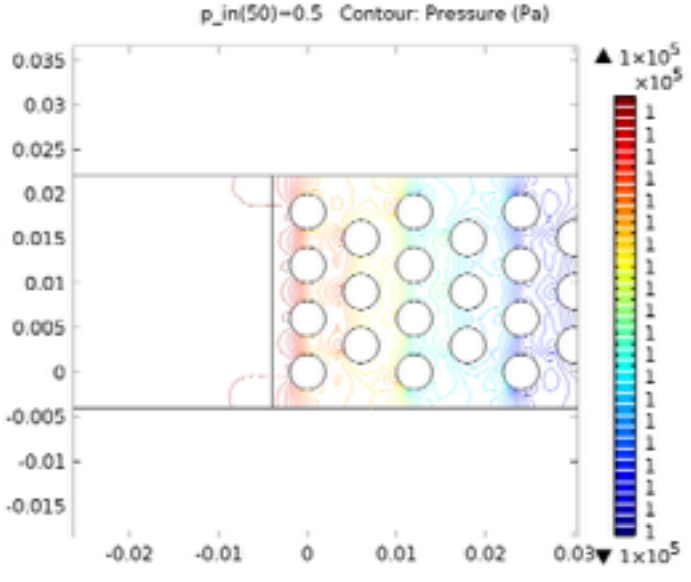

p_in(50)=0.5 Contour: Pressure (Pa)

4.3.3. Outlet Velocity

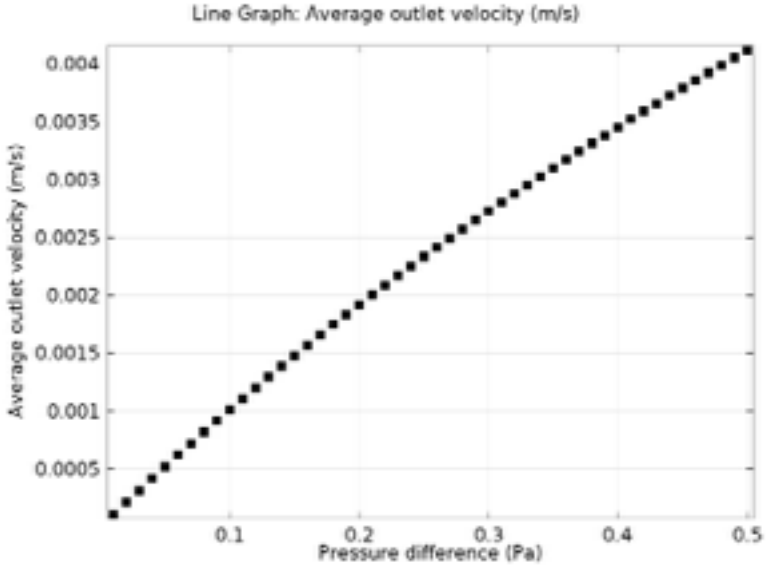

Line Graph: Average outlet velocity (m/s)

4.3.4. Max Reynolds Number

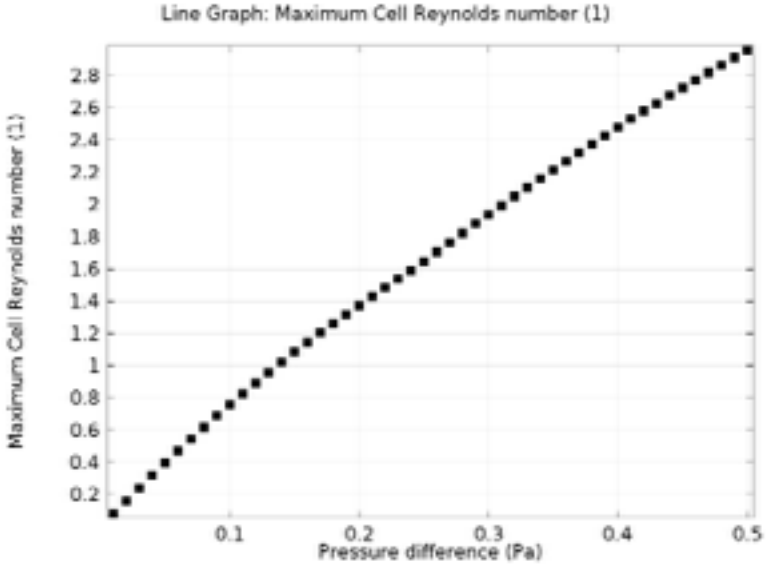

Line Graph: Maximum Cell Reynolds number (1)

4.3.5. Velocity (spf) 1

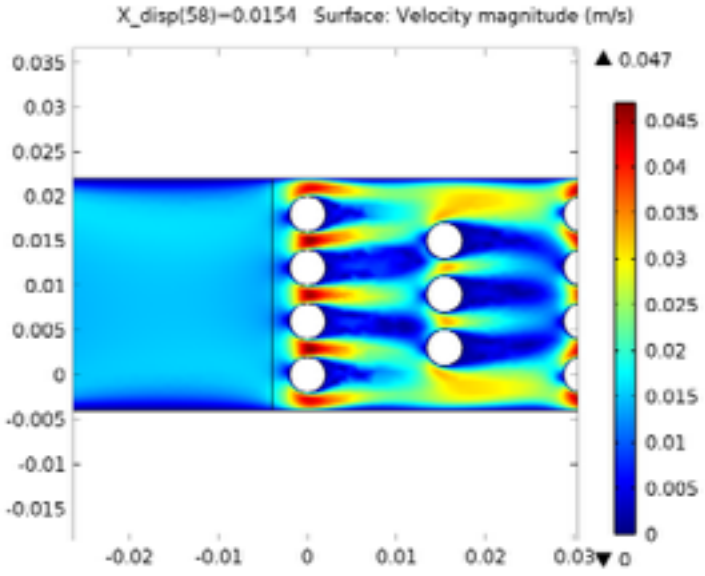

X_disp(58)=0.0154 Surface: Velocity magnitude (m/s)

4.3.6. Pressure (spf) 1

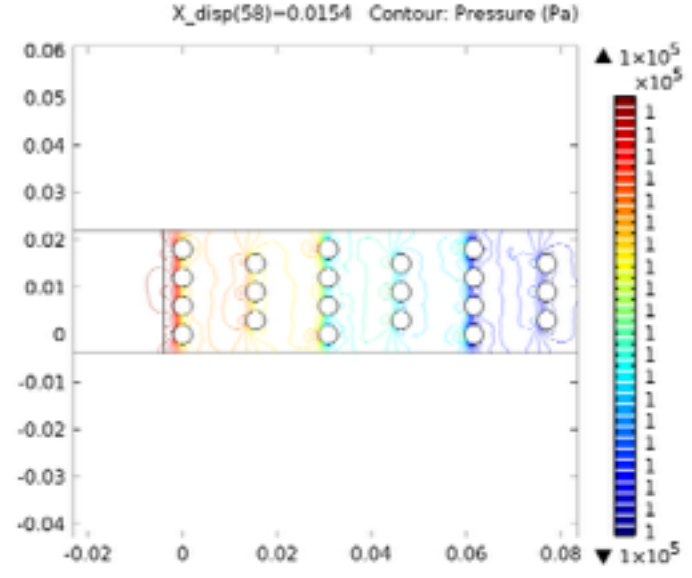

X_disp(58)=0.0154 Contour: Pressure (Pa)

1. Global Definitions

1.1. Parameters 1

Parameters

Name	Expression	Description
R	R_const	
L_r	270[mm]	length of reactor
R_r	135[mm]	radius of reactor
V_r	L_r*pi*R_r^2	Volume of reactor
A_r	L_r*2*pi*R_r	Surface area of reactor
p_r	250[mbar]	pressure of reactor
T_o	2073[K]	initial temperature
c_SiH4_o	(3/12)*p_r/(R_const*T_o)	inital silane concentration
c_H2_o	(8/12)*p_r/(R_const*T_o)	initial hydrogen concentration
c_C3H8_o	(1/12)*p_r/(R_const*T_o)	initial propane concnetration
Temp	2073[K]	Initial temperature

2. Model 1 (mod1)

2.1. Definitions

2.1.1. Variables

Variables 1

Selection

Geometric entity level	Entire model

Name	Expression	Description
Si_gas	mod1.re.c_SiH4 + mod1.re.c_SiH2 + 2*mod1.re.c_Si2H6 + mod1.re.c_Si + 2*mod1.re.c_Si2 + 2*mod1.re.c_Si2C + mod1.re.c_SiCH2	Total Concentration of Si in Gas Form
C_gas	3*mod1.re.c_C3H8 + mod1.re.c_CH3 + 2*mod1.re.c_C2H5 + mod1.re.c_CH4 + 2*mod1.re.c_C2H6 + 2*mod1.re.c_C2H4 + 2*mod1.re.c_C2H2 + mod1.re.c_Si2C + mod1.re.c_SiCH2 + mod1.re.c_CH2	Total Concentration of C in Gas phase
Si_solid	c_SiH4_o - Si_gas	Concentration of Si atoms deposited onto surface
C_solid	3*c_C3H8_o - C_gas	Concentration of C atoms deposited onto surface

2.2. Reaction Engineering (re)

Selection

Geometric entity level	Entire model

Settings

Description	Value
Equation form	Study controlled

Description	Value
Old pressure	R_const*T*(c_SiH4 + c_SiH2 + c_H2 + c_Si2H6 + c_Si + c_H + c_C3H8 + c_CH3 + c_C2H5 + c_CH4 + c_C2H6 + c_C2H4 + c_C2H2 + c_Si2 + c_Si2C + c_SiCH2 + c_C_bulk + c_Si_surf + c_C_surf + c_Si_bulk + c_SiH2_surf + c_CH2)
Reactor volume	V_r
Volumetric flow rate	1
Old volumetric flow rate	1
Volumetric production rate	R_const*T*Vr*(r_1 + r_2 + r_3 + r_4 - r_7 - r_8 + r_9 + r_10 + r_11 + r_14)/p
Old volumetric production rate	R_const*T*Vr*(r_1 + r_2 + r_3 + r_4 - r_7 - r_8 + r_9 + r_10 + r_11 + r_14)/p
Reaction sequence number	17
Sequence number	26
Surface reaction sequence number	15
Temperature	User defined
Temperature	T_o
Pressure	User defined
Pressure	R_const*T*(c_SiH4 + c_SiH2 + c_H2 + c_Si2H6 + c_Si + c_H + c_C3H8 + c_CH3 + c_C2H5 + c_CH4 + c_C2H6 + c_C2H4 + c_C2H2 + c_Si2 + c_Si2C + c_SiCH2 + c_CH2)
Importing...	0
Calculate thermodynamic properties	On
Calculate transport properties	On
Reactor type	Batch, constant volume
Mixture	Gas

Description	Value
Solve for reactions of type	Volumetric
Species numbering	Off
Solvent is set	Off
Uniform scaling of concentration variables	0
Show equation assuming	std1/time

2.2.1. 1: SiH4<=>SiH2+H2

The settings for the first homogeneous reaction is given. Subsequent reactions follow a similar method but with the reaction-specific data listed in Appendix B.

Selection

Geometric entity level	Entire model

Settings

Description	Value
Formula	SiH4<=>SiH2 + H2
Valid reaction	1
Reaction defined	0
Third body	
Reset to default	0
Use Arrhenius expressions	One
Forward frequency factor	1.67E-6
Reverse frequency factor	2.17E8
Forward temperature exponent	18.23
Reverse temperature exponent	3.1
Forward rate constant	Af_1*T^nf_1*exp(-Ef_1/(R_const*T))

Chemical Reaction Model

Description	Value
Reverse rate constant	Ar_1*T^nr_1*exp(-Er_1/(R_const*T))
Equilibrium constant	1
Specify equilibrium constant	Zero
Equilibrium expression	1.0
Equilibrium expression numerator	0
Equilibrium expression denominator	1.0
Reaction rate	kf_1*c_SiH4 - kr_1*c_SiH2*c_H2
Enthalpy of reaction	-h_SiH4 + h_SiH2 + h_H2
Entropy of reaction	-s_SiH4 + s_SiH2 + s_H2
Heat source of reaction	-r_1*H_1
Forward stoichiometric array	{-1, 0, 0, 0, 0, 0, 0, 0, 0, 0, 0, 0, 0, 0, 0, 0, 0, 0, 0, 0, 0, 0, 0, 0, 0, 0, 0, 0, 0, 0, 0, 0, 0, 0, 0}
Reverse stoichiometric array	{0, 1, 1, 0, 0, 0, 0, 0, 0, 0, 0, 0, 0, 0, 0, 0, 0, 0, 0, 0, 0, 0, 0, 0, 0, 0, 0, 0, 0, 0, 0, 0, 0, 0, 0}
Stoichiometric array	{-1, 1, 1, 0, 0, 0, 0, 0, 0, 0, 0, 0, 0, 0, 0, 0, 0, 0, 0, 0, 0, 0, 0, 0, 0, 0, 0, 0, 0, 0, 0, 0, 0, 0, 0}
Reactant species	SiH4
Product species	{SiH2, H2}
Species	{SiH4, SiH2, H2}
Reaction sequence number	1
Reaction type	Reversible
Forward activation energy	-6.26E4
Reverse activation energy	-1.06E4
Reaction S	0
Reaction Q	0
Reset to default	0
Reset to default	0

Description	Value
Reset to default	0
Reset to default	0
Reset to default	0
Reaction rate	User defined
Enthalpy of reaction	User defined
Entropy of reaction	Automatic
Heat source of reaction	Automatic
Equilibrium constant	User defined
Rate	0
Equilibrium Settings	0
Forward rate constant	0
Reverse rate constant	0

2.2.2. 2: Si2H6<=>SiH2+SiH4

2.2.3. 3: SiH2<=>Si+H2

2.2.4. 5: C3H8<=>CH3+C2H5

2.2.5. 6: CH4+H<=>CH3+H2

2.2.6. 7: C2H5+H<=>2CH3

2.2.7. 8: 2CH3<=>C2H6

2.2.8. 9: C2H4+H<=>C2H5

2.2.9. 10: C2H4<=>C2H2+H2

2.2.10. 13: Si2<=>2Si

2.2.11. 14: Si2+CH4<=>Si2C+2H2

2.2.12. 15: SiH2+Si<=>Si2+H2

2.2.13. 16: CH3+Si<=>SiCH2+H

2.2.14. 17: SiCH2+SiH2<=>Si2C+2H2

2.2.15. 1: C(b)+Si(s)+H2=>SiH2+C(s)

The settings for the first surface reaction is given. Subsequent surface reactions follow a similar method but with the reaction-specific data taken from Blanquet, *et al*.

Selection

Geometric entity level	Entire model

Settings

Description	Value
Formula	C(b) + Si(s) + H2=>SiH2 + C(s)
Valid reaction	1
Reaction defined	0
Reset to default	0
Reaction type	Irreversible
Third body	

Description	Value
Use Arrhenius expressions	1
Forward sticking coefficient frequency factor	2.200e18
Forward sticking coefficient exponent	0
Forward sticking coefficient activation energy	52786[K]*R
Forward rate constant	af_1*T^bf_1*exp(-ef_1/(R_const*T))
Reaction rate	ksf_1*c_H2*c_C_bulk*c_Si_surf
Enthalpy of reaction	h_SiH2 - h_H2 - h_C_bulk - h_Si_surf + h_C_surf
Entropy of reaction	s_SiH2 - s_H2 - s_C_bulk - s_Si_surf + s_C_surf
Surface heat source of reaction	-q_1*H_1
Forward stoichiometric array	{0, 0, -1, 0, 0, 0, 0, 0, 0, 0, 0, 0, 0, 0, 0, 0, 0, 0, -1, -1, 0, 0, 0, 0}
Reverse stoichiometric array	{0, 1, 0, 0, 0, 0, 0, 0, 0, 0, 0, 0, 0, 0, 0, 0, 0, 0, 0, 0, 1, 0, 0, 0}
Stoichiometric array	{0, 1, -1, 0, 0, 0, 0, 0, 0, 0, 0, 0, 0, 0, 0, 0, 0, 0, -1, -1, 1, 0, 0, 0}
Reactant species	{C(b), Si(s), H2}
Product species	{SiH2, C(s)}
Species	{C_bulk, Si_surf, H2, SiH2, C_surf}
Reaction sequence number	1

2.2.16. 2: 2Si(b)+2C(s)+H2=>C2H2+2Si(s)

2.2.17. 3: SiH4+C(s)=>SiH2(s)+H2+C(b)

2.2.18. 4: SiH2(s)=>H2+Si(s)

2.2.19. 5: SiH2+C(s)=>SiH2(s)+C(b)

2.2.20. 6: Si+C(s)=>Si(s)+C(b)

2.2.21. 7: C2H2+Si(s)=>2C(s)+H2+2Si(b)

2.2.22. 8: C2H4+2Si(s)=>2C(s)+2H2+2Si(b)

2.2.23. 9: CH4+Si(s)=>C(s)+2H2+Si(b)

2.2.24. 11: CH3+Si(s)=>C(s)+1.5H2+Si(b)

2.2.25. 12: Si2+2C(s)=>2Si(s)+2C(b)

2.2.26. 13: Si2C+Si(s)=>Si2+C(s)+Si(b)

2.2.27. 14: SiCH2+C(s)=>Si(s)+CH2+C(b)

2.2.28. 15: CH2+Si(s)=>C(s)+H2+Si(b)

2.2.29. Species: SiH4

The settings for the first species is given. Subsequent species follow a similar method but with the species-specific data listed in Appendix A.

Selection

Geometric entity level	Entire model

Settings

Description	Value
Species is defined	1
Dependent	0
Sequence number	2
Lock concentration/ activity	0
Species name	SiH4

Description	Value
Species label	SiH4
Reset to default	0
Molecular weight	0.032117[kg/mol]
Charge	0
Old rate expression	-r_1 + r_2
Rate expression	-r_1 + r_2
Surface rate expression	-q_3
Old surface rate expression	-q_3
Lower temperature limit	298[K]
Middle temperature limit	1300[K]
Upper temperature limit	6000[K]
Polynomial coefficients	{6.060189, 139.9632, -77.88474, 16.24095, 0.135509, -6.91824, 174.3351}
Polynomial coefficients	{99.84949, 4.25153, -0.809269, 0.053437, -20.39005, -74.8492, 266.8015}

Description	Value
Molar entropy	(T<=Tlo_SiH4)*1[J/(mol*K)]*(aLo1_SiH4*log(Tlo_SiH4/1000[K]) + aLo2_SiH4*(Tlo_SiH4/1000) + (1/2)*aLo3_SiH4*(Tlo_SiH4/1000)^2 + (1/3)*aLo4_SiH4*(Tlo_SiH4/1000)^3 - (1/2)*aLo5_SiH4*1[K^6]*(Tlo_SiH4/1000)^ - 2 + aLo7_SiH4) + (T>Tlo_SiH4)*(T<=Tmid_SiH4)*1[J/(mol*K)]*(aLo1_SiH4*log(T/1000[K]) + aLo2_SiH4*(T/1000) + (1/2)*aLo3_SiH4*(T/1000)^2 + (1/3)*aLo4_SiH4*(T/1000)^3 - (1/2)*aLo5_SiH4*1[K^6]*(T/1000)^ - 2 + aLo7_SiH4) + (T>Tmid_SiH4)*(T<=Thi_SiH4)*1[J/(mol*K)]*(aHi1_SiH4*log(T/1000[K]) + aHi2_SiH4*(T/1000) + (1/2)*aHi3_SiH4*(T/1000)^2 + (1/3)*aHi4_SiH4*(T/1000)^3 - (1/2)*aHi5_SiH4*1[K^6]*(T/1000)^ - 2 + aHi7_SiH4) + (T>Thi_SiH4)*1[J/(mol*K)]*(aHi1_SiH4*log(Thi_SiH4/1000[K]) + aHi2_SiH4*(Thi_SiH4/1000) + (1/2)*aHi3_SiH4*(Thi_SiH4/1000)^2 + (1/3)*aHi4_SiH4*(Thi_SiH4/1000)^3 - (1/2)*aHi5_SiH4*1[K^6]*(Thi_SiH4/1000)^ - 2 + aHi7_SiH4)
Molar enthalpy	(T<=Tlo_SiH4)*1[J/(mol*K)]*(aLo1_SiH4*(Tlo_SiH4/1000) + (1/2)*aLo2_SiH4*((Tlo_SiH4/1000)^2) + (1/3)*aLo3_SiH4*((Tlo_SiH4/1000)^3) + (1/4)*aLo4_SiH4*((Tlo_SiH4/1000)^4) - aLo5_SiH4*1[K^6]*((Tlo_SiH4/1000)^ - 1) + aLo6_SiH4) + (T>Tlo_SiH4)*(T<=Tmid_SiH4)*1[J/(mol*K)]*(aLo1_SiH4*(T/1000) + (1/2)*aLo2_SiH4*((T/1000)^2) + (1/3)*aLo3_SiH4*((T/1000)^3) + (1/4)*aLo4_SiH4*((T/1000)^4) - aLo5_SiH4*1[K^6]*((T/1000)^ - 1) + aLo6_SiH4) + (T>Tmid_SiH4)*(T<=Thi_SiH4)*1[J/(mol*K)]*(aHi1_SiH4*(T/1000) + (1/2)*aHi2_SiH4*((T/1000)^2) + (1/3)*aHi3_SiH4*((T/1000)^3) + (1/4)*aHi4_SiH4*((T/1000)^4) - aHi5_SiH4*1[K^6]*((T/1000)^ - 1) + aHi6_SiH4) + (T>Thi_SiH4)*1[J/(mol*K)]*(aHi1_SiH4*(Thi_SiH4/1000) + (1/2)*aHi2_SiH4*((Thi_SiH4/1000)^2) + (1/3)*aHi3_SiH4*((Thi_SiH4/1000)^3) + (1/4)*aHi4_SiH4*((Thi_SiH4/1000)^4) - aHi5_SiH4*1[K^6]*((Thi_SiH4/1000)^ - 1) + aHi6_SiH4)

Description	Value
Heat capacity at constant pressure	(T<=Tlo_SiH4)*1[J/(mol*K)]*(aLo1_SiH4 + aLo2_SiH4*(Tlo_SiH4/1000) + aLo3_SiH4*(Tlo_SiH4/1000)^2 + aLo4_SiH4*(Tlo_SiH4/1000)^3 + aLo5_SiH4*1[K^6]*(Tlo_SiH4/1000)^ - 2) + (T>Tlo_SiH4)*(T<=Tmid_SiH4)*1[J/(mol*K)]*(aLo1_SiH4 + aLo2_SiH4*(T/1000) + aLo3_SiH4*(T/1000)^2 + aLo4_SiH4*(T/1000)^3 + aLo5_SiH4*1[K^6]*(T/1000)^ - 2) + (T>Tmid_SiH4)*(T<=Thi_SiH4)*1[J/(mol*K)]*(aHi1_SiH4 + aHi2_SiH4*(T/1000) + aHi3_SiH4*(T/1000)^2 + aHi4_SiH4*(T/1000)^3 + aHi5_SiH4*1[K^6]*(T/1000)^ - 2) + (T>Thi_SiH4)*1[J/(mol*K)]*(aHi1_SiH4 + aHi2_SiH4*(Thi_SiH4/1000) + aHi3_SiH4*(Thi_SiH4/1000)^2 + aHi4_SiH4*(Thi_SiH4/1000)^3 + aHi5_SiH4*1[K^6]*(Thi_SiH4/1000)^ - 2)
Potential characteristic length	3.458[angstrom]
Potential energy minimum	107.4[K]
Dipole moment	0
Diffusivity	2.6950000000000004E-22*sqrt(5.0E-4*(M_SiH4 + M_H2)*T^3/(M_SiH4*M_H2))/(p*sigma_SiH4*sigma_H2*(1.06036/(T/sqrt(epsilonkb_SiH4*epsilonkb_H2))^0.1561 + 0.193*exp(-(0.47635*T/sqrt(epsilonkb_SiH4*epsilonkb_H2))) + 1.03587*exp(-(1.52996*T/sqrt(epsilonkb_SiH4*epsilonkb_H2))) + 1.76474*exp(-(3.89411*T/sqrt(epsilonkb_SiH4*epsilonkb_H2)))))
Mobility	re.D_SiH4*e_const/k_B_const/T
Dynamic viscosity	2.669e-6*sqrt(T*M_SiH4*1e3)/((sigma_SiH4)*1e10)^2*(1.16145/(T/epsilonkb_SiH4)^0.14874 + 0.52487/exp(0.77320*T/epsilonkb_SiH4) + 2.16178/exp(2.43787*T/epsilonkb_SiH4) + 4.998e-40*mu_SiH4^4/(((sigma_SiH4)*1e10)^6*k_B_const^2*epsilonkb_SiH4*T))^ - 1
Thermal conductivity	eta_SiH4/M_SiH4*(1.15*Cp_SiH4 + 0.88*R_const)

Description	Value
Feed stream molar enthalpy	R_const*((Tf_SiH4<=Tlo_SiH4)*Tlo_SiH4*(aLo1_SiH4 + 0.5*aLo2_SiH4*Tlo_SiH4 + aLo3_SiH4*Tlo_SiH4^2/3 + 0.25*aLo4_SiH4*Tlo_SiH4^3 + 0.2*aLo5_SiH4*Tlo_SiH4^4 + aLo6_SiH4/Tlo_SiH4) + (Tf_SiH4>Tlo_SiH4)*(Tf_SiH4<=Tmid_SiH4)*Tf_SiH4*(aLo1_SiH4 + 0.5*aLo2_SiH4*Tf_SiH4 + aLo3_SiH4*Tf_SiH4^2/3 + 0.25*aLo4_SiH4*Tf_SiH4^3 + 0.2*aLo5_SiH4*Tf_SiH4^4 + aLo6_SiH4/Tf_SiH4) + (Tf_SiH4>Tmid_SiH4)*(Tf_SiH4<=Thi_SiH4)*Tf_SiH4*(aHi1_SiH4 + 0.5*aHi2_SiH4*Tf_SiH4 + aHi3_SiH4*Tf_SiH4^2/3 + 0.25*aHi4_SiH4*Tf_SiH4^3 + 0.2*aHi5_SiH4*Tf_SiH4^4 + aHi6_SiH4/Tf_SiH4) + (Tf_SiH4>Thi_SiH4)*Thi_SiH4*(aHi1_SiH4 + 0.5*aHi2_SiH4*Thi_SiH4 + aHi3_SiH4*Thi_SiH4^2/3 + 0.25*aHi4_SiH4*Thi_SiH4^3 + 0.2*aHi5_SiH4*Thi_SiH4^4 + aHi6_SiH4/Thi_SiH4))
Volumetric feed rate	0
Feed stream temperature	0
Additional enthalpy contribution	0
Species type	None
Density	c_SiH4*M_SiH4
Initial concentration	c_SiH4_o
Specify diffusivity and mobility	1
Rate expression	Automatic
Surface rate expression	User defined
Species rate	0
Reset to default	0
Reset to default	0

2.2.30. Species: SiH2

2.2.31. Species: H2

2.2.32. Species: Si2H6

2.2.33. Species: Si

2.2.34. Species: H

2.2.35. Species: C3H8

2.2.36. Species: CH3

2.2.37. Species: C2H5

2.2.38. Species: CH4

2.2.39. Species: C2H6

2.2.40. Species: C2H4

2.2.41. Species: C2H2

2.2.42. Species: Si2

2.2.43. Species: Si2C

2.2.44. Species: SiCH2

2.2.45. Species: C(b)

2.2.46. Species: Si(s)

2.2.47. Species: C(s)

2.2.48. Species: Si(b)

2.2.49. Species: SiH2(s)

2.2.50. Species: CH2

3. Study 1

3.1. Parametric Sweep

Parameter name: T_o

Parameters:

3.2. Time Dependent

Study settings

Property	Value
Include geometric nonlinearity	Off

Times: range(0,1e-8,2e-6)

Physics selection

Physics	Discretization
Reaction Engineering (re)	physics

3.3. Solver Configurations

3.3.1. Solver 1

Compile Equations: Time Dependent (st1)

Study and step

Name	Value
Use study	Study 1
Use study step	Time Dependent

Dependent Variables 1 (v1)

General

Name	Value
Defined by study step	Time Dependent

Initial values of variables solved for

Name	Value
Solution	Zero

Values of variables not solved for

Name	Value
Solution	Zero

Concentration (mod1.ODE1) (mod1_ODE1)

General

Name	Value
State components	mod1.re.c_SiH4

Concentration (mod1.ODE2) (mod1_ODE2)

General

Name	Value
State components	mod1.re.c_SiH2

Concentration (mod1.ODE3) (mod1_ODE3)

General

Name	Value
State components	mod1.re.c_H2

Concentration (mod1.ODE4) (mod1_ODE4)

General

Name	Value
State components	mod1.re.c_Si2H6

Concentration (mod1.ODE5) (mod1_ODE5)

General

Name	Value
State components	mod1.re.c_Si

Concentration (mod1.ODE6) (mod1_ODE6)

General

Name	Value
State components	mod1.re.c_H

Concentration (mod1.ODE7) (mod1_ODE7)

General

Name	Value
State components	mod1.re.c_C3H8

Concentration (mod1.ODE8) (mod1_ODE8)

General

Name	Value
State components	mod1.re.c_CH3

Concentration (mod1.ODE9) (mod1_ODE9)

General

Name	Value
State components	mod1.re.c_C2H5

Concentration (mod1.ODE10) (mod1_ODE10)

General

Name	Value
State components	mod1.re.c_CH4

Concentration (mod1.ODE11) (mod1_ODE11)

General

Name	Value
State components	mod1.re.c_C2H6

Concentration (mod1.ODE12) (mod1_ODE12)

General

Name	Value
State components	mod1.re.c_C2H4

Concentration (mod1.ODE13) (mod1_ODE13)

General

Name	Value
State components	mod1.re.c_C2H2

Concentration (mod1.ODE14) (mod1_ODE14)

General

Name	Value
State components	mod1.re.c_Si2

Concentration (mod1.ODE15) (mod1_ODE15)

General

Name	Value
State components	mod1.re.c_Si2C

Concentration (mod1.ODE16) (mod1_ODE16)

General

Name	Value
State components	mod1.re.c_SiCH2

Concentration (mod1.ODE17) (mod1_ODE17)

General

Name	Value
State components	mod1.re.c_C_bulk

Concentration (mod1.ODE18) (mod1_ODE18)

General

Name	Value
State components	mod1.re.c_Si_surf

Concentration (mod1.ODE19) (mod1_ODE19)

General

Name	Value
State components	mod1.re.c_C_surf

Concentration (mod1.ODE20) (mod1_ODE20)

General

Name	Value
State components	mod1.re.c_Si_bulk

Concentration (mod1.ODE21) (mod1_ODE21)

General

Name	Value
State components	mod1.re.c_CH2

Time-Dependent Solver 1 (t1)

General

Name	Value
Defined by study step	User defined

Name	Value
Time	{0, 1.0E-8, 2.0E-8, 3.0000000000000004E-8, 4.0E-8, 5.0E-8, 6.000000000000001E-8, 7.0E-8, 8.0E-8, 9.0E-8, 1.0E-7, 1.1E-7, 1.2000000000000002E-7, 1.3E-7, 1.4E-7, 1.5E-7, 1.6E-7, 1.7000000000000001E-7, 1.8E-7, 1.9E-7, 2.0E-7, 2.1E-7, 2.2E-7, 2.3E-7, 2.4000000000000003E-7, 2.5E-7, 2.6E-7, 2.7E-7, 2.8E-7, 2.9000000000000003E-7, 3.0E-7, 3.1E-7, 3.2E-7, 3.3E-7, 3.4000000000000003E-7, 3.5E-7, 3.6E-7, 3.7E-7, 3.8E-7, 3.9E-7, 4.0E-7, 4.1E-7, 4.2E-7, 4.3E-7, 4.4E-7, 4.5000000000000003E-7, 4.6E-7, 4.7E-7, 4.800000000000001E-7, 4.9E-7, 5.0E-7, 5.1E-7, 5.2E-7, 5.3E-7, 5.4E-7, 5.5E-7, 5.6E-7, 5.7E-7, 5.800000000000001E-7, 5.9E-7, 6.0E-7, 6.1E-7, 6.2E-7, 6.3E-7, 6.4E-7, 6.5E-7, 6.6E-7, 6.7E-7, 6.800000000000001E-7, 6.900000000000001E-7, 7.0E-7, 7.1E-7, 7.2E-7, 7.3E-7, 7.4E-7, 7.5E-7, 7.6E-7, 7.7E-7, 7.8E-7, 7.900000000000001E-7, 8.0E-7, 8.1E-7, 8.2E-7, 8.3E-7, 8.4E-7, 8.5E-7, 8.6E-7, 8.7E-7, 8.8E-7, 8.900000000000001E-7, 9.000000000000001E-7, 9.1E-7, 9.2E-7, 9.3E-7, 9.4E-7, 9.5E-7, 9.600000000000001E-7, 9.7E-7, 9.8E-7, 9.9E-7, 1.0E-6}
Relative tolerance	1e-9

Absolute tolerance

Name	Value
Tolerance	1.0E-4

Output

Name	Value
Times to store	Steps taken by solver

Advanced

Name	Value
Consistent initialization	Off

Name	Value
Solution	Solver 1

1. Global Definitions

1.1. Parameters 1

Parameters

Name	Expression	Description
R_fib	0.005[m]	fiber radius

2. Model 1 (mod1)

2.1. Definitions

2.1.1. Variables

Variables 1a

Selection

Geometric entity level	Entire model

Name	Expression	Description
density	10[mol/m^3]	material density
vx_int	-(chds.ntflux_c*chds.nx)/density	surface velocity in x-direction
vy_int	-(chds.ntflux_c*chds.ny)/density	surface velocity in y-direction

2.1.2. Coordinate Systems

Boundary System 1

Coordinate system type	Boundary system
Identifier	sys1

Settings

Name	Value
Coordinate names	{t1, n, to}
Create first tangent direction from	Global Cartesian (spatial)

2.2. Geometry 1

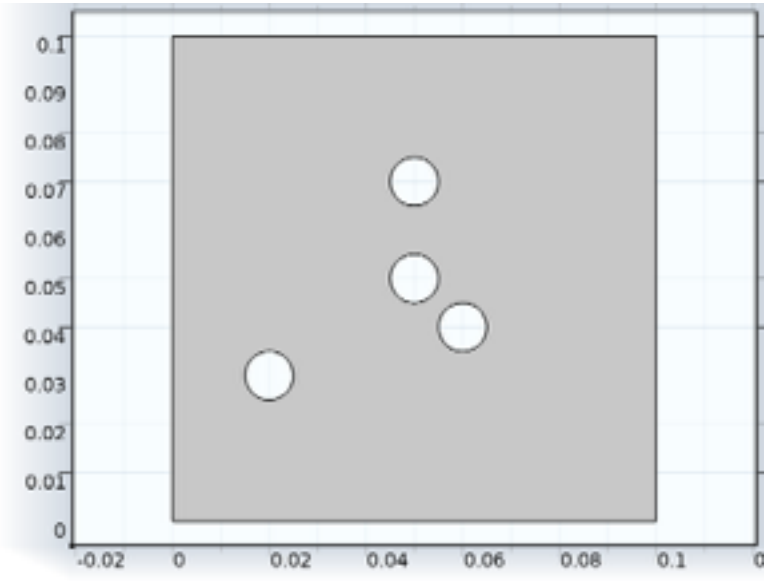

Geometry 1

Units

Length unit	m
Angular unit	deg

Geometry statistics

Property	Value
Space dimension	2
Number of domains	1
Number of boundaries	20

2.2.1. Square 1 (sq1)

Position

Name	Value
Position	{0, 0}

Name	Value
Side length	0.1
Side length	0.1

2.2.2. Circle 1 (c1)

Position

Name	Value
Position	{0.05, 0.05}
Radius	R_fib

2.2.3. Circle 2 (c2)

Position

Name	Value
Position	{0.05, 0.07}
Radius	R_fib

2.2.4. Circle 3 (c3)

Position

Name	Value
Position	{0.02, 0.03}
Radius	R_fib

2.2.5. Circle 4 (c4)

Position

Name	Value
Position	{0.06, 0.04}
Radius	R_fib

2.2.6. Compose 1 (co1)

Selections of resulting entities

Name	Value
Create selections	On
Set formula	sq1 - c1 - c2 - c3 - c4

2.3. Transport of Diluted Species (chds)

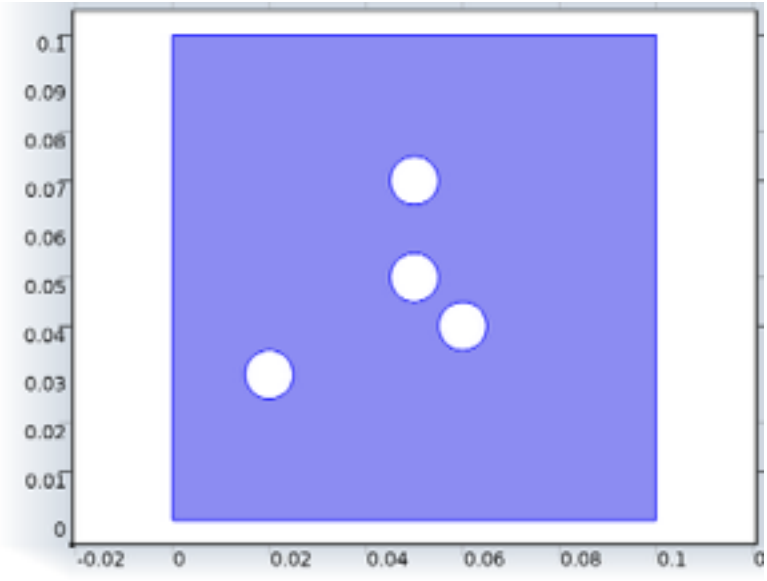

Transport of Diluted Species

Selection

Geometric entity level	Domain
Selection	Domain 1

Settings

Description	Value
Concentration	Linear
Compute boundary fluxes	1
Apply smoothing to boundary fluxes	1

Description	Value
Value type when using splitting of complex variables	Real
Equation form	Study controlled
Migration in electric field	0
Convection	0
Convective term	Non - conservative form
Equation residual	Approximate residual
Streamline diffusion	1
Crosswind diffusion	1
Crosswind diffusion type	Do Carmo and Galeão
Enable space-dependent physics interfaces	0
Synchronize with COMSOL Multiphysics	
Show equation assuming	std1/time

2.3.1. Diffusion

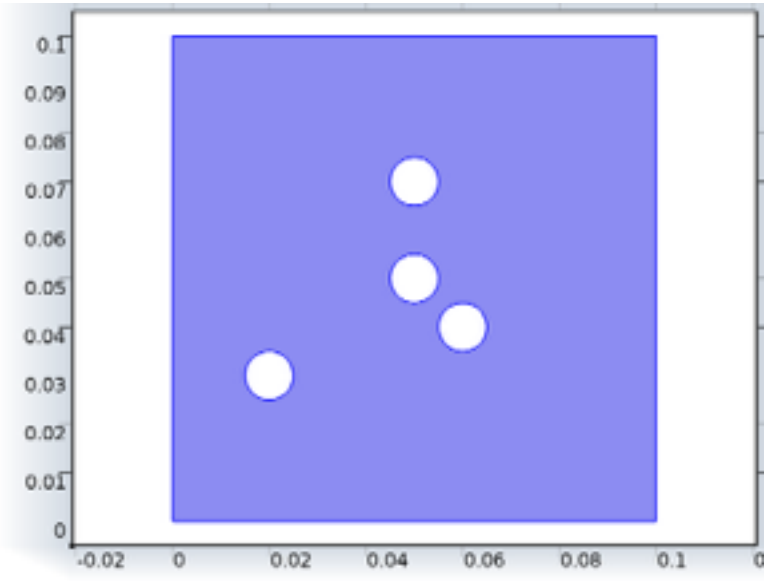

Diffusion

Selection

Geometric entity level	Domain
Selection	Domain 1

Settings

Description	Value
Velocity field	User defined
Velocity field	{0, 0, 0}
Electric potential	User defined
Electric potential	0
Diffusion coefficient	User defined
Diffusion coefficient	{{1e-9[m^2/s], 0, 0}, {0, 1e-9[m^2/s], 0}, {0, 0, 1e-9[m^2/s]}}
Bulk material	None

2.3.2. No Flux 1

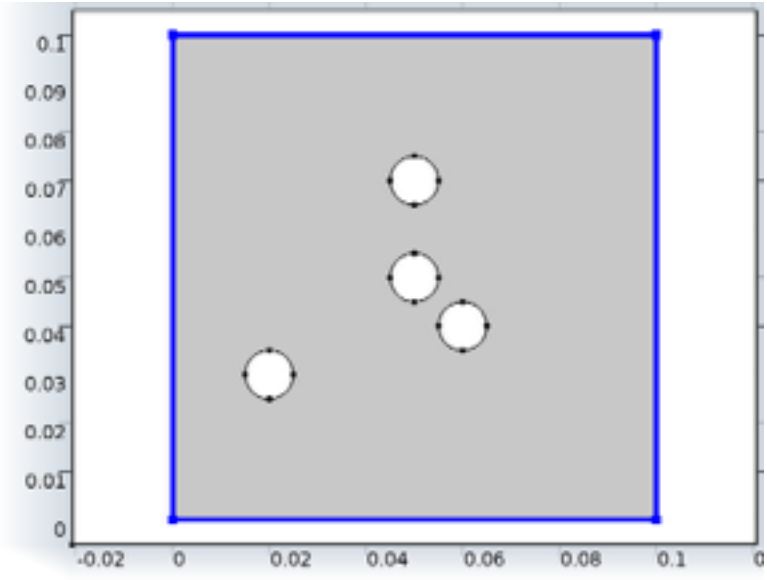

No Flux 1

Selection

Geometric entity level	Boundary
Selection	Boundaries 1–4

Settings

Description	Value
Apply for all species	Apply for all species

2.3.3. Initial Values 1

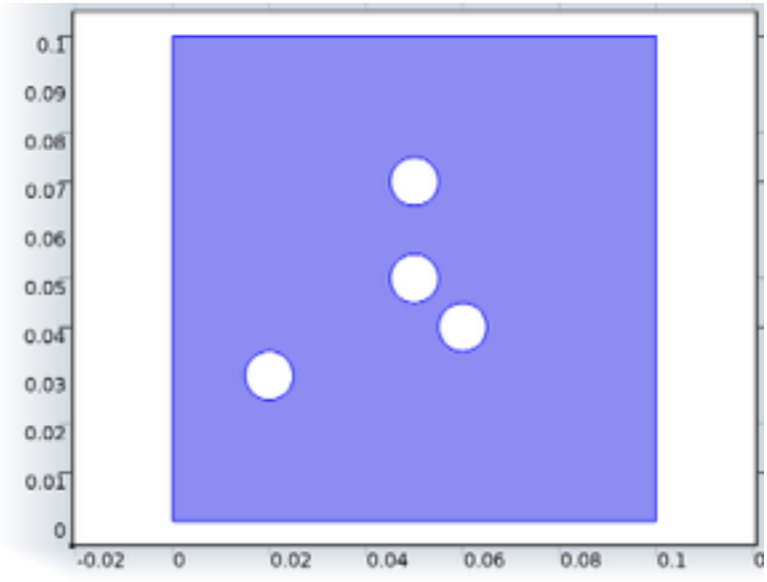

Initial Values 1

Selection

Geometric entity level	Domain
Selection	Domain 1

Settings

Description	Value
Concentration	20

2.3.4. Concentration 1

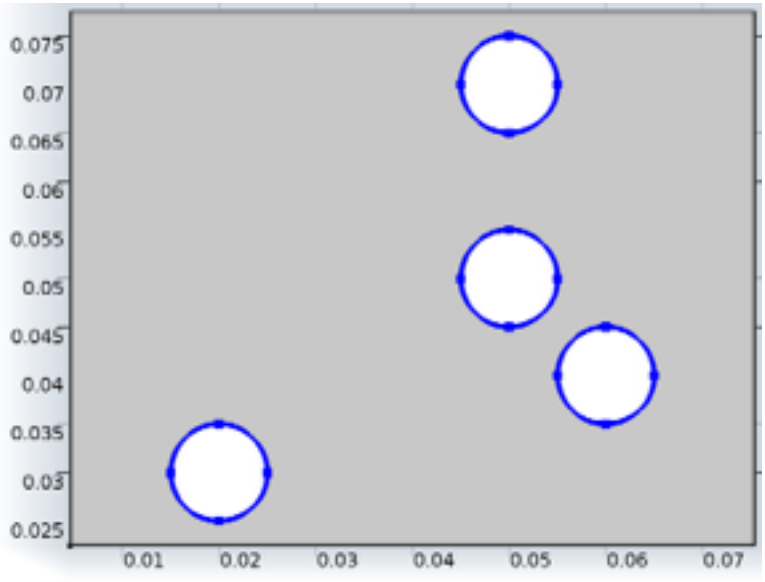

Concentration 1

Selection

Geometric entity level	Boundary
Selection	Boundaries 5–20

Settings

Description	Value
Concentration	0
Species c	1
Apply reaction terms on	All physics (symmetric)
Use weak constraints	0

2.4. Deformed Geometry (dg)

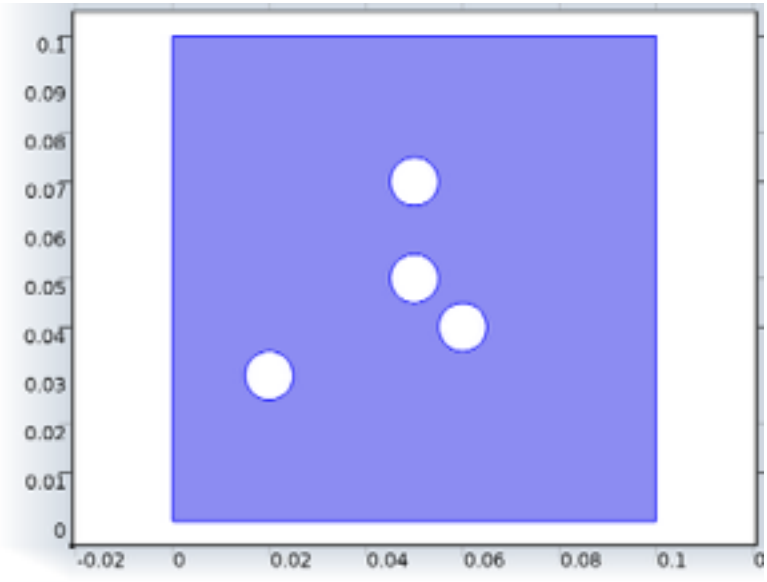

Deformed Geometry

Selection

Geometric entity level	Domain
Selection	Domain 1

Settings

Description	Value
Equation form	Study controlled
Geometry frame coordinates	{Xg, Yg, Zg}
Geometry shape order	1
Mesh smoothing type	Laplace
Show equation assuming	0

2.4.1. Fixed Mesh 1

Selection

Geometric entity level	Domain
Selection	No domains

2.4.2. Prescribed Mesh Displacement 1

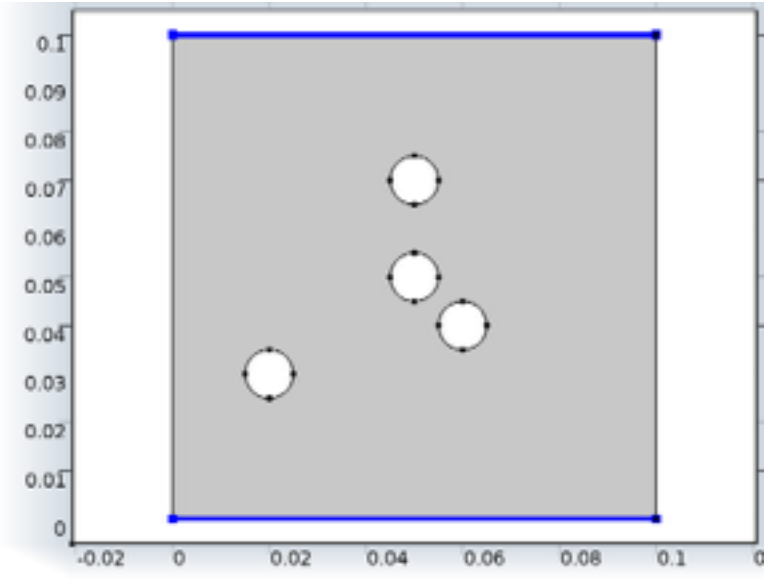

Prescribed Mesh Displacement 1

Selection

Geometric entity level	Boundary
Selection	Boundaries 2–3

Settings

Description	Value
Prescribed # displacement	{0, 1}
Prescribed mesh displacement	{0, 0}
Use weak constraints	0

2.4.3. Free Deformation 1

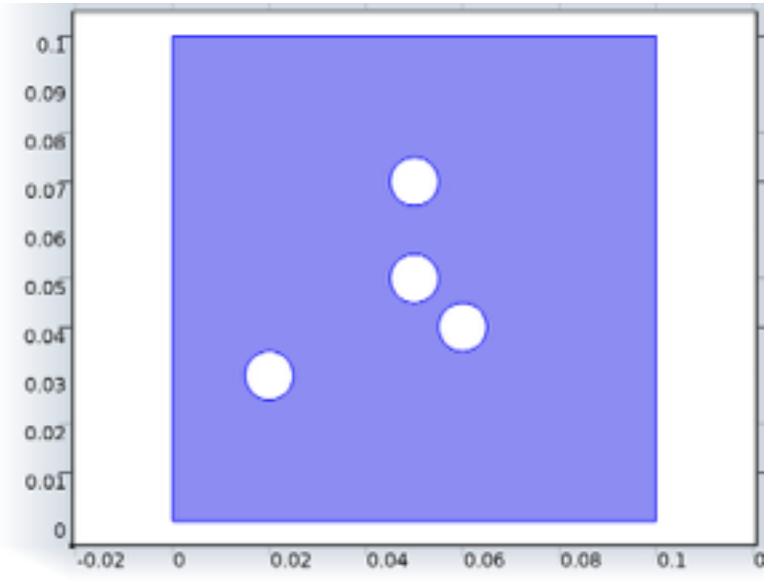

Free Deformation 1

Selection

Geometric entity level	Domain
Selection	Domain 1

Settings

Description	Value
Initial mesh displacement	{0, 0}

2.4.4. Prescribed Mesh Displacement 2

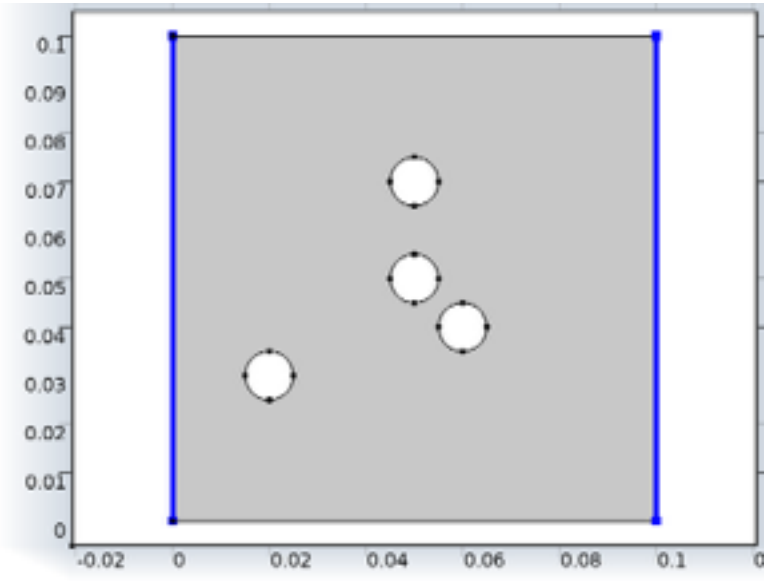

Prescribed Mesh Displacement 2

Selection

Geometric entity level	Boundary
Selection	Boundaries 1, 4

Settings

Description	Value
Prescribed # displacement	{1, 0}
Prescribed mesh displacement	{0, 0}
Use weak constraints	0

2.4.5. Prescribed Mesh Velocity 1

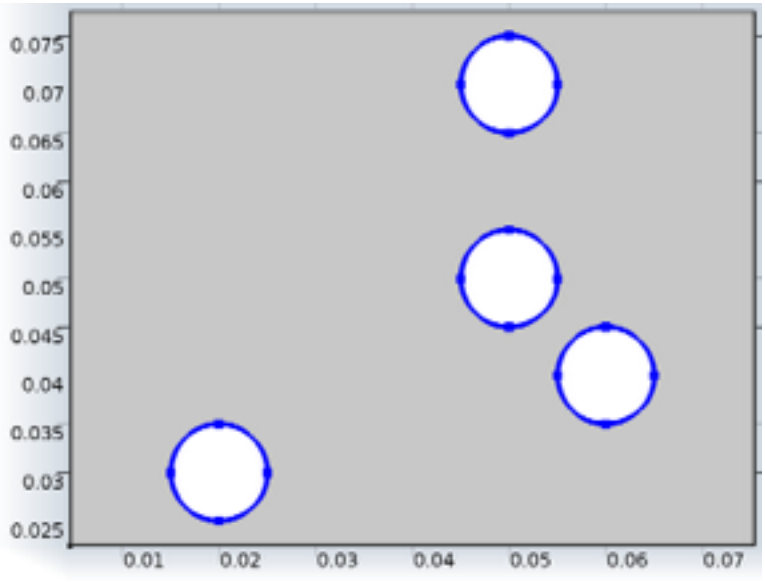

Prescribed Mesh Velocity 1

Selection

Geometric entity level	Boundary
Selection	Boundaries 5–20

Settings

Description	Value
Prescribed # velocity	{1, 1}
Prescribed mesh velocity	{vx_int, vy_int}
Use weak constraints	0

2.5. Meshes

2.5.1. Mesh 1

Mesh statistics

Property	Value
Minimum element quality	0.6886
Average element quality	0.9202
Triangular elements	2364
Edge elements	172
Vertex elements	20

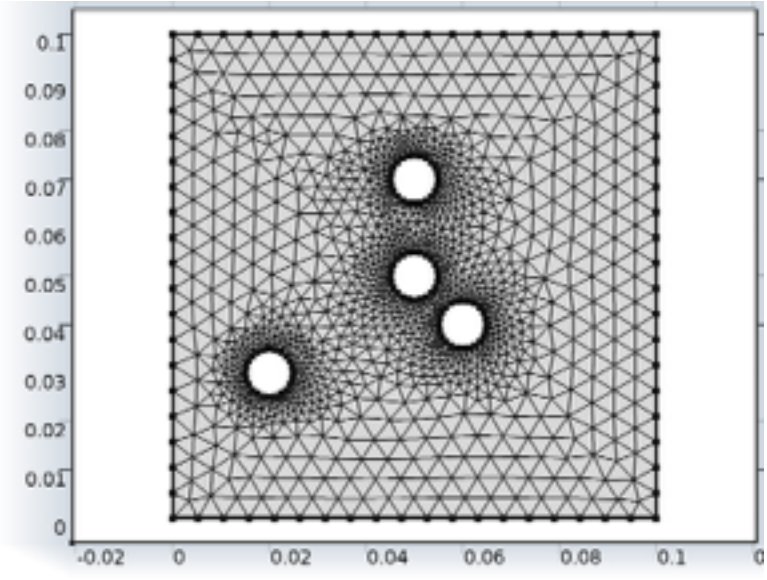

Mesh 1

Size (size)

Settings

Name	Value
Maximum element size	0.0053
Minimum element size	3.0E-5
Resolution of curvature	0.3
Maximum element growth rate	1.3
Predefined size	Fine

Free Triangular 1 (ftri1)

Selection

Geometric entity level	Remaining

3. Study 1

3.1. Time Dependent

Study settings

Property	Value
Include geometric nonlinearity	Off

Times: range(0,100,10^6)

Mesh selection

Geometry	Mesh
Geometry 1 (geom1)	mesh1

Physics selection

Physics	Discretization
Transport of Diluted Species (chds)	physics
Deformed Geometry (dg)	physics

3.2. Solver Configurations

3.2.1. Solver 1

Compile Equations: Time Dependent (st1)

Study and step

Name	Value
Use study	Study 1
Use study step	Time Dependent

Dependent Variables 1 (v1)

General

Name	Value
Defined by study step	Time Dependent

Initial values of variables solved for

Name	Value
Solution	Zero

Values of variables not solved for

Name	Value
Solution	Zero

Concentration (mod1.c) (mod1_c)

General

Name	Value
Field components	mod1.c

mod1.xy (mod1_xy)

General

Name	Value
Field components	{x, y}

mod1.XgYg (mod1_XgYg)

General

Name	Value
Field components	{Xg, Yg}
Solve for this field	Off

Time-Dependent Solver 1 (t1)

General

Name	Value
Defined by study step	Time Dependent

Name	Value
Time	{0, 100, 200, 300, 400, 500, 600, 700, 800, 900, 1000, 1100, 1200, 1300, 1400, 1500, 1600, 1700, 1800, 1900, 2000, 2100, 2200, 2300, 2400, 2500, 2600, 2700, 2800, 2900, 3000, 3100, 3200, 3300, 3400, 3500, 3600, 3700, 3800, 3900, 4000, 4100, 4200, 4300, 4400, 4500, 4600, 4700, 4800, 4900, 5000, 5100, 5200, 5300, 5400, 5500, 5600, 5700, 5800, 5900, 6000, 6100, 6200, 6300, 6400, 6500, 6600, 6700, 6800, 6900, 7000, 7100, 7200, 7300, 7400, 7500, 7600, 7700, 7800, 7900, 8000, 8100, 8200, 8300, 8400, 8500, 8600, 8700, 8800, 8900, 9000, 9100, 9200, 9300, 9400, 9500, 9600, 9700, 9800, 9900, 10000, 10100, 10200, 10300, 10400, 10500, 10600, 10700, 10800, 10900, 11000, 11100, 11200, 11300, 11400, 11500, 11600, 11700, 11800, 11900, 12000, 12100, 12200, 12300, 12400, 12500, 12600, 12700, 12800, 12900, 13000, 13100, 13200, 13300, 13400, 13500, 13600, 13700, 13800, 13900, 14000, 14100, 14200, 14300, 14400, 14500, 14600, 14700, 14800, 14900, 15000, 15100, 15200, 15300, 15400, 15500, 15600, 15700, 15800, 15900, 16000, 16100, 16200, 16300, 16400, 16500, 16600, 16700, 16800, 16900, 17000, 17100, 17200, 17300, 17400, 17500, 17600, 17700, 17800, 17900, 18000, 18100, 18200, 18300, 18400, 18500, 18600, 18700, 18800, 18900, 19000, 19100, 19200, 19300, 19400, 19500, 19600, 19700, 19800, 19900, 20000, 20100, 20200, 20300, 20400, 20500, 20600, 20700, 20800, 20900, 21000, 21100, 21200, 21300, 21400, 21500, 21600, 21700, 21800, 21900, 22000, 22100, 22200, 22300, 22400, 22500, 22600, 22700, 22800, 22900, 23000, 23100, 23200, 23300, 23400, 23500, 23600, 23700, 23800, 23900, 24000, 24100, 24200, 24300, 24400, 24500, 24600, 24700, 24800, 24900, 25000, 25100, 25200, 25300, 25400, 25500, 25600, 25700, 25800, 25900, 26000, 26100, 26200, 26300, 26400, 26500, 26600, 26700, 26800, 26900, 27000, 27100, 27200, 27300, 27400, 27500, 27600, 27700, 27800, 27900, 28000, 28100, 28200, 28300, 28400, 28500, 28600, 28700, 28800, 28900, 29000, 29100, 29200, 29300, 29400, 29500, 29600, 29700, 29800, 29900, 30000, 30100, 30200, 30300, 30400, 30500, 30600, 30700, 30800, 30900, 31000, 31100, 31200, 31300, 31400, 31500, 31600, 31700, 31800, 31900, 32000, 32100, 32200, 32300, 32400, 32500, 32600, 32700, 32800, 32900, 33000, 33100, 33200, 33300, 33400, 33500, 33600, 33700, 33800, 33900, 34000, 34100, 34200, 34300, 34400, 34500, 34600, 34700, 34800, 34900, 35000, 35100, 35200, 35300, 35400, 35500, 35600, 35700, 35800, 35900, 36000, 36100, 36200, 36300, 36400, 36500, 36600, 36700, 36800, 36900, 37000, 37100, 37200, 37300, 37400, 37500, 37600, 37700, 37800, 37900, 38000, 38100, 38200, 38300, 38400, 38500, 38600, 38700, 38800, 38900, 39000, 39100, 39200, 39300, 39400, 39500, 39600, 39700, 39800, 39900, 40000, 40100, 40200, 40300, 40400, 40500, 40600, 40700, 40800, 40900, 41000, 41100, 41200, 41300, 41400, 41500, 41600, 41700, 41800, 41900, 42000, 42100, 42200, 42300, 42400, 42500, 42600, 42700, 42800, 42900, 43000, 43100, 43200, 43300, 43400, 43500, 43600, 43700, 43800, 43900, 44000, 44100, 44200, 44300, 44400, 44500, 44600, 44700, 44800, 44900, 45000, 45100, 45200, 45300, 45400, 45500, 45600, 45700,

General

Name	Value
Remesh in geometry	Geometry 1

Output

Name	Value
Solution	Automatic Remeshing 2
Meshes	{mesh2, mesh3, mesh4, mesh5, mesh6}

Fully Coupled 1 (fc1)

General

Name	Value
Linear solver	Direct 1

Automatic Remeshing 2

4. Results

4.1. Data Sets

4.1.1. Solution 1

Selection

Geometric entity level	Domain
Selection	Geometry geom1

Solution

Name	Value
Solution	Solver 1
Model	Save Point Geometry 1

4.1.2. Solution 2

Selection

Geometric entity level	Domain
Selection	Geometry geom1

Solution

Name	Value
Solution	Automatic Remeshing 2
Model	Save Point Geometry 1

4.2. Plot Groups

4.2.1. Concentration (chds)

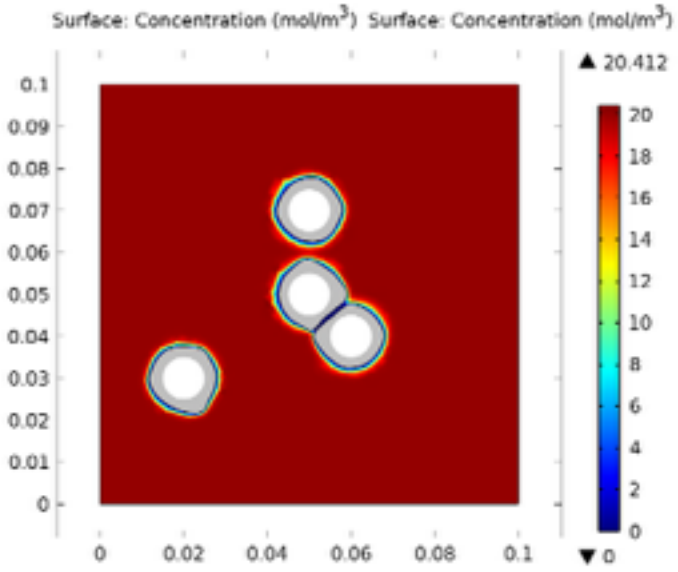

Surface: Concentration (mol/m³) Surface: Concentration (mol/m³)

Bibliography

1. Heimann, R. (2010). *Classic and Advanced Ceramics: From Fundamentals to Applications*. Weinheim: Wiley-VCH CmbH & Co. KGaA.

2. Interrante, L., C. Whitmarsh & W. Sherwood. (1994). Fabrication of SiC Matrix Composites by Liquid Phase Infiltration With a Polymeric Precursor. *Materials Research Society Symposia Proceedings*, 139-146.

3. Ionescu, E. & R. Riedel. (2012). Polymer Processing of Ceramics. *Ceramics and Composites: Processing Methods*. Eds. N. Bandal & A. Boccaccini. (pp 235-270) Hoboken: John Wiley and Sons.

4. Lazzeri, A. (2012). CVI Processing of Ceramic Matrix Composites. C*eramics and Composites: Processing Methods*. Eds. N. Bandal & A. Boccaccini. (pp 313-349) Hoboken: John Wiley and Sons.

5. Blanquet, E., et al. (2006). High Temperature Silicon Carbide Chemical Vapor Deposition Processes: From Pure Thermodynamic to Mass Transport Modeling. *European Conference on Computational Fluid Dynamics*.

6. de Jong, F. & M. Meyyappan. (1996). Numerical Simulation of Silicon Carbide Chemical Vapor Deposition. *Diamond and Related Materials*, 141-150.

7. de Persis, S., A. Dollet & F. Teyssandier. (2003). Gas-phase Kinetics Analysis and Reduction of Large Reaction Mechanisms Exemplified in the Case of SiC Deposition. *Journal of Analytical and Applied Pyrolysis*, 55-71.

8. Dollet, A., et al. (2004). Simulation of SiC Deposition from $SiH_4/C_3H_8/Ar/H_2$ Mixtures in a Cold-Wall CVD Reactor. *Surface & Coatings Technology*, 382-388.

9. Fischman, G. & W. Petuskey. (1985). Thermodynamic Analysis and Kinetic Implications of Chemical Vapor Deposition of SiC from Si-C-Cl-H Gas Systems. *Journal of the American Ceramic Society*, 185-190.

10. Kingon, A., et al. (1983). Thermodynamic Calculations for the Chemical Vapor Deposition of Silicon Carbide. *Journal of the American Ceramic Society*, 558-566.

11. Li, A., et al. (2008). Modeling and Simulation of Materials Synthesis: Chemical Vapor Deposition and Infiltration of Pyrolytic Carbon. *Composites Science and Technology*, 1097-1104.

12. Loumagne, F., F. Langlais & R. Naslain. (1993). Kinetic Laws of the Chemical Process in the CVD of SiC Ceramics from CH3SiCl3-H2 Precursor. *Journal de Physique IV*, C3527-C3533.

13. ———— (1995). Experimental Kinetic Study of the Chemical Vapour Deposition of SiC-based ceramics from CH_3SiCl_3/H_2 Gas Precursor. *Journal of Crystal Growth*, 198-204.

14. Neuschutz, D., M. Schierling & S. Zimdahl. (1995). Simulation of Chemical Vapour Deposition of SiC from Methyltrichlorosilane in a Hot Wall Reactor. *Journal de Physique IV*, C5253-C5260.

15. Oh, I., C. Takoudis & G. Neudeck. (1991). Mathematical Modeling of Epitaxial Silicon Growth in Pancake Chemical Vapor Deposition Reactors. *Journal of the Electrochemical Society*, 554-567.

16. Pons, M., et al.. (1996). Thermodynamic Heat Transfer and Mass Transport Modeling of the Sublimation Growth of Silicon Carbide Crystals. *Journal of the Electrochemical Society*, 3727-3735.

17. Gupte, S. & J. Tsamopoulos. (1989). Densification of Porous Materials by Chemical Vapor Infiltration. *Journal of the Electrochemical Society*, 555-561.

18. Maizza, G. & M. Longhin. (2009). Modeling of SiC Chemical Vapor Infiltration Process (CVI) Assisted by Microwave Heating. *Proceedings of the COMSOL Conference 2009 Milan*.

19. Ros, W., et al. (2011). Simulation of Chemical Vapor Infiltration and Deposition Based on 3D Images: A Local Scale Approach. *Chemical Vapor Deposition*, 312-320.

20. Schnack, E., F. Wang & A. Li. (2010). Phase-Field Model for the Chemical Vapor Infiltration of Silicon Carbide. *Journal of the Electrochemical Society*, D377-D386.

21. Vignoles, G., et al. (2011). Pearson Random Walk Algorithms for Fiber-Scale Modeling of Chemical Vapor Infiltration. *Computational Materials Science*, 1157-1168.

22. Vignoles, G., et al. (2011). A Brownian Motion Algorithm for Tow Scale Modeling of Chemical Vapor Infiltration. *Computational Materials Science,* 1871-1878.

23. Wang, C. & D. Tsai. (2000). Low Pressure Chemical Vapor Deposition of Silicon Carbide from Dichlorosilane and Acetylene. *Materials Chemistry and Physics,* 196-201.

24. Wei, X., et al. (2006). A Two-Dimensional Model for Densification Behavior of C/SiC Composites in Isothermal Chemical Vapor Infiltration. *Modeling and Simulation in Materials Science and Engineering*, 891-904.

25. Geiser, J. (2013). Multiscale Modeling of Chemical Vapor Deposition (CVD) Apparatus: Simulations and Approximations. *Polymers*, 142-160.

26. Rodgers, S. & K. Jensen. (1998). Multiscale Modeling of Chemical Vapor Deposition. *Journal of Applied Physics*, 524-530.

27. Carlsson, J. (2010). Chemical Vapor Deposition. *Handbook of Deposition Technologies for Films and Coatings, 3rd ed.* Ed. P. Martin. (pp. 314-363). Boston: William Andrew Publishing.

28. Kern, W. & G. Schnable. (1979). Low-Pressure Chemical Vapor Deposiion for Very Large-Scale Integration Processing—A Review. *IEEE Transactions of Electron Devices*, 647-657.

29. Blocher, J. (1974). Structure/Property/Process Relationships in Chemical Vapor Deposition CVD. *Journal of Vacuum Science & Technology*, 680-686.

30. Powell, A. & L. Rowland. (2002). SiC Materials—Progress, Status, and Potential Roadblocks. *Proceedings of the IEEE*, 942-955.

31. Kong, H., J. Glass & R. Davis. (1988). Chemical Vapor Deposition and Characterization of 6HSiC Films on Offaxis 6HSiC Substrates. *Journal of Applied Physics*, 2672-2679.

32. Moene, R., et al. (1996). Coating of Activated Carbon With Silicon Carbide by Chemical Vapor Deposition. *Carbon*, 567-579.

33. Sone, H., T. Kaneko & N. Miyakawa. (2000). In Situ Measurements and Growth Kinetics of Silicon Carbide Chemical Vapor Deposition from Methyltrichlorosilane. *Journal of Crystal Growth*, 245-252.

34. Wei, X., et al. (2006). Numerical Simulation of Effect of Methyltrichlorosilane Flux on Isothermal Chemical Vapor Infiltration Process of C/SiC Composites. *Journal of the American Ceramic Society*, 2762-2768.

35. Narushima, T., et al. (1991). High-Temperature Active Oxidation of Chemically Vapro-Deposited Silicon Carbide in an Ar-O_2 Atmosphere. *Journal of the American Ceramic Society*, 2583-2586.

36. Yang, Y. & W. Zhang. (2009). Kinetic and Microstructure of SiC Deposited from $SiCl_4$-CH_4-H_2. *Chinese Journal of Chemical Engineering*, 419-426.

37. Anzalone, R., et al. (2010). Low Stress Heteroepitaxial 3C-SiC Films Characterized by Microstructure Fabrication and Finite Element Analysis. *Journal of the Electrochemical Society*, H438-H442.

38. Shi, B., et al. (2012). Effect of Propane/Silane Ratio on the Growth of 3C-SiC Thin Films on Si(1 0 0) Substrates by APCVD. *Applied Surface Science*, 685-690.

39. COMSOL, Inc. (2012) *COMSOL Multiphysics User's Guide, Version 4.3.*

40. Kundu, P. & I. Cohen. (2008). *Fluid Mechanics, 4th ed*. Boston: Elsevier Inc.

41. Chang, H. &R. Adomaitis. (1998). Analysis of Heat Transfer in a Chemical Vapor Depostion Reactor: An Eigenfunction Expansion Solution Approach. *International Journal of Heat and Fluid Flow*, 74-83.

42. National Institute of Standards and Technology. (2011). *NIST Chemistry WebBook*. Retrieved from http://webbook.nist.gov/chemistry/

43. Murdoch, L. (2013). *Tutorial 9 Models with changing geometries. Hydro Model Gallery.* Retrieved from http://www.clemson.edu/ces/hydromodelgallery/index.php

44. Reddy, J. (2006). *An Introduction to the Finite Element Method, 3rd ed*. Boston: McGraw-Hill.

45. Dickinson, E., H. Ekstrom & E. Fontes. (2014). COMSOL Multiphysics: Finite Element Software for Electrochemical Analysis. A Mini-Review. *Electrochemistry Communications,* 71-74.

46. COMSOL, Inc. (2014) *COMSOL Model Gallery*. Retrieved from http://www.comsol.com/models

REPORT DOCUMENTATION PAGE

Form Approved
OMB No. 0704-0188

1. REPORT DATE *(DD-MM-YYYY)*	2. REPORT TYPE	3. DATES COVERED *(From - To)*
19-06-2014	Master's Thesis	September 2007- June 2014

4. TITLE AND SUBTITLE

Finite Element Analysis Modeling of Chemical Vapor Deposition of Silicon Carbide

5a. CONTRACT NUMBER

5b. GRANT NUMBER

5c. PROGRAM ELEMENT NUMBER

6. AUTHOR(S)

Allen, Brandon M., Mr.

5d. PROJECT NUMBER

5e. TASK NUMBER

5f. WORK UNIT NUMBER

7. PERFORMING ORGANIZATION NAME(S) AND ADDRESS(ES)

Air Force Institute of Technology
Graduate School of Engineering and Management (AFIT/EN)
2950 Hobson Way Wright-Patterson AFB OH 45433-7765

8. PERFORMING ORGANIZATION REPORT NUMBER

AFIT-ENP-T-14-J-38

9. SPONSORING/MONITORING AGENCY NAME(S) AND ADDRESS(ES)

Air Force Research Laboratory
Dr. Ming Y. Chen
2941 Hobson Way Wright-Patterson AFB OH 45433-7750
ming.chen@us.af.mil

10. SPONSOR/MONITOR'S ACRONYM(S)

AFRL

11. SPONSOR/MONITOR'S REPORT NUMBER(S)

12. DISTRIBUTION/AVAILABILITY STATEMENT

Distribution Statement A. Approved for Public Release; Distribution Unlimited

13. SUPPLEMENTARY NOTES

14. ABSTRACT

Fiber-reinforced silicon carbide (SiC) composite materials are important for many applications due to their high temperature strength, excellent thermal shock and impact resistance, high hardness, and good chemical stability. The microstructureand phase composition of SiC composites can be tailored by fiber surface modification, the process parameters, and/orfiber preform architecture. One process by which SiC composites can be produced is chemical vapor deposition (CVD). This thesis primarily focuses on mass transport by gas-phase flow and diffusion, chemical reaction in gas phase and on solid surfaces, and thin film formation on curved surfaces, which are fundamental to the CVD process. We highlighted process parameters that can potentially affect the structures and properties of the CMCs using simple model material systems. We also analyzed the use of a finite element modeling tool, COMSOL Multiphysics, to build the series of models.

15. SUBJECT TERMS

Ceramic Matrix Composite, Silicon Carbide, Finite Element Analysis Modeling, Chemical Vapor Deposition

16. SECURITY CLASSIFICATION OF:			17. LIMITATION OF ABSTRACT	18. NUMBER OF PAGES	19a. NAME OF RESPONSIBLE PERSON
a. REPORT	b. ABSTRACT	c. THIS PAGE			Dr. Alex G. Li, AFIT/ENP
U	U	U	UU	181	19b. TELEPHONE NUMBER *(Include area code)* (937)255-3636x4576 alex.li@afit.edu

Reset

Standard Form 298 (Rev. 8/98)
Prescribed by ANSI Std. Z39.18